

NOTE TO USERS

This reproduction is the best copy available.

UMI[®]

**Analysis of Product-separable 2-D IIR Discrete Filters with
Feedbacks for Variable Characteristics**

Jun Xiao

A Thesis

in

The Department

of

Electrical and Computer Engineering

Presented in Partial Fulfillment of the Requirements

for the Degree of Master of Applied Science at

Concordia University

Montreal, Quebec, Canada

September, 2005

© Jun Xiao, 2005



Library and
Archives Canada

Bibliothèque et
Archives Canada

Published Heritage
Branch

Direction du
Patrimoine de l'édition

395 Wellington Street
Ottawa ON K1A 0N4
Canada

395, rue Wellington
Ottawa ON K1A 0N4
Canada

Your file *Votre référence*
ISBN: 0-494-10256-X
Our file *Notre référence*
ISBN: 0-494-10256-X

NOTICE:

The author has granted a non-exclusive license allowing Library and Archives Canada to reproduce, publish, archive, preserve, conserve, communicate to the public by telecommunication or on the Internet, loan, distribute and sell theses worldwide, for commercial or non-commercial purposes, in microform, paper, electronic and/or any other formats.

The author retains copyright ownership and moral rights in this thesis. Neither the thesis nor substantial extracts from it may be printed or otherwise reproduced without the author's permission.

AVIS:

L'auteur a accordé une licence non exclusive permettant à la Bibliothèque et Archives Canada de reproduire, publier, archiver, sauvegarder, conserver, transmettre au public par télécommunication ou par l'Internet, prêter, distribuer et vendre des thèses partout dans le monde, à des fins commerciales ou autres, sur support microforme, papier, électronique et/ou autres formats.

L'auteur conserve la propriété du droit d'auteur et des droits moraux qui protègent cette thèse. Ni la thèse ni des extraits substantiels de celle-ci ne doivent être imprimés ou autrement reproduits sans son autorisation.

In compliance with the Canadian Privacy Act some supporting forms may have been removed from this thesis.

Conformément à la loi canadienne sur la protection de la vie privée, quelques formulaires secondaires ont été enlevés de cette thèse.

While these forms may be included in the document page count, their removal does not represent any loss of content from the thesis.

Bien que ces formulaires aient inclus dans la pagination, il n'y aura aucun contenu manquant.


Canada

ABSTRACT

Analysis of Product-separable 2-D IIR Discrete Filters with Feedbacks for Variable Characteristics

Jun Xiao

In order to design 2-D digital systems with variable characteristics, product-separable IIR filters with feedbacks in each dimension are studied. The stability and response of such systems with different situations are analyzed and discussed.

Belonging to one of the methods of generation of VSHP in z-domain, product-separable IIR filters with dimensional feedbacks offer variable characteristics. The variable feedback gain in one-dimension is analyzed with all the other coefficients based on Schussler's Theorem. The stable conditions for the feedback in terms of other coefficients are obtained and hence a stable range of the feedback gain is determined.

Within the stable range of feedback in each dimension, different filters' 2-D frequency responses have been studied and observed with different situations. Significant variable characteristics and different 2-D symmetries are shown with stable responses. Relations between the feedback and response are discussed. Furthermore, to extend this analysis to higher order systems, a computerized analysis method and algorithm is proposed and implemented. This approximation method can work with any order of IIR or FIR filters and has low computation complexity.

More complex systems with variable characteristics can be composed and examples of Image Processing with these filters are simulated as space-domain applications.

ACKNOWLEDGMENTS

Most of all, I would like to express my great gratitude to my research advisor Professor Dr. Venkat Ramachandran for his support and guidance over the past two and a half years. His high expectation and enlightening advice have helped me stay improved, and made this thesis possible. I am grateful to Professor Dr. Weiping Zhu, for his DSP and digital image processing lectures and materials. And also I thank Dr. Henry Hong and Dr. O. Ait Mohamed for their helpful suggestions in the preparation of the final version of the thesis.

I would like to thank Aide Financiere Aux Etudes Quebec for the financial support.

Learning together with other members in DSP field has greatly enriched my education and life. I would like to thank all of them for their support and encouragement: Xiaojun Zhang, Xibin Han. Their suggestions made the task of research enjoyable.

Finally, and most importantly, I would like to thank my dear wife Yongmei Zhu, my parents, their love and encouragement made me overcome difficulties and complete this degree.

TABLE OF CONTENTS

1	Introduction.....	1
1.1	Importance of 2-D filtering.....	1
1.2	Stability of 2-D IIR systems.....	3
1.3	Some properties of VSHP.....	6
1.4	Methods of generation of VSHP.....	7
1.5	Symmetry of 2-D systems.....	12
1.5.1	Rotational symmetry.....	12
1.5.2	Centro-symmetry.....	12
1.5.3	Reflection symmetry.....	12
1.5.4	Quadrantal symmetry.....	13
1.5.5	Diagonal four-fold reflection symmetry.	13
1.5.6	Octagonal symmetry.....	13
1.5.7	Circular symmetry.....	13
1.6	Separable and non-separable 2-D transfer functions.....	14
1.7	Scope of the thesis.....	14
2	Product-separable 2-D transfer functions.....	16
2.1	Introduction.....	16
2.2	The structure considered.....	17

2.3	Schussler's theorem for 1-D systems.....	18
2.4	Stability conditions of 1-D systems.....	20
2.5	Stability conditions for different numerators.....	22
2.5.1	Typical forms with order up to 2.....	22
2.5.2	The Generic Biquadratic Transfer Functions.....	26
2.6	Summary and discussions.....	31
3	Response of different conditions.....	34
3.1	Introductions.....	34
3.2	1-D Responses with stable range of k	34
3.3	Specifications for 2-D filter design.....	38
3.3.1	Quadrantal frequency requirements.....	39
3.3.2	Circular frequency requirements.....	40
3.4	Frequency response of various filters with $k_1=k_2$	40
3.4.1	LP00 with different values of k	41
3.4.2	LP01 with different values of k	42
3.4.3	LP02 with different values of k	43
3.4.4	LP11 with different values of k	44
3.4.5	LP20 with different values of k	45
3.4.6	HP with different values of k	47

3.4.7	BP01 with different values of k	49
3.4.8	BP10 with different values of k	50
3.5	Frequency response of various filters with $k_1 \neq k_2$	52
3.5.1	Dimension-unbalanced LP00.....	52
3.5.2	Dimension-unbalanced LP01.....	52
3.5.3	Dimension-unbalanced LP02.....	53
3.5.4	Dimension-unbalanced LP11.....	53
3.5.5	Dimension-unbalanced LP20.....	54
3.5.6	Dimension-unbalanced HP.....	55
3.5.7	Dimension-unbalanced BP01.....	56
3.5.8	Dimension-unbalanced BP10.....	56
3.6	Frequency response of combinations of filters with $k_1 = k_2$	57
3.6.1	LP20/HP.....	58
3.6.2	LP20/BP10.....	59
3.6.3	HP/BP10.....	60
3.7	Frequency response of combinations of filters with $k_1 \neq k_2$	61
3.7.1	LP20/HP.....	62
3.7.2	LP20/BP10.....	63
3.7.3	HP/BP10.....	64
3.8	Summary and discussions.....	65

4	Analysis and response of higher order filters.....	66
4.1	Algorithms for higher order filters.....	66
4.1.1	Algorithm Selection.....	67
4.1.2	Implementation and simulation.....	72
4.1.2.1	Algorithm flow chart.....	72
4.1.2.2	Implementation examples.....	74
4.2	2-D response of higher order filters.....	75
4.2.1	IIR filters.....	75
4.2.2	FIR filters.....	81
4.3	Summary.....	83
5	2-D Applications and simulations.....	85
5.1	2-D filters derived from low-pass and high-pass filters.....	85
5.2	Space-domain response.....	88
5.3	Summaries.....	95
6	Conclusions.....	96
6.1	The works have been done.....	96
6.2	Related and future works.....	99
	References.....	101

LIST OF FIGURES

Fig.1.1	Signal-flow graph of a basic structure.....	2
Fig.2.1	2-D product-separable system.....	16
Fig.2.2	1-D analog IIR filter with variable feedback.....	17
Fig.2.3	2-D IIR VCTR system to be analyzed.....	18
Fig.2.4	Poles and zeros of F_1/F_2 , if $D(z) = z^n$ and $n = 4$ or $n = 5$	20
Fig.2.5	Poles and zeros of F_1/F_2 , if $D(z) = z^n$ and $n = 4$ or $n = 5$, their real parts separate each other on the real axis between -1 and 1	21
Fig.2.6	1-D discrete system.....	22
Fig.3.1	Butterworth of LP00.....	36
Fig.3.2	Butterworth of LP01.....	36
Fig.3.3	Butterworth of LP11.....	37
Fig.3.4	Butterworth of LP02.....	37
Fig.3.5	Butterworth of BP01.....	38
Fig.3.6	Quadrantal requirements for typical filters, (a)Low-pass; (b)High-pass; (c)Band-pass; (d)Band-elimination.....	39
Fig.3.7	2-D Butterworth of LP00, (a) $k_1=k_2=0$; (b) $k_1=k_2=1.8$; (c) $k_1=k_2=-1.8$	41
Fig.3.8	2-D Butterworth of LP01, (a) $k_1=k_2=0$; (b) $k_1=k_2=2.5$; (c) $k_1=k_2=-2.5$	42
Fig.3.9	2-D Butterworth of LP02, (a) $k_1=k_2=0$; (b) $k_1=k_2=2.5$; (c) $k_1=k_2=-2.5$	43
Fig.3.10	2-D Butterworth of LP11, (a) $k_1=k_2=0$; (b) $k_1=k_2=0.7$	44

Fig.3.11	2-D Butterworth of LP20, (a) $k_1=k_2=0$; (b) $k_1=k_2=0.3$; (c) $k_1=k_2=0.7$; (d) $k_1=k_2=-0.3$; (e) $k_1=k_2=-0.7$	46
Fig.3.12	2-D Butterworth of HP, (a) $k_1=k_2=0$; (b) $k_1=k_2=0.2$; (c) $k_1=k_2=0.4$; (d) $k_1=k_2=-0.2$; (e) $k_1=k_2=-0.5$	48
Fig.3.13	2-D Butterworth of BP01, (a) $k_1=k_2=0$; (b) $k_1=k_2=0.5$; (c) $k_1=k_2=-1.5$	49
Fig.3.14	2-D Butterworth of BP10, $k_1=k_2=0$; (b) $k_1=k_2=0.1$; (c) $k_1=k_2=0.5$; (d) $k_1=k_2=-0.5$; (e) $k_1=k_2=-1.5$	51
Fig.3.15	2-D Butterworth of LP00, $k_1=1.5$, $k_2=-2$	52
Fig.3.16	2-D Butterworth of LP01, $k_1=2.5$, $k_2=-2.5$	52
Fig.3.17	2-D Butterworth of LP02, $k_1=2$, $k_2=-2$	53
Fig.3.18	2-D Butterworth of LP11, $k_1=1.5$, $k_2=-2$	53
Fig.3.19	2-D Butterworth of LP20, (a) $k_1=0.7$, $k_2=0.1$; (b) $k_1=0.97$, $k_2=0.1$	54
Fig.3.20	2-D Butterworth of HP, (a) $k_1=0.45$, $k_2=0.2$; (b) $k_1=0.45$, $k_2=-0.4$	55
Fig.3.21	2-D Butterworth of BP01, $k_1=1$, $k_2=-1$	56
Fig.3.22	2-D Butterworth of BP10, (a) $k_1=0.5$, $k_2=-0.5$; (b) $k_1=0.5$, $k_2=-2.5$	57
Fig.3.23	Butterworth of LP20/HP, (a) $k_1=k_2=0.4$; (b) $k_1=k_2=0.1$; (c) $k_1=k_2=-0.3$	58
Fig.3.24	Butterworth of LP20/BP10, (a) $k_1=k_2=0.4$; (b) $k_1=k_2=0.2$; (c) $k_1=k_2=-0.5$	60
Fig.3.25	Butterworth of HP/BP10, (a) $k_1=k_2=0.4$; (b) $k_1=k_2=0.1$; (c) $k_1=k_2=-0.5$...	61
Fig.3.26	Butterworth of LP20/HP, (a) $k_1=-0.4$, $k_2=0.4$; (b) $k_1=0.95$, $k_2=-0.9$	62
Fig.3.27	Butterworth of LP20/BP10, (a) $k_1=-0.5$, $k_2=0.5$; (b) $k_1=0.95$, $k_2=-0.95$	63

Fig.3.28	Butterworth of HP/BP10, (a) $k_1=-0.5, k_2=0.5$; (b) $k_1=0.95, k_2=-0.95$	64
Fig.4.1	Variable z picked from -1 to 1 on the unit circle with small step value of Δz	69
Fig.4.2	Example of $G_1(z)$ along semi unit circle, $n=6, \Delta z = 0.001$	70
Fig.4.3	Example of $G_2(z)$ along semi unit circle, $n=6, \Delta z = 0.001$	71
Fig.4.4	The flow chart of the algorithm.....	73
Fig.4.5	Calculated stable range of k ($\Delta k = 0.08, \Delta z = 0.001\pi$).....	75
Fig.4.6	1-D response with stable range of k	74
Fig.4.7	2-D response with 6 th order Butterworth low-pass filters(0.5π), (a) $k_1=k_2=0$; (b) $k_1=k_2=0.05$; (c) $k_1=k_2=0.55$; (d) $k_1=k_2=-0.55$	77
Fig.4.8	2-D response with 6 th order Butterworth high-pass filters(0.5π), (a) $k_1=k_2=0$; (b) $k_1=k_2=0.3$; (c) $k_1=k_2=-0.7$	78
Fig.4.9	2-D response of modified 6 th order Butterworth low-pass filter, coefficients a_2 and a_3 are changed to 0.5558 and 0.2959	80
Fig.4.10	2-D response of modified 6 th order Butterworth high-pass filter, Coefficients a_2 and a_3 are changed to 0.467 and 0.3965	80
Fig.4.11	2-D magnitude response of 6 th order FIR high-pass filters with feedbacks, (a) FIR with feedback $k_1=k_2=0$; (b) $k_1=k_2=0.1$	82
Fig.4.12	1-D group delay of 6 th order FIR high-pass filters with feedbacks, (a) FIR with feedback $k=0$; (b) $k=0.1$	82

Fig.5.1	2-D band-pass filters built with 6 th order Butterworth filters, Pass-band: 0.3 π ~0.8 π ; (a)k=0; (b) k=0.5; (c)k=-0.5.....	86
Fig.5.2	2-D band-elimination filters built with 6 th order Butterworth filters, Pass-band: 0~0.3 π , 0.5 π ~ π ; (a)k=0; (b) k=0.5; (c)k=-0.5.....	88
Fig.5.3	(a) Image Lena and Photographer; (b) Noised added.....	89
Fig.5.4	(a) Image denoised with 2-D LP11 Biquadratic filters (k ₁ = k ₂ =0.2) (b) Output matrix values.....	90
Fig.5.5	(a) Original images processed with 2-D BP01 Biquadratic filters (k ₁ = k ₂ =0.2); (b) Output matrix values.....	91
Fig.5.6	(a) Processed with 2-D Butterworth high-pass filters (2 nd order, 0.05 π , k ₁ = k ₂ =0.1); (b) Output matrix.....	92
Fig.5.7	(a) Processed with 2-D Butterworth band-elimination filters (0.15 π ~0.5 π); (b) Output matrix.....	93
Fig.5.8	(a) Plain white and template images; Middle: Processed with LP00-LP02 Biquadratic filters (k ₁ = k ₂ =0.1); (b) Output matrix values.....	94

LIST OF TABLES

Table 2.1	Generic biquadratic transfer functions.....	26
Table 2.2	Summary of analysis of different filters	31
Table 3.1	Stable conditions for Generic Biquadratic Butterworth filters.....	34
Table 4.1	Example of high order coefficients.....	74
Table 4.2	Example of high order FIR coefficients.....	81

LIST OF IMPORTANT SYMBOLS, CHARACTERS AND ACRONYMS

z_1, z_2	Z-domain complex variables in two dimensions
s_1, s_2	S-domain complex variables in two dimensions
k_1, k_2	Feedback gain of filters in two dimensions
ω_1, ω_2	Frequencies in radians in two dimensions
$H(z_1, z_2)$	Z-domain response of 2-D digital filters
$H(s_1, s_2)$	S-domain response of 2-D analog filters
$D(z_1, z_2)$	Denominator of 2-D digital filters' transfer function
$N(z_1, z_2)$	Nominator of 2-D digital filters' transfer function
LP/HP/BPij	Low-pass/high-pass/band-pass Biquadratic filters i: order of factor of $(z^{-1} + 1)$, j: order of factor of z^{-1}
Σ	Summation of
Π	Product of
\forall	For all values
FFT	Fast Fourier Transformation
IFFT	Inverse Fast Fourier Transformation
IIR	Infinite Impulse Response
FIR	Finite Impulse Response
VSHP	Very Strict Hurwitz Polynomials
VCTF	Variable Characteristics Transfer Functions

CHAPTER 1 Introduction

1.1 Importance of 2-D filtering

Nowadays, two-dimensional (2-D) digital filters are widely used in the image processing, telecommunication, radar systems, medical diagnosis and other applications where 2-dimensional data array is used.

The transfer function of these filters can be described as:

$$H(z_1, z_2) = \frac{\sum_{m=0}^M \sum_{n=0}^N b_{mn} z_1^{-m} z_2^{-n}}{\sum_{i=0}^I \sum_{j=0}^J a_{ij} z_1^{-i} z_2^{-j}} \quad (1.1)$$

When $a_{00} \neq 0$ and $a_{ij} = 0$ for $i \neq 0$ and $j \neq 0$, it is a 2-D FIR (Finite Impulse Response) filter, otherwise it is a 2-D IIR (Infinite Impulse Response) filter.

In order to design a 2-D system optimally satisfying the specifications, the characteristics, (which include magnitude response, phase or group delay, etc.), need to be variable. First, one can choose a certain type of filter, and then change one or more of the coefficients of the transfer function as shown in Fig.1.1. This can give variable characteristics but also simultaneously change the pole-zero locations of the system. For FIR filters, there is no stability problem to worry about because they are inherently stable with any set of coefficients. The main job then is to find an algorithm to vary the characteristics of the filter according to the specifications. But usually the order of this

kind of filters is so high that it is difficult to implement them.

The IIR filters, on the other hand, are more suitable to achieve this job. With lower order, and by adding one or more feedback paths as shown in Fig.1.1, it is easy to obtain variable characteristics. However, IIR filters can be unstable while changing any of the coefficients. So the main concern is to ensure the stability.

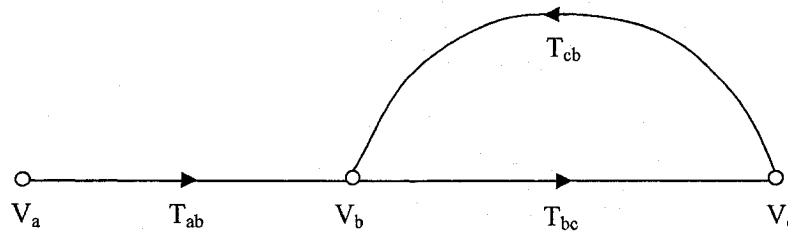


Fig.1.1 Signal-flow graph of a basic structure

The overall transfer function is:

$$T_{ac} = \frac{V_c}{V_a} = \frac{T_{ab}T_{bc}}{1 - T_{bc}T_{cb}} \quad (1.2)$$

Without lose of generality, consider $T_{ab} = 1$ in (1.2). In order to obtain variable characteristics, one of the transmittances needs to change. It is easy to make T_{cb} a variable quantity. When $T_{cb} = 0$, it is required that T_{bc} must be stable.

For 1-D systems, there exists an extensive literature about both analog and discrete filters with variable characteristics. The stability has already been investigated in these researches. But for 2-D system, the stability test procedure can be so complex that it is impractical to conduct the test every time when any coefficient is changed. So one can

obtain the ranges of one or more coefficients, which ensure the system to be stable.

In 2-D systems, the frequency response is a function of two independent variables. For 2-D discrete systems, one can focus on the plane with each dimension ranging from $-\pi$ to π . Although the magnitude frequency response of 1-D system is always symmetrical about the origin, the symmetry of 2-D magnitude response is more than this.

In this thesis, the main concern of variable characteristics is about magnitude and its symmetry, group delays will also be discussed in some cases.

1.2 Stability of 2-D IIR systems

In 1-D IIR systems (both analog and discrete), the transfer function is a relative function without any common factors between the numerator and the denominator. Mathematically,

$$H_a(s) = \frac{N_a(s)}{D_a(s)} \quad (1.3)$$

describes the transfer function in the analog domain with $N_a(s)$ and $D_a(s)$ to be relatively prime. In order that this system is stable, all the zeros of $D_a(s)$ must be strictly located in the left-half of the s-plane, namely, $D_a(s)$ must be a strict Hurwitz polynomial (SHP) [1].

Likewise, there is

$$H_d(z) = \frac{N_d(z)}{D_d(z)} \quad (1.4)$$

which is a transfer function in the discrete domain with $N_d(z)$ and $D_d(z)$ to be relatively prime. In order of this system to be stable, all the zeros of $D_d(z)$ must be strictly located

inside the unit circle, or $D_d(z)$ must be a Schur polynomial [2].

In 2-D analog systems, a popular method of discrete filter design is starting from an analog filter transfer function and then use the well-known generalized bilinear transformations [2]:

$$s_i = k_i \frac{z_i - b_i}{z_i + a_i} \quad i = 1, 2, \quad (1.5a)$$

the stability conditions being:

$$k_i > 0, \quad |a_i| \leq 1, \quad |b_i| \leq 1 \quad (1.5b)$$

Then the corresponding discrete filter transfer function can be obtained. So one can consider the stability of analog systems first. There is

$$H_a(s_1, s_2) = \frac{N_a(s_1, s_2)}{D_a(s_1, s_2)} \quad (1.6)$$

being the transfer function. According to [4], if both the even and the odd parts of the denominator polynomial become simultaneously zero at any specified set of points but not in their neighbourhood, it belongs to the non-essential singularity of the first kind.

And if both the numerator and denominator become zero simultaneously at any specified set of points, it is called non-essential singularity of the second kind (NSSK).

Specifically,

(a) if $D_a(s_{10}, s_{20}) = 0$ and $H_a(s_{10}, s_{20}) \neq 0$, it has non-essential singularity of the first kind at

(s_{10}, s_{20}) ;

(b) if $D_a(s_{10}, s_{20}) = 0$ and $H_a(s_{10}, s_{20}) = 0$, it has non-essential singularity of the second kind

at (s_{10}, s_{20}) ;

The definition of a 2-D polynomial to be an SHP is: if $1/D_a(s_1, s_2)$ does not have any singularity in the region $\{ (s_1, s_2) \mid \text{Re } s_1 \geq 0, \text{Re } s_2 \geq 0, |s_1| < \infty, |s_2| < \infty \}$, then $D_a(s_1, s_2)$ is an SHP.

So the polynomial of a denominator having occurrence of non-essential singularity of the first kind is not a SHP and hence the filter is not stable. However, even if a polynomial is an SHP, it may also have the occurrence of the non-essential singularity of the second kind. And the NSSK can also make a system unstable. Therefore, having to be an SHP as the denominator is only a necessary condition for a 2-D system to be stable.

Then the Very Strict Hurwitz Polynomials (VSHP), which does not have any of the two kinds of singularities, is defined [4]: if $1/D_a(s_1, s_2)$ does not have any singularity in the region $\{ (s_1, s_2) \mid \text{Re } s_1 \geq 0, \text{Re } s_2 \geq 0, |s_1| \leq \infty, |s_2| \leq \infty \}$, $D_a(s_1, s_2)$ is a VSHP.

From above, a VSHP must be an SHP first. So once a polynomial has been ensured to be an SHP, the remaining job is to inspect the absence of singularities at the combination points including infinity. To do this, one can substitute the original variable that tends to be infinity with their reciprocals. There are three possibilities to consider:

- (a) $s_1 \rightarrow \infty, s_2 = \text{finite}$, inspect $D_a(1/s_1, s_2)$;
- (b) $s_1 = \text{finite}, s_2 \rightarrow \infty$, inspect $D_a(s_1, 1/s_2)$;
- (c) $s_1 \rightarrow \infty, s_2 \rightarrow \infty$, inspect $D_a(1/s_1, 1/s_2)$;

According to the bilinear transformation, zero and ∞ in s-domain correspond to 1 and -1 in z-domain, which stand for the DC and the highest frequency components of a

discrete system. So the study of VSHP shows the importance in 2-D analog-to-digital filter design.

1.3 Some properties of VSHP [4]

Property I:

That $D_a(s_1, s_2)$ is a VSHP, is the necessary and sufficient condition for $H_a(s_1, s_2)$ to have no singularity in the closed right-half biplane $\{ (s_1, s_2) \mid \text{Re } s_1 \geq 0, \text{Re } s_2 \geq 0, |s_1| \leq \infty, |s_2| \leq \infty \}$.

Property II:

If $D(s_{10}, s_{20}) = D_1(s_1, s_2) \cdot D_2(s_1, s_2)$ is to be a VSHP, the necessary and sufficient conditions are that $D_1(s_1, s_2)$ and $D_2(s_1, s_2)$ are individually VSHPs.

Property III:

If $D_a(s_1, s_2)$ is a VSHP, $\frac{\partial D_a(s_1, s_2)}{\partial s_1}$ and $\frac{\partial D_a(s_1, s_2)}{\partial s_2}$ are also VSHPs.

Property IV:

Consider $D_a(s_1, s_2)$ to be a VSHP, then the polynomials $E_i(s_2)$ and $F_j(s_1)$ ($i=0, 1, \dots, p$ and $j=0, 1, \dots, q$) defined below are SHPs in s_2 and s_1 respectively, where:

$$D_a(s_1, s_2) = E_p(s_2)s_1^p + E_{p-1}(s_2)s_1^{p-1} + \dots + E_1(s_2)s_1 + E_0(s_2)$$

or
$$D_a(s_1, s_2) = F_q(s_1)s_2^q + F_{q-1}(s_1)s_2^{q-1} + \dots + F_1(s_1)s_2 + F_0(s_1)$$

$E_i(s_2)$ and $F_j(s_1)$ ($i=0,1,\dots,p$ and $j=0,1,\dots,q$) are the polynomial coefficients of the powers of s_1 and s_2 respectively.

Property V:

The functions $\frac{E_i(s_2)}{E_{i-1}(s_2)}$ and $\frac{F_j(s_1)}{F_{j-1}(s_1)}$ ($i=0,1,\dots,p$ and $j=0,1,\dots,q$) are minimum

reactive positive real functions defined below in s_2 and s_1 respectively.

Definition 1: A rational function $F(s) = \frac{P(s)}{Q(s)}$ with real coefficients is a positive real

function, if and only if

- (a) $P(s)+Q(s)$ is an SHP;
- (b) $Re F(s) \geq 0$, for $Re s \geq 0$.

Definition 2: $F(s)$ is a minimum reactive positive real function, if there is no pole or zero on the imaginary axis of s .

1.4 Methods of generation of VSHP

Based on the properties of VSHPs (which are omitted here) [4], there are different methods to generate this kind of polynomials, some of which are briefly reviewed below:

Method I

Consider $D_n = A \Psi A^t s_1 + B \Lambda B^t s_2 + R \Gamma R^t + G$

$$= A_1 S_1 + B_1 S_2 + R_1 + G$$

where A_1 , B_1 and R_1 are lower triangular matrices given by (1.7, 1.8, 1.9), and G is a skew-symmetric matrix given by (1.10) and they are:

$$A = \begin{bmatrix} a_{11} & 0 & \dots & \dots & 0 \\ a_{12} & a_{22} & 0 & \dots & 0 \\ \dots & \dots & \dots & \dots & \dots \\ \dots & \dots & \dots & \dots & \dots \\ a_{1n} & a_{2n} & \dots & \dots & a_{nn} \end{bmatrix} \quad (1.7)$$

$$B = \begin{bmatrix} b_{11} & 0 & \dots & \dots & 0 \\ b_{12} & b_{22} & 0 & \dots & 0 \\ \dots & \dots & \dots & \dots & \dots \\ \dots & \dots & \dots & \dots & \dots \\ b_{1n} & b_{2n} & \dots & \dots & b_{nn} \end{bmatrix} \quad (1.8)$$

$$R = \begin{bmatrix} r_{11} & 0 & \dots & \dots & 0 \\ r_{12} & r_{22} & 0 & \dots & 0 \\ \dots & \dots & \dots & \dots & \dots \\ \dots & \dots & \dots & \dots & \dots \\ r_{1n} & r_{2n} & \dots & \dots & r_{nn} \end{bmatrix} \quad (1.9)$$

$$G = \begin{bmatrix} 0 & g_{12} & g_{13} & \dots & g_{1n} \\ -g_{12} & 0 & g_{23} & \dots & g_{2n} \\ -g_{13} & -g_{23} & 0 & \dots & \dots \\ \dots & \dots & \dots & \dots & \dots \\ -g_{1n} & -g_{2n} & -g_{3n} & \dots & 0 \end{bmatrix} \quad (1.10)$$

and Ψ , Λ and Γ are diagonal matrices:

$$\Psi = \text{diag}[\psi_1 \quad \psi_2 \quad \dots \quad \psi_n] \quad (1.11)$$

$$\Lambda = \text{diag}[\lambda_1 \quad \lambda_2 \quad \dots \quad \lambda_n] \quad (1.12)$$

$$\Gamma = \text{diag}[\gamma_1 \quad \gamma_2 \quad \dots \quad \gamma_n] \quad (1.13)$$

If all the Ψ_i , λ_i and γ_i are positive, A_i , B_i and R_i are positive-definite matrices, and they are realizable in circuits. By making some of Ψ_i , λ_i and γ_i to zero and Γ to null matrix, determinant of D_n becomes either an even or an odd polynomial. VSHPs can be obtained by taking derivatives as shown in the example:

$$D_2 = \begin{bmatrix} 1 & 0 \\ a & 0 \end{bmatrix} \begin{bmatrix} \psi_1 & 0 \\ 0 & \psi_2 \end{bmatrix} \begin{bmatrix} 1 & a \\ 0 & 1 \end{bmatrix} s_1 + \begin{bmatrix} 1 & 0 \\ b & 0 \end{bmatrix} \begin{bmatrix} \lambda_1 & 0 \\ 0 & \lambda_2 \end{bmatrix} \begin{bmatrix} 1 & b \\ 0 & 1 \end{bmatrix} s_2 \\ + \begin{bmatrix} 1 & 0 \\ c & 0 \end{bmatrix} \begin{bmatrix} \gamma_1 & 0 \\ 0 & \gamma_2 \end{bmatrix} \begin{bmatrix} 1 & c \\ 0 & 1 \end{bmatrix} + \begin{bmatrix} 0 & g \\ -g & 0 \end{bmatrix}$$

By making Ψ_2 to zero, s_1^2 term will be zero. And if $\Psi_1=0$, parameter a will not be in the determinant. Likewise, λ_2 and λ_1 equals zero can cause that s_1^2 term will be zero and b does not show up in the determinant. The results in D_2 is:

$$\begin{bmatrix} \psi_1 s_1 + \lambda_1 s_2 + \gamma_1 & a\psi_1 s_1 + b\lambda_1 s_2 + c\gamma_1 + g \\ a\psi_1 s_1 + b\lambda_1 s_2 + c\gamma_1 - g & a^2\psi_1 s_1 + b^2\lambda_1 s_2 + c^2\gamma_1 + \gamma_2 \end{bmatrix}$$

Therefore the determinant of D_2 :

$$\det D_2 = \psi_1 \lambda_1 (a-b)^2 s_1 s_2 + \psi_1 [\gamma_1 (a-c)^2 + \gamma_2] s_1 + \lambda_1 [\gamma_1 (b-c)^2 + \gamma_2] s_2 + (\gamma_1 \gamma_2 + g^2)$$

is a VSHP if $a \neq b$, $\gamma_2 \neq 0$.

If $\gamma_1 = \gamma_2 = 0$, $a \neq b$, one can obtain an even polynomial:

$$M_a = \psi_1 \lambda_1 (a-b)^2 s_1 s_2 + g^2$$

Therefore a VSHP can be generated as:

$$M_a + k_1 \frac{\partial M_a}{\partial s_1} + k_2 \frac{\partial M_a}{\partial s_2} = \psi_1 \lambda_1 k_1 (a-b)^2 s_1 s_2 + k_2 \psi_1 \lambda_1 (a-b)^2 s_1 + k_1 \psi_1 \lambda_1 (a-b)^2 s_2 + g^2 \quad (1.14)$$

Method II

This method starts from the VSHP,

$$D(s_1, s_2) = a_{11}s_1s_2 + a_{10}s_1 + a_{01}s_2 + a_{00} \quad (1.15)$$

and one can get the reactance function [4],

$$G(s_1, s_2) = \frac{a_{11}s_1s_2 + a_{00}}{a_{10}s_1 + a_{01}s_2} \quad (1.16)$$

Then by choosing $b_{11} > 0$, $b_{10} > 0$, $b_{01} > 0$ and $b_{00} > 0$, one can use the transformation,

$$s_1 = \frac{b_{11}s_1s_2 + b_{00}}{b_{10}s_1 + b_{01}s_2} \quad (1.17)$$

and substitute variable s_1 in (1.16) to get a VSHP with s_1 of order one and s_2 of order two.

Likewise, by using following transformation with $c_{11} > 0$, $c_{10} > 0$, $c_{01} > 0$ and $c_{00} > 0$,

$$s_2 = \frac{c_{11}s_1s_2 + c_{00}}{c_{10}s_1 + c_{01}s_2} \quad (1.18)$$

a VSHP can be obtained with s_1 of order two and s_2 of order one.

For specific order of s_1 and s_2 , the procedures above can be repeated accordingly. The sum of the numerators and the denominators gives a VSHP.

Method III

For the 2-D systems with product-separable [5] denominators described as $D_{a1}(s_1)D_{a2}(s_2)$, the condition is that $D_{a1}(s_1)$ and $D_{a2}(s_2)$ are SHPs in s_1 and s_2 domains respectively. Instead of using method I, according to Schussler's theorem [6], one can generate Schur polynomials in discrete domains directly as following:

Let $D(z)$ be a real polynomial of degree n , described as

$$D(z) = \sum_{v=0}^n c_v z^v = c \prod_{v=1}^n (z - z_{\infty v}) = F_1(z) + F_2(z) \quad (1.19)$$

where $F_1(z)$ is a mirror-image polynomial defined as

$$F_1(z) = \sum_{v=0}^n d_v z^v \quad \text{with} \quad d_v = \frac{1}{2}(c_v + c_{n-v}) \quad (1.20)$$

and $F_2(z)$ is an anti-mirror-image polynomial defined as

$$F_2(z) = \sum_{v=0}^n g_v z^v \quad \text{with} \quad d_v = \frac{1}{2}(c_v - c_{n-v}) \quad (1.21)$$

The necessary and sufficient conditions for $D(z)$ to be a Schur polynomial are:

Condition 1: $\left| \frac{c_0}{c_n} \right| < 1;$

Condition 2: (a) For n even:

$$F_1(z) = k_e \prod_{i=1}^{n/2} (z^2 - 2\alpha_i z + 1) \quad (1.22)$$

$$F_2(z) = (z^2 - 1) \prod_{i=1}^{(n-2)/2} (z^2 - 2\beta_i z + 1) \quad (1.23)$$

with $1 > \alpha_1 > \beta_1 > \alpha_2 > \beta_2 > \dots > \beta_{\frac{n-2}{2}} > \alpha_{\frac{n}{2}} > -1$ (1.24)

(b) For n odd:

$$F_1(z) = k_o (z + 1) \prod_{i=1}^{(n-1)/2} (z^2 - 2\alpha_i z + 1) \quad (1.25)$$

$$F_2(z) = (z - 1) \prod_{i=1}^{(n-1)/2} (z^2 - 2\beta_i z + 1) \quad (1.26)$$

with $1 > \alpha_1 > \beta_1 > \alpha_2 > \beta_2 > \dots > \alpha_{\frac{n-1}{2}} > \beta_{\frac{n-1}{2}} > -1$ (1.27)

Working backward through the theorem one can construct stable 1-D filters for each dimension, and hence construct a stable separable 2-D discrete system.

1.5 Symmetry of 2-D systems

There are different kinds of symmetries of frequency response of 2-D discrete systems [7,15]. Not to name all the categories exhaustively, but only the important ones are introduced.

With two dimensional radium frequency variables ω_1 and ω_2 with ranges from $-\pi$ to π , one can construct a close square of plane. The symmetry is based on this plane and its coordinates.

1.5.1 Rotational symmetry

Let the origin be the rotation centre and the rotation angle is $\pi/2$ radians, it is a four-fold symmetry:

$$H_d(\omega_1, \omega_2) = H_d(-\omega_2, \omega_1) = H_d(-\omega_1, -\omega_2) = H_d(\omega_2, -\omega_1) \quad (1.28)$$

1.5.2 Centro-symmetry

If the rotation angle is π radians, it is a two-fold symmetry:

$$H_d(\omega_1, \omega_2) = H_d(-\omega_1, -\omega_2) \quad (1.29)$$

1.5.3 Reflection symmetry

Reflections about the ω_1 axis, ω_2 axis, or $\omega_1 = \omega_2$ line or $\omega_1 = -\omega_2$ line, the symmetry can be any of the following:

$$\begin{aligned} H_d(\omega_1, \omega_2) &= H_d(-\omega_1, \omega_2) \\ H_d(\omega_1, \omega_2) &= H_d(\omega_1, -\omega_2) \\ H_d(\omega_1, \omega_2) &= H_d(\omega_2, \omega_1) \end{aligned} \quad (1.30)$$

$$H_d(\omega_1, \omega_2) = H_d(-\omega_2, -\omega_1) \quad (1.31)$$

1.5.4 Quadrantal symmetry

If the symmetry is about the ω_1 and ω_2 axis simultaneously, there is:

$$H_d(\omega_1, \omega_2) = H_d(-\omega_1, \omega_2) = H_d(-\omega_1, -\omega_2) = H_d(\omega_1, -\omega_2)$$

1.5.5 Diagonal four-fold reflection symmetry

Likewise, if the symmetry is about $\omega_1 = \omega_2$ and $\omega_1 = -\omega_2$ line simultaneously, there is:

$$H_d(\omega_1, \omega_2) = H_d(\omega_2, \omega_1) = H_d(-\omega_2, -\omega_1) = H_d(-\omega_1, -\omega_2)$$

1.5.6 Octagonal symmetry

If both Quadrantal and Diagonal symmetry hold simultaneously, there is:

$$\begin{aligned} H_d(\omega_1, \omega_2) &= H_d(-\omega_1, \omega_2) = H_d(\omega_2, \omega_1) = H_d(-\omega_2, -\omega_1) \\ &= H_d(-\omega_1, -\omega_2) = H_d(\omega_1, -\omega_2) \end{aligned}$$

1.5.7 Circular symmetry

$$H_d(\omega_1, \omega_2) = \begin{cases} a_1 & (\omega_1^2 + \omega_2^2 = r_1) \\ \vdots & \vdots \\ a_n & (\omega_1^2 + \omega_2^2 = r_n) \end{cases} \quad (1.32)$$

The relationship between the symmetry and the 2-D filter will be discussed in Chapter 3.

1.6 Separable and non-separable 2-D transfer functions

For both analog and discrete transfer functions of 2-D systems, they can be classified

into two groups: product-separable and non-product-separable. If the transfer functions

are like
$$H_a(s_1, s_2) = \frac{N_{a1}(s_1)}{D_{a1}(s_1)} \cdot \frac{N_{a2}(s_2)}{D_{a2}(s_2)} \quad (1.33)$$

$$H_d(z_1, z_2) = \frac{N_{d1}(z_1)}{D_{d1}(z_1)} \cdot \frac{N_{d2}(z_2)}{D_{d2}(z_2)} \quad (1.34)$$

they can be studied as two cascade independent 1-D systems working in different dimensions. For this case, the stability problem can be simplified to the stability of both of the 1-D systems. So once both of their denominators are SHPs in s-domain or Schur polynomials in z-domain, the whole system will be stable.

For discrete separable transfer functions, since each 1-D system has the frequency response symmetry about the vertical axis, the 2-D response symmetry will be about both horizontal and vertical axes.

The 2-D transfer functions that can not be written like (1.33) or (1.34), are non-product-separable. For this case, one must consider conditions of VSHP in analog domain.

1.7 Scope of this thesis

In this thesis, a 2-D product-separable discrete system design with variable characteristics is discussed. The stability with ranges of one or more coefficients of the system is to be discussed.

In Chapter 1, the background knowledge of 2-D IIR filtering has been introduced, especially, the original stability theorem about VSHP from analog domain. Also the 2-D

symmetries in frequency domain as well as product-separable and non-product-separable 2-D transfer functions are introduced.

The 2-D digital filter VCTR structure is described in Chapter 2. Since this structure's stability analysis can be decomposed into 1-D systems, Schussler's theorem, which is also a special case of VSHP corresponding to analog domain, is introduced and mathematically expressed in this chapter. Then analysis with typical numerators and general denominators up to 2nd order is discussed.

Chapter 3 extends the analysis from 1-D to 2-D by combining different typical filters such as Biquadratic filters with variable but stable value of feedback gain. Low order filters and different situations are simulated. The variable response are observed and studied in detail.

Further analysis for higher order is in Chapter 4. An algorithm is proposed and simulated for arbitrary order of filters. 2-D responses of higher order filters including FIR filters with feedbacks are observed and studied.

In Chapter 5, responses of composed 2-D filters with component filters with variable characteristics are briefly discussed. Some of the stable 2-D IIR filters are applied in image processing. The stability and variable effect are further confirmed with practical applications.

The conclusions and future works are discussed in Chapter 6.

CHAPTER 2 Product-separable 2-D Transfer Functions

2.1 Introduction

Since product-separable 2-D transfer functions are concluded with (1.33) and (1.34), it can be shown in Fig.2.1:

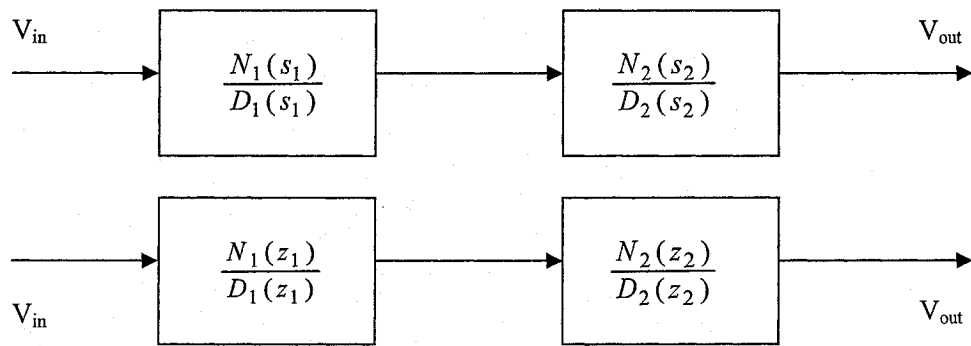


Fig.2.1 2-D product-separable system

For the analog transfer functions, the stability discussion about VSHP can be simplified into 1-D stability with SHPs. And also the design of 2-D variable characteristics can be simplified to two 1-D variable characteristics. In order to design 1-D analog variable transfer functions (VCTF) [5], a most often used method is to add a variable feedback to the IIR filter (shown in Fig.2.2). By adjusting the gain of the feedback, variable characteristics can be obtained.

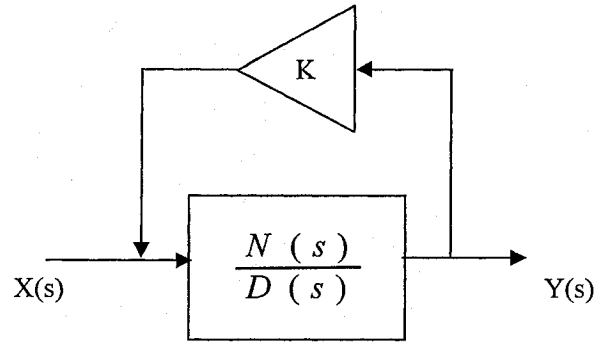


Fig.2.2 1-D analog IIR filter with variable feedback

The transfer function of the system is,

$$H(s) = \frac{N(s)}{D(s) - kN(s)} \quad (2.1)$$

with $D(s) - kN(s)$ being an SHP to make it stable.

However, by using the bilinear transformation to obtain the corresponding product-separable discrete systems, the k parameter will be dispersed into coefficients of different order of z^{-1} . This can cause difficulties of VCTF design for discrete filters [5].

So a 2-D discrete product-separable IIR VCTF will be discussed. And the stability will be ensured based on Schussler's theorem as a special case of VSHP by using method III [4].

2.2 The structure considered

A 2-D discrete VCTF can be designed directly in z -domain as shown in Fig.2.3. This is a product-separable system with a variable feedback gain attached to each 1-D filter. Likewise, by adjusting the feedback gain, variable characteristics of the system can be obtained. In order to make the system stable, the analysis is to obtain the constraint of

the variable gain k in terms of other coefficients of the filter.

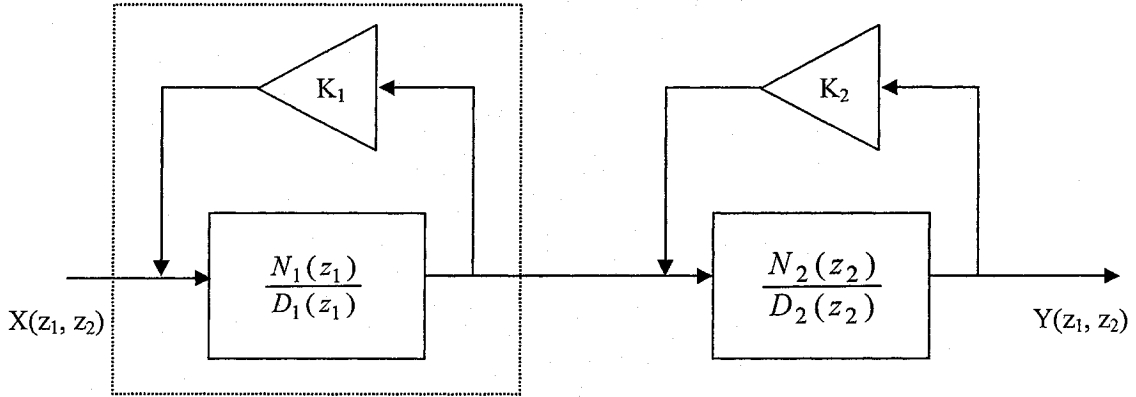


Fig.2.3 2-D IIR VCTR system to be analyzed

According to method III in 1.4, the condition of VSHP for this case is equivalent to Schussler's theorem in both 1-D discrete systems.

2.3 Schussler's Theorem for 1-D systems

The basic necessary and sufficient conditions for a 1-D IIR discrete system to be stable is that all the poles are located within the unit circle in z -domain.

Let $D(z)$ be a real polynomial of degree n , described as

$$D(z) = \sum_{v=0}^n c_v z^v = c \prod_{v=1}^n (z - z_{\infty v}) \quad (2.5)$$

and

$$D(z) = F_1(z) + F_2(z) \quad (2.6)$$

where $F_1(z)$ is a mirror-image polynomial defined as

$$F_1(z) = \sum_{v=0}^n d_v z^v \quad \text{with} \quad d_v = \frac{1}{2}(c_v + c_{n-v}) \quad (2.7)$$

and $F_2(z)$ is an anti-mirror-image polynomial defined as

$$F_2(z) = \sum_{v=0}^n g_v z^v \quad \text{with} \quad d_v = \frac{1}{2}(c_v - c_{n-v}) \quad (2.8)$$

For $D(z)$ to be a stable polynomial, characterized by $|z_{\infty v}| < 1 \quad \forall \quad v$, it is necessary and sufficient that:

Condition 1a: The zeros of $F_1(z)$ and $F_2(z)$ are located on the unit circle;

Condition 1b: They are simple;

Condition 1c: They separate each other.

These conditions are equivalent to the following of the function $F_1(z) / F_2(z)$ [or $F_2(z) / F_1(z)$]:

Condition 2a: The poles and zeros of $F_1(z) / F_2(z)$ are located on the unit circle, they are simple.

Condition 2b: If a pole of $F_1(z) / F_2(z)$ [or $F_2(z) / F_1(z)$] is located at $e^{j\psi_v}$, the angle of the residue of $F_1(z) / F_2(z)$ [or $F_2(z) / F_1(z)$] is ψ_v .

Condition 2c: The slope of the imaginary part of $F_1(z) / F_2(z)$ [or $F_2(z) / F_1(z)$] on the unit circle $e^{j\Omega}$ in dependence of Ω is always positive.

The theorem is equivalent to the well-known properties of a Hurwitz polynomial [4]. $F_1(z) / F_2(z)$ correspond to the even and odd part of a Hurwitz polynomial, respectively; $F_1(z) / F_2(z)$ is the discrete counterpart of a reactance function in the continuous domain. In [6] it has been mentioned, if and only if the zeros of $\text{Re}\{D(e^{j\Omega})\}$ and of $\text{Im}\{D(e^{j\Omega})\}$ separate each other, the system will be stable. Fig.2.4 demonstrates possible locations of poles and zeros of $F_1(z) / F_2(z)$.

It is possible to prove the theorem by transforming the mentioned properties of a Hurwitz polynomial into the z-domain using the bilinear transformation. The proof can also be found exclusively in the z-domain.

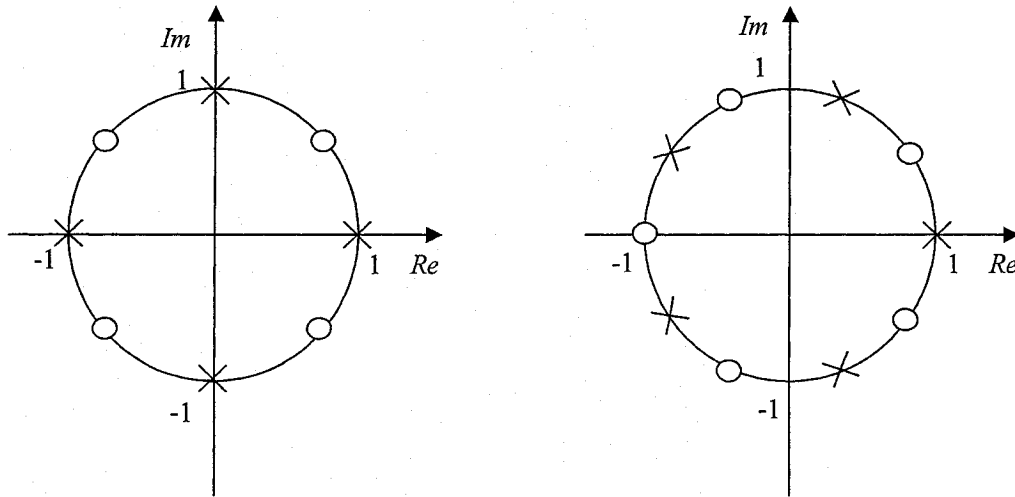


Fig.2.4 Poles and zeros of F_1/F_2 , if $D(z) = z^n$ and $n = 4$ or $n = 5$

2.4 Stability conditions of 1-D systems

According to Schussler's theorem, a further more mathematical expression can be derived as following [8]:

Condition 1: $\left| \frac{c_0}{c_n} \right| < 1$;

Condition 2: (a) For n even:

$$F_1(z) = k_e \prod_{i=1}^{n/2} (z^2 - 2\alpha_i z + 1) \quad (2.9)$$

$$F_2(z) = (z^2 - 1) \prod_{i=1}^{(n-2)/2} (z^2 - 2\beta_i z + 1) \quad (2.10)$$

with $1 > \alpha_1 > \beta_1 > \alpha_2 > \beta_2 > \dots > \beta_{\frac{n-2}{2}} > \alpha_{\frac{n}{2}} > -1$ (2.11)

(b) For n odd:

$$F_1(z) = k_o(z+1) \prod_{i=1}^{(n-1)/2} (z^2 - 2\alpha_i z + 1) \quad (2.12)$$

$$F_2(z) = (z-1) \prod_{i=1}^{(n-1)/2} (z^2 - 2\beta_i z + 1) \quad (2.13)$$

with $1 > \alpha_1 > \beta_1 > \alpha_2 > \beta_2 > \dots > \alpha_{\frac{n-1}{2}} > \beta_{\frac{n-1}{2}} > -1$ (2.14)

Since each pair of complex conjugate zeros on the unit circle can be described as a factor of $(z^2 - 2\phi z + 1)$ with ϕ to be the common real part of the them. This can be shown in

Fig.2.5:

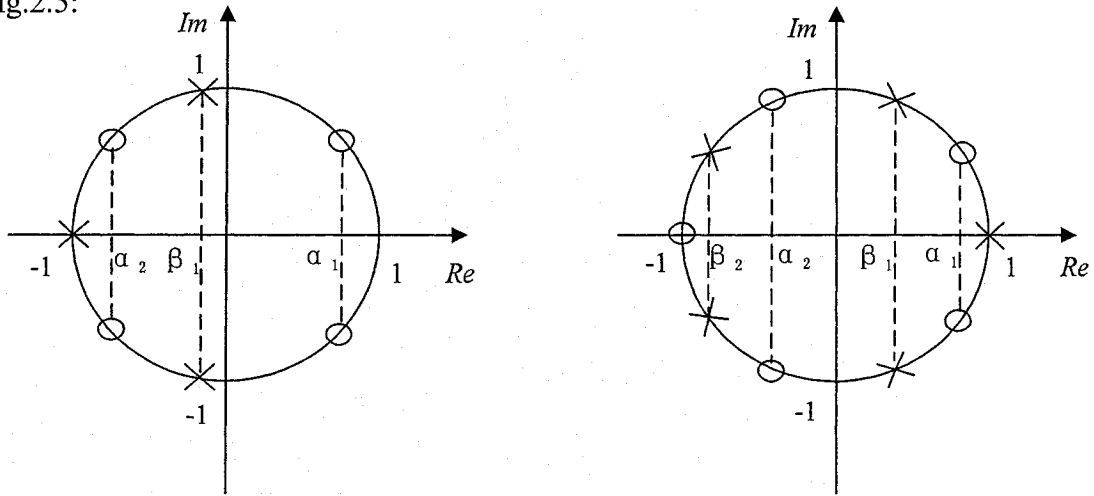


Fig.2.5 Poles and zeros of F_1/F_2 , if $D(z) = z^n$ and $n = 4$ or $n = 5$, their real parts separate each other on the real axis between -1 and 1

Therefore, the parameters of α_n and β_n , which correspond to the real part of those zeros and poles, can be extracted with the coefficients of the polynomial and the stability conditions can be directly applied on those coefficients.

2.5 Stability conditions of 1-D for different numerators

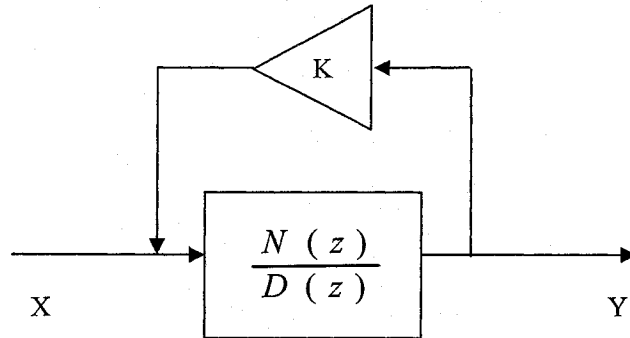


Fig.2.6 1-D discrete system

For each 1-D block as Fig.2.6, similar with (2.1) the transform function of the whole block is:

$$H(z) = \frac{N(z)}{D(z) - kN(z)} = \frac{N(z)}{D_d(z)} \quad (2.15)$$

In order this system to be stable, the denominator of $H(z)$ must satisfy the stable conditions. Consider different numerators $N(z)$ and general forms of $D(z)$ s, one can get the following conditions for the coefficients. The first and second order systems are considered only, because higher order systems can be cascaded using such blocks.

2.5.1 Typical forms with order up to 2

I Low-pass filter (order of 1)

Assume:
$$\begin{cases} N(z) = z + 1 \\ D(z) = a_1 z + a_0 \end{cases}$$

Therefore:
$$H(z) = \frac{N(z)}{D(z) - kN(z)} = \frac{z + 1}{(a_1 - k)z + (a_0 - k)} \quad (2.16c)$$

$$D_d(z) = (a_1 - k)z + (a_0 - k) \quad (2.16d)$$

According to Schussler's Theorem, there is:

$$D_d(z) = F_1(z) + F_2(z) \quad (2.16e)$$

Which

$$\begin{cases} F_1(z) = \frac{1}{2}(a_1 + a_0 - 2k)(z + 1) \\ F_2(z) = \frac{1}{2}(a_1 - a_0)(z - 1) \end{cases} \quad (2.16f)$$

$$(2.16g)$$

There is no parameter of α and β , but zero points of +1 and -1 are already separated with each other on the unit circle. So the only stability condition is:

$$\left| \frac{a_0 - k}{a_1 - k} \right| < 1 \quad (2.16h)$$

II Low-pass filter (order of 2)

Assume:

$$\begin{cases} N(z) = (z + 1)^2 = z^2 + 2z + 1 \\ D(z) = a_2 z^2 + a_1 z + a_0 \end{cases} \quad (2.17a)$$

$$(2.17b)$$

Therefore:

$$D_d(z) = (a_2 - k)z^2 + (a_1 - 2k)z + (a_0 - k) \quad (2.17c)$$

And

$$\begin{cases} F_1(z) = \frac{1}{2}(a_2 + a_0 - 2k) \left[z^2 + \frac{2(a_1 - 2k)}{(a_2 + a_0 - 2k)} z + 1 \right] \\ F_2(z) = \frac{1}{2}(a_2 - a_0)(z^2 - 1) \end{cases} \quad (2.17d)$$

$$(2.17e)$$

Therefore,

$$\alpha_1 = \frac{2k - a_1}{a_2 + a_0 - 2k} \quad (2.17f)$$

There is no β , but zeros of $F_2(z)$ are +1 and -1. So the stability conditions are:

$$\left| \frac{a_0 - k}{a_2 - k} \right| < 1 \quad (2.17g)$$

$$\left| \frac{a_1 - 2k}{a_2 + a_0 - 2k} \right| < 1 \quad (2.17h)$$

III High-pass filter (order of 1)

$$\text{Assume: } \begin{cases} N(z) = z - 1 & (2.18a) \\ D(z) = a_1 z + a_0 & (2.18b) \end{cases}$$

$$\text{Therefore: } D_d(z) = (a_1 - k)z + (a_0 + k) \quad (2.18c)$$

$$\text{Then } \begin{cases} F_1(z) = \frac{1}{2}(a_1 + a_0)(z + 1) & (2.18d) \\ F_2(z) = \frac{1}{2}(a_1 - a_0 - 2k)(z - 1) & (2.18e) \end{cases}$$

$$\text{The condition is: } \left| \frac{a_0 + k}{a_1 - k} \right| < 1 \quad (2.18f)$$

IV High-pass filter (order of 2)

$$\text{Assume: } \begin{cases} N(z) = (z - 1)^2 = z^2 - 2z + 1 & (2.19a) \\ D(z) = a_2 z^2 + a_1 z + a_0 & (2.19b) \end{cases}$$

$$\text{Therefore: } D_d(z) = (a_2 - k)z^2 + (a_1 + 2k)z + (a_0 - k) \quad (2.19c)$$

$$\text{And: } \begin{cases} F_1(z) = \frac{1}{2}(a_2 + a_0 - 2k) \left[z^2 + \frac{2(a_1 + 2k)}{(a_2 + a_0 - 2k)} z + 1 \right] & (2.19d) \\ F_2(z) = \frac{1}{2}(a_2 - a_0)(z^2 - 1) & (2.19e) \end{cases}$$

$$\text{Therefore, } \alpha_1 = \frac{-a_1 - 2k}{a_2 + a_0 - 2k} \quad (2.19f)$$

$$\text{Conditions are: } \left| \frac{a_0 - k}{a_2 - k} \right| < 1 \quad (2.19g)$$

$$\left| \frac{a_1 + 2k}{a_2 + a_0 - 2k} \right| < 1 \quad (2.19h)$$

V Band-pass filter (order of 2)

$$\text{Assume: } \begin{cases} N(z) = (z+1)(z-1) = z^2 - 1 & (2.20a) \\ D(z) = a_2 z^2 + a_1 z + a_0 & (2.20b) \end{cases}$$

$$\text{Therefore: } D_d(z) = (a_2 - k)z^2 + a_1 z + (a_0 + k) \quad (2.20c)$$

$$\text{And: } \begin{cases} F_1(z) = \frac{1}{2}(a_2 + a_0) \left(z^2 + \frac{2a_1}{a_2 + a_0} z + 1 \right) & (2.20d) \\ F_2(z) = \frac{1}{2}(a_2 - a_0 - 2k)(z^2 - 1) & (2.20e) \end{cases}$$

$$\text{Therefore, } \alpha_1 = \frac{-a_1}{a_2 + a_0} \quad (2.20f)$$

$$\text{Conditions are: } \begin{cases} \left| \frac{a_0 + k}{a_2 - k} \right| < 1 & (2.20g) \\ \left| \frac{a_1}{a_2 + a_0} \right| < 1 & (2.20h) \end{cases}$$

VI Band-elimination filter (order of 2)

$$\text{Assume: } \begin{cases} N(z) = (z+j)(z-j) = z^2 + 1 & (2.21a) \\ D(z) = a_2 z^2 + a_1 z + a_0 & (2.21b) \end{cases}$$

$$\text{Therefore: } D_d(z) = (a_2 - k)z^2 + a_1 z + (a_0 - k) \quad (2.21c)$$

$$\text{And: } \begin{cases} F_1(z) = \frac{1}{2}(a_2 + a_0 - 2k) \left(z^2 + \frac{2a_1}{a_2 + a_0 - 2k} z + 1 \right) & (2.21d) \\ F_2(z) = \frac{1}{2}(a_2 - a_0)(z^2 - 1) & (2.21e) \end{cases}$$

$$\text{Therefore, } \alpha_1 = \frac{-a_1}{a_2 + a_0 - 2k} \quad (2.21f)$$

$$\text{Conditions are: } \begin{cases} \left| \frac{a_0 - k}{a_2 - k} \right| < 1 & (2.21g) \\ \left| \frac{a_1}{a_2 + a_0 - 2k} \right| < 1 & (2.21h) \end{cases}$$

2.5.2 The Generic Biquadratic Transfer Functions

The Active Switched Capacitor filter's transfer functions are biquadratic in z-domain [9], which are widely used in application of Integrated Circuit design:

$$H(z) = \frac{N(z)}{D(z)} = \frac{\nu + \varepsilon z^{-1} + \delta z^{-2}}{1 + \alpha z^{-1} + \beta z^{-2}} \quad (2.22)$$

The numerators of generic biquadratic transfer functions are listed in Table.3.1. These are the same used in active switched capacitor filters. The LP and BP functions are particularly interesting in that there are several different forms which can be used, the notch filter and all-pass filter are not included here. These forms are referred to in Table.2.1 as LP_{ij} and BP_{ij}, where *i* denotes the number of 1+z⁻¹ factors and *j* the number of z⁻¹ factors.

Table 2.1 Generic Biquadratic transfer functions

Generic Form	Numerator N(z)
LP 20	$K(1 + z^{-1})^2$
LP 11	$K z^{-1} (1 + z^{-1})$
LP 10	$K(1 + z^{-1})$
LP 02	$K z^{-2}$
LP 01	$K z^{-1}$
LP 00	K
BP 10	$K(1 + z^{-1})(1 - z^{-1})$
BP 01	$K z^{-1} (1 - z^{-1})$

BP 00	$K(1 - z^{-1})$
HP 20	$K(1 - z^{-1})^2$

Note: LP20, LP10, BP10, BP00 and HP have been analyzed equivalently in the 2.5.1.

I LP11

Assume:
$$\begin{cases} N(z) = z^{-1}(z^{-1} + 1) \\ D(z) = a_2 + a_1z^{-1} + a_0z^{-2} \end{cases}$$

equivalent to:
$$\begin{cases} N(z) = z + 1 & (2.23a) \\ D(z) = a_2z^2 + a_1z + a_0 & (2.23b) \end{cases}$$

Therefore:
$$D_d(z) = a_2z^2 + (a_1 - k)z + (a_0 - k) \quad (2.23c)$$

Then:
$$\begin{cases} F_1(z) = \frac{1}{2}(a_2 + a_0 - k)(z^2 + \frac{2a_1 - 2k}{a_2 + a_0 - k}z + 1) & (2.23d) \end{cases}$$

$$F_2(z) = \frac{1}{2}(a_2 - a_0 + k)(z^2 - 1) \quad (2.23e)$$

Therefore:
$$\alpha_1 = \frac{k - a_1}{a_2 + a_0 - k} \quad (2.23f)$$

Conditions are:
$$\left| \frac{a_0 - k}{a_2} \right| < 1 \quad (2.23g)$$

$$\left| \frac{a_1 - k}{a_2 + a_0 - k} \right| < 1 \quad (2.23h)$$

II LP02

Assume:
$$\begin{cases} N(z) = z^{-2} \\ D(z) = a_2 + a_1z^{-1} + a_0z^{-2} \end{cases}$$

equivalent to:
$$\begin{cases} N(z) = 1 & (2.24a) \\ D(z) = a_2z^2 + a_1z + a_0 & (2.24b) \end{cases}$$

Therefore: $D_d(z) = a_2 z^2 + a_1 z + a_0$ (2.24c)

Then:
$$\begin{cases} F_1(z) = \frac{1}{2}(a_2 + a_0 - k)(z^2 + \frac{2a_1}{a_2 + a_0 - k}z + 1) \end{cases}$$
 (2.24d)

$$\begin{cases} F_2(z) = \frac{1}{2}(a_2 - a_0 + k)(z^2 - 1) \end{cases}$$
 (2.24e)

Therefore: $\alpha_1 = \frac{-a_1}{a_2 + a_0 - k}$ (2.24f)

Conditions are: $\left| \frac{a_0 - k}{a_2} \right| < 1$ (2.24g)

$\left| \frac{a_1}{a_2 + a_0 - k} \right| < 1$ (2.24h)

III LP01 (order of 1)

Assume:
$$\begin{cases} N(z) = z^{-1} \\ D(z) = a_1 + a_0 z^{-1} \end{cases}$$

equivalent to:
$$\begin{cases} N(z) = 1 \\ D(z) = a_1 z + a_0 \end{cases}$$
 (2.25a)

(2.25b)

Therefore: $D_d(z) = a_1 z + a_0 - k$ (2.25c)

Then:
$$\begin{cases} F_1(z) = \frac{1}{2}(a_1 + a_0 - k)(z + 1) \end{cases}$$
 (2.25d)

$$\begin{cases} F_2(z) = \frac{1}{2}(a_1 - a_0 + k)(z - 1) \end{cases}$$
 (2.25e)

The condition is: $\left| \frac{a_0 - k}{a_1} \right| < 1$ (2.25f)

IV LP01 (order of 2)

Assume:
$$\begin{cases} N(z) = z^{-1} \\ D(z) = a_2 + a_1 z^{-1} + a_0 z^{-2} \end{cases}$$

$$\text{equivalent to: } \begin{cases} N(z) = z & (2.26a) \\ D(z) = a_2 z^2 + a_1 z + a_0 & (2.26b) \end{cases}$$

$$\text{Therefore: } D_d(z) = a_2 z^2 + (a_1 - k)z + a_0 \quad (2.26c)$$

$$\text{Then: } \begin{cases} F_1(z) = \frac{1}{2}(a_2 + a_0)[z^2 + \frac{2(a_1 - k)}{a_2 + a_0}z + 1] & (2.26d) \end{cases}$$

$$\begin{cases} F_2(z) = \frac{1}{2}(a_2 - a_0)(z^2 - 1) & (2.26e) \end{cases}$$

$$\text{Therefore: } \alpha_1 = \frac{k - a_1}{a_2 + a_0} \quad (2.26f)$$

$$\text{Conditions are: } \begin{cases} \left| \frac{a_0}{a_2} \right| < 1 & (2.26g) \end{cases}$$

$$\begin{cases} \left| \frac{a_1 - k}{a_2 + a_0} \right| < 1 & (2.26h) \end{cases}$$

V LP00 (originally order of 1 for D(z))

$$\text{Assume: } \begin{cases} N(z) = 1 \\ D(z) = a_1 + a_0 z^{-1} \end{cases}$$

$$\text{equivalent to: } \begin{cases} N(z) = z & (2.27a) \\ D(z) = a_1 z + a_0 & (2.27b) \end{cases}$$

$$\text{Therefore: } D_d(z) = (a_1 - k)z + a_0 \quad (2.27c)$$

$$\text{Then: } \begin{cases} F_1(z) = \frac{1}{2}(a_1 + a_0 - k)(z + 1) & (2.27d) \end{cases}$$

$$\begin{cases} F_2(z) = \frac{1}{2}(a_1 - a_0 - k)(z - 1) & (2.27e) \end{cases}$$

$$\text{The condition is: } \left| \frac{a_0}{a_1 - k} \right| < 1 \quad (2.27f)$$

VI LP00 (originally order of 2 for D(z))

Assume:
$$\begin{cases} N(z) = 1 \\ D(z) = a_2 + a_1 z^{-1} + a_0 z^{-2} \end{cases}$$

equivalent to:
$$\begin{cases} N(z) = z^2 & (2.28a) \\ D(z) = a_2 z^2 + a_1 z + a_0 & (2.28b) \end{cases}$$

Therefore:
$$D_d(z) = (a_2 - k)z^2 + a_1 z + a_0 \quad (2.28c)$$

Then:
$$\begin{cases} F_1(z) = \frac{1}{2}(a_2 + a_0 - k)(z^2 + \frac{2a_1}{a_2 + a_0 - k}z + 1) & (2.28d) \end{cases}$$

$$\begin{cases} F_2(z) = \frac{1}{2}(a_2 - a_0 - k)(z^2 - 1) & (2.28e) \end{cases}$$

Therefore:
$$\alpha_1 = \frac{-a_1}{a_2 + a_0 - k} \quad (2.28f)$$

Conditions are:
$$\left| \frac{a_0}{a_2 - k} \right| < 1 \quad (2.28g)$$

$$\left| \frac{a_1}{a_2 + a_0 - k} \right| < 1 \quad (2.28h)$$

VII BP01

Assume:
$$\begin{cases} N(z) = z^{-1}(z^{-1} - 1) \\ D(z) = a_2 + a_1 z^{-1} + a_0 z^{-2} \end{cases}$$

equivalent to:
$$\begin{cases} N(z) = z - 1 & (2.29a) \\ D(z) = a_2 z^2 + a_1 z + a_0 & (2.29b) \end{cases}$$

Therefore:
$$D_d(z) = a_2 z^2 + (a_1 - k)z + (a_0 + k) \quad (2.29c)$$

Then:
$$\begin{cases} F_1(z) = \frac{1}{2}(a_2 + a_0 + k)(z^2 + \frac{2a_1 - 2k}{a_2 + a_0 - k}z + 1) & (2.29d) \end{cases}$$

$$\begin{cases} F_2(z) = \frac{1}{2}(a_2 - a_0 - k)(z^2 - 1) & (2.29e) \end{cases}$$

Therefore:
$$\alpha_1 = \frac{k - a_1}{a_2 + a_0 + k} \quad (2.29f)$$

Conditions are:
$$\left\{ \begin{array}{l} \left| \frac{a_0 + k}{a_2} \right| < 1 \\ \left| \frac{a_1 - k}{a_2 + a_0 + k} \right| < 1 \end{array} \right. \quad (2.29g)$$

$$\left\{ \begin{array}{l} \left| \frac{a_1 - k}{a_2 + a_0 + k} \right| < 1 \end{array} \right. \quad (2.29h)$$

2.6 Summary and discussions

In this chapter, first the product-separable 2-D transfer function has been discussed. Then the discrete structure considered in this thesis is given. To conduct the product-separate 1-D stability analysis, the well-known Schussler's theorem is introduced. Since the situation is equivalent to VSHP analysis of method III [4], the mathematic stability conditions of 1-D system are given. Lastly different numerators were considered with general denominators to find their constraints.

All the analysis result above are summarized in Table.2.2:

Table 2.2: Summary of analysis of different filters

Class	Name of filters	N(z)	D(z)	Constraint of k
Typical forms of transfer functions (Same order for both N(z) and D(z))	LP (order of 1)	$z+1$	$a_1z + a_0$	$\left \frac{a_0 - k}{a_1 - k} \right < 1$
	LP (order of 2) "LP20"	$z^2 + 2z + 1$	$a_2z^2 + a_1z + a_0$	$\left\{ \begin{array}{l} \left \frac{a_0 - k}{a_2 - k} \right < 1 \\ \left \frac{a_1 - 2k}{a_2 + a_0 - 2k} \right < 1 \end{array} \right.$
	HP (order of 1)	$z-1$	$a_1z + a_0$	$\left \frac{a_0 + k}{a_1 - k} \right < 1$

	HP (order of 2) "HP"	$z^2 - 2z + 1$	$a_2 z^2 + a_1 z + a_0$	$\left\{ \begin{array}{l} \left \frac{a_0 - k}{a_2 - k} \right < 1 \\ \left \frac{a_1 + 2k}{a_2 + a_0 - 2k} \right < 1 \end{array} \right.$
	BP (order of 2) "BP10"	$z^2 - 1$	$a_2 z^2 + a_1 z + a_0$	$\left\{ \begin{array}{l} \left \frac{a_0 + k}{a_2 - k} \right < 1 \\ \left \frac{a_1}{a_2 + a_0} \right < 1 \end{array} \right.$
	BE (order of 2)	$z^2 + 1$	$a_2 z^2 + a_1 z + a_0$	$\left\{ \begin{array}{l} \left \frac{a_0 - k}{a_2 - k} \right < 1 \\ \left \frac{a_1}{a_2 + a_0 - 2k} \right < 1 \end{array} \right.$
Generic Biquadratic transfer functions	LP00 (1)	1	$a_1 + a_0 z^{-1}$	$\left \frac{a_0}{a_1 - k} \right < 1$
	LP00 (2)	1	$a_2 + a_1 z^{-1} + a_0 z^{-2}$	$\left\{ \begin{array}{l} \left \frac{a_0}{a_2 - k} \right < 1 \\ \left \frac{a_1}{a_2 + a_0 - k} \right < 1 \end{array} \right.$
	LP01 (1)	z^{-1}	$a_1 + a_0 z^{-1}$	$\left \frac{a_0 - k}{a_1} \right < 1$
	LP01 (2)	z^{-1}	$a_2 + a_1 z^{-1} + a_0 z^{-2}$	$\left\{ \begin{array}{l} \left \frac{a_0}{a_2} \right < 1 \\ \left \frac{a_1 - k}{a_2 + a_0} \right < 1 \end{array} \right.$
	LP11	$z^{-1}(z^{-1} + 1)$	$a_2 + a_1 z^{-1} + a_0 z^{-2}$	$\left\{ \begin{array}{l} \left \frac{a_0 - k}{a_2} \right < 1 \\ \left \frac{a_1 - k}{a_2 + a_0 - k} \right < 1 \end{array} \right.$
	LP02	z^{-2}	$a_2 + a_1 z^{-1} + a_0 z^{-2}$	$\left\{ \begin{array}{l} \left \frac{a_0 - k}{a_2} \right < 1 \\ \left \frac{a_1}{a_2 + a_0 - k} \right < 1 \end{array} \right.$

	BP01	$z^{-1}(z^{-1} - 1)$	$a_2 + a_1z^{-1} + a_0z^{-2}$	$\begin{cases} \left \frac{a_0 + k}{a_2} \right < 1 \\ \left \frac{a_1 - k}{a_2 + a_0 + k} \right < 1 \end{cases}$
--	------	----------------------	-------------------------------	--

From above, by using the stable conditions of the 1-D discrete system, the constraints of k are related with all of the coefficients of the filter. So for any given filter with a certain set of coefficients, k must be bound within a certain range to make the system stable. And the adjustment of k to obtain variable characteristics can be safely done within these ranges.

For the whole product-separable 2-D system, the two 1-D filters and their feedback gains are not necessary to be the same. According to the 2-D system specification, they can be chosen differently and their corresponding stable ranges can be obtained differently. By adjusting both of them, one can obtain 2-D variable characteristics.

CHAPTER 3 Response of low-order filters

3.1 Introductions

Having established the range of k to ensure overall stability of a filter, now the effect of k with the resulting magnitude response needs to be studied. Both 1-D and 2-D frequency responses of low-order filters with variable characteristics are illustrated and studied. 1-D responses with various and stable k values show variable magnitude contours while 2-D responses give us variable 2-D characteristics and symmetries.

3.2 1-D Response with stable range of k

Considering all-pole Butterworth filters' denominators of 2nd order, there is

$$D(z) = (2 + \sqrt{2})z^2 + 2 - \sqrt{2} \quad (3.1)$$

For denominators of order 2, substitute the Generic Biquadratic transfer functions in

Table 2.2, examples of results are listed in Table 3.1:

Table 3.1 Stable conditions of k for Generic Biquadratic Butterworth filters

Name of filters	$N(z)$	$D(z)$	Constraint of k
LP00 (2)	1	$a_2 + a_1z^{-1} + a_0z^{-2}$	$k < 2\sqrt{2}$ or $k > 4$
LP01 (2)	z^{-1}	$\begin{cases} a_0 = 2 - \sqrt{2} \\ a_1 = 0 \\ a_2 = 2 + \sqrt{2} \end{cases}$	$-4 < k < 4$
LP11	$z^{-1}(z^{-1} + 1)$		$-2\sqrt{2} < k < 2$

LP02	z^{-2}		$-2\sqrt{2} < k < 4$
LP20	$(z^{-1} + 1)^2$		$k < 1$
HP	$(z^{-1} - 1)^2$		$k < \frac{1}{2}$
BP01	$z^{-1}(z^{-1} - 1)$		$-2\sqrt{2} < k < 2$
BP10	$z^{-2} - 1$		$-2 < k < 2\sqrt{2}$

Since the stability theorem has been proven, the main concern in this simulation is not to verify the result but to show the general effect of the analysis. Of course the simulation result must not show any contradiction to the theorem.

According to Table 3.1, the k values are taken from the stable ranges and each k can have a corresponding system frequency response curve. So one can take parameter k , radius frequency w and the absolute response and draw them in 3-dimensional coordinate. Those responses in unstable areas of k are forced to be minus showing like gaps.

First, the stable area is divided with m and the step value of k . Then one can start from the first step greater than the lower border of the range and stop by the first step less than the higher border. For the open area like Butterworth LP00, 0 and 8 are considered as the lowest and highest interesting stable k values and the same kind of scan is done as above.

The following figures show the 1-D frequency response within stable areas:

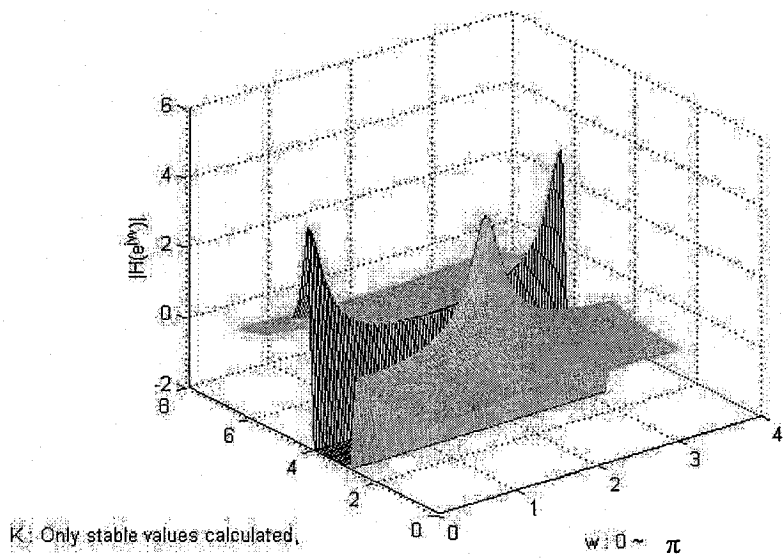


Fig.3.1 Butterworth of LP00 (2)

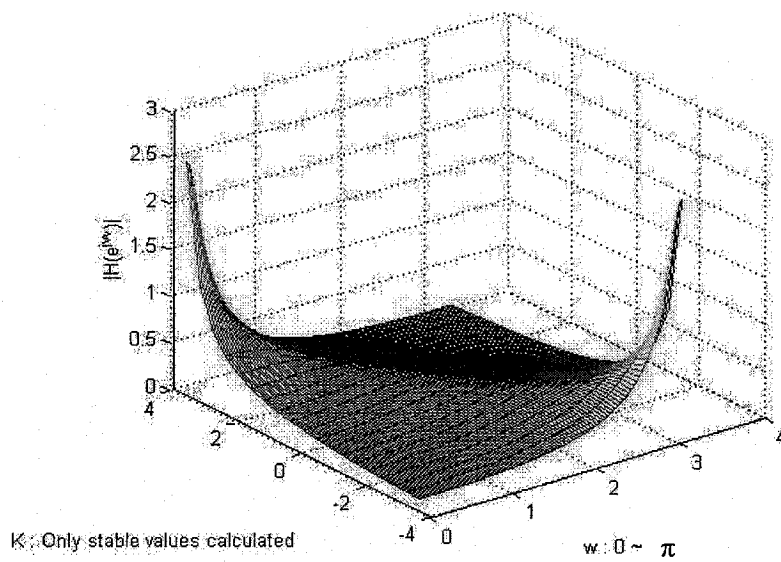


Fig.3.2 Butterworth of LP01(2)

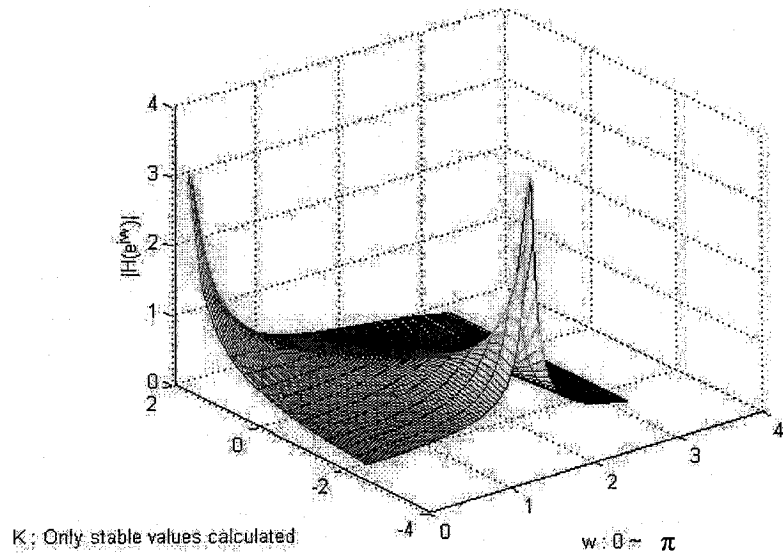


Fig.3.3 Butterworth of LP11

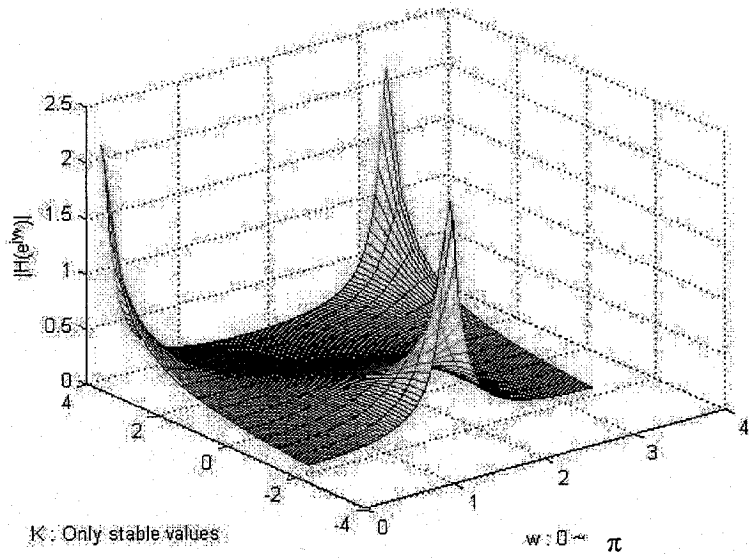


Fig.3.4 Butterworth of LP02

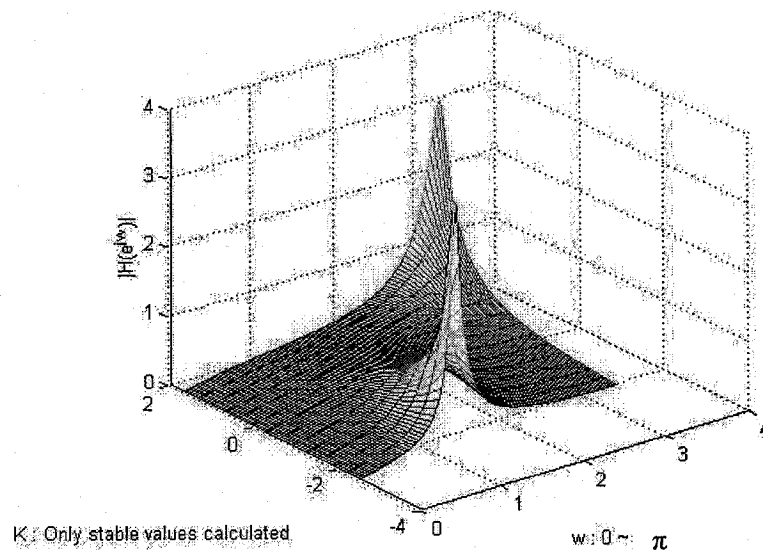


Fig.3.5 Butterworth of BP01

As one can see from the figures above, even in the frequency domain, the unstable area of k is likely to have the trend to reach infinite value. At the border between the stable area and unstable area, the response tends to be significantly great. Obviously the smaller step value is choose, the closer it will approach the border and also the greater response can be obtained. But it will still be finite.

So in the stable area, those different k values can allow us to obtain different system response characteristics in frequency domain according to the design requirement without worrying about the stability.

3.3 Specifications for 2-D filter design

Not to mention all of the specifications for 2-D filter design, only those important are listed below:

3.3.1 Quadrantal frequency requirements

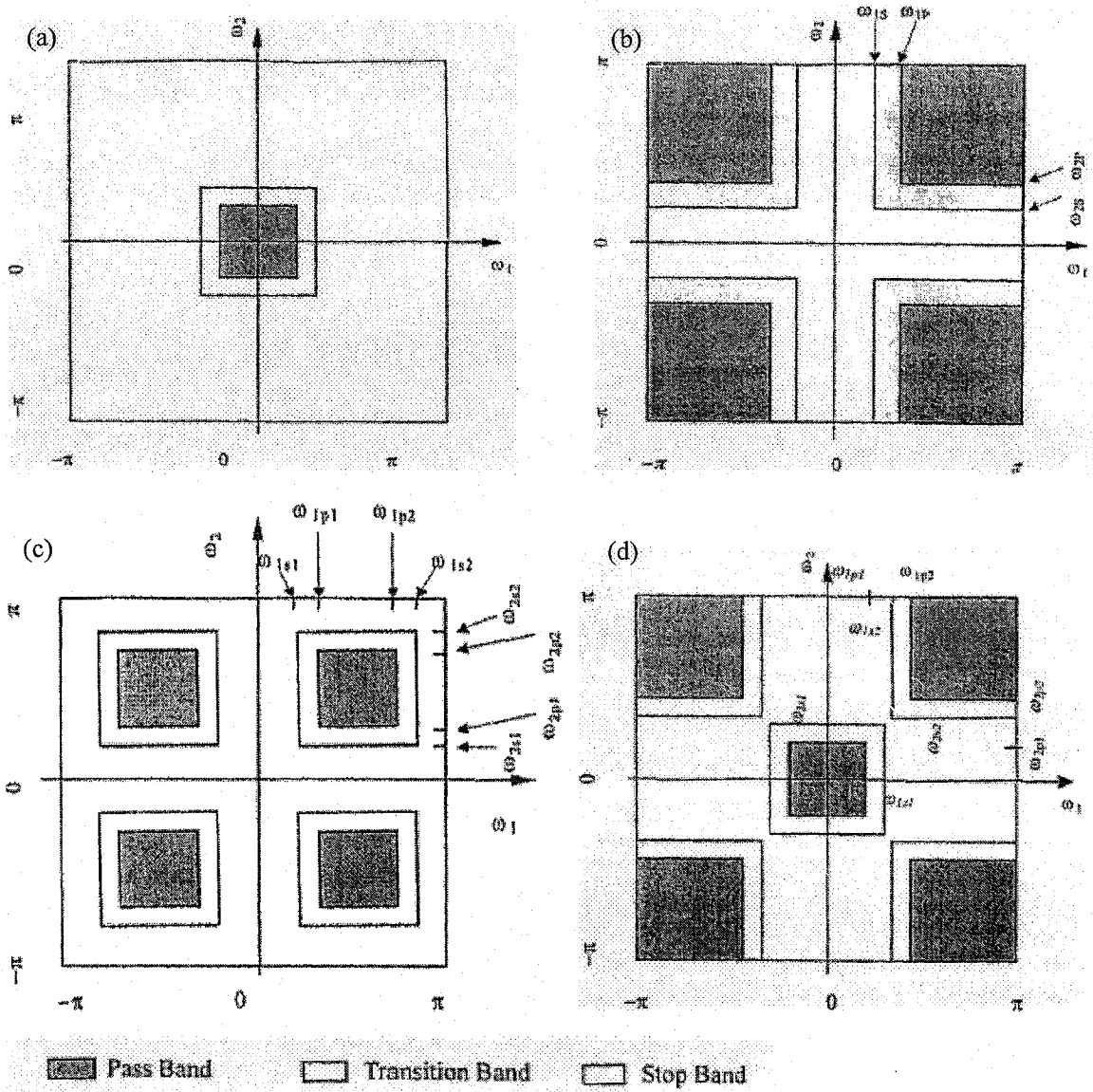


Fig.3.6 Quadrantal requirements for typical filters

(a)Low-pass; (b)High-pass; (c)Band-pass; (d)Band-elimination

The mathematic descriptions for the requirements are:

Low-pass filter:

$$H(\omega_1, \omega_2) = \begin{cases} 1, & |\omega_i| \leq \omega_p \\ 0, & \omega_s < |\omega_i| \leq \pi \end{cases}$$

High-pass filter:

$$H(\omega_1, \omega_2) = \begin{cases} 0, & 0 \leq |\omega_i| \leq \omega_p \\ 1, & \omega_p < |\omega_i| \leq \pi \end{cases}$$

Band-pass filter:

$$H(\omega_1, \omega_2) = \begin{cases} 0, & |\omega_i| \leq \omega_{iis1} \\ 1, & \omega_{ip1} \leq |\omega_i| \leq \omega_{ip2} \\ 0, & \omega_{iis2} \leq |\omega_i| \leq \pi \end{cases}$$

Band-elimination filter:

$$H(\omega_1, \omega_2) = \begin{cases} 1, & |\omega_i| \leq \omega_{iis1} \\ 0, & \omega_{ip1} \leq |\omega_i| \leq \omega_{ip2} \\ 1, & \omega_{iis2} \leq |\omega_i| \leq \pi \end{cases}$$

3.3.2 Circular frequency requirements

Let
$$\omega_i = \sqrt{\omega_1^2 + \omega_2^2} \quad (3.2)$$

Substitute (3.2) into the descriptions above, one can get 2-D circular symmetry of different filters. The shapes are either circles or rings.

3.4 Frequency responses of various filters with $k_1=k_2$

Now the 2-D frequency responses of the different types of filters can be examined, with each having the types of numerators listed in Table 3.1. In each case, the range of values of k selected will be within the stability range. The same type of filters is used in both the domains z_1 and z_2 initially.

3.4.1 LP00 with different values of k

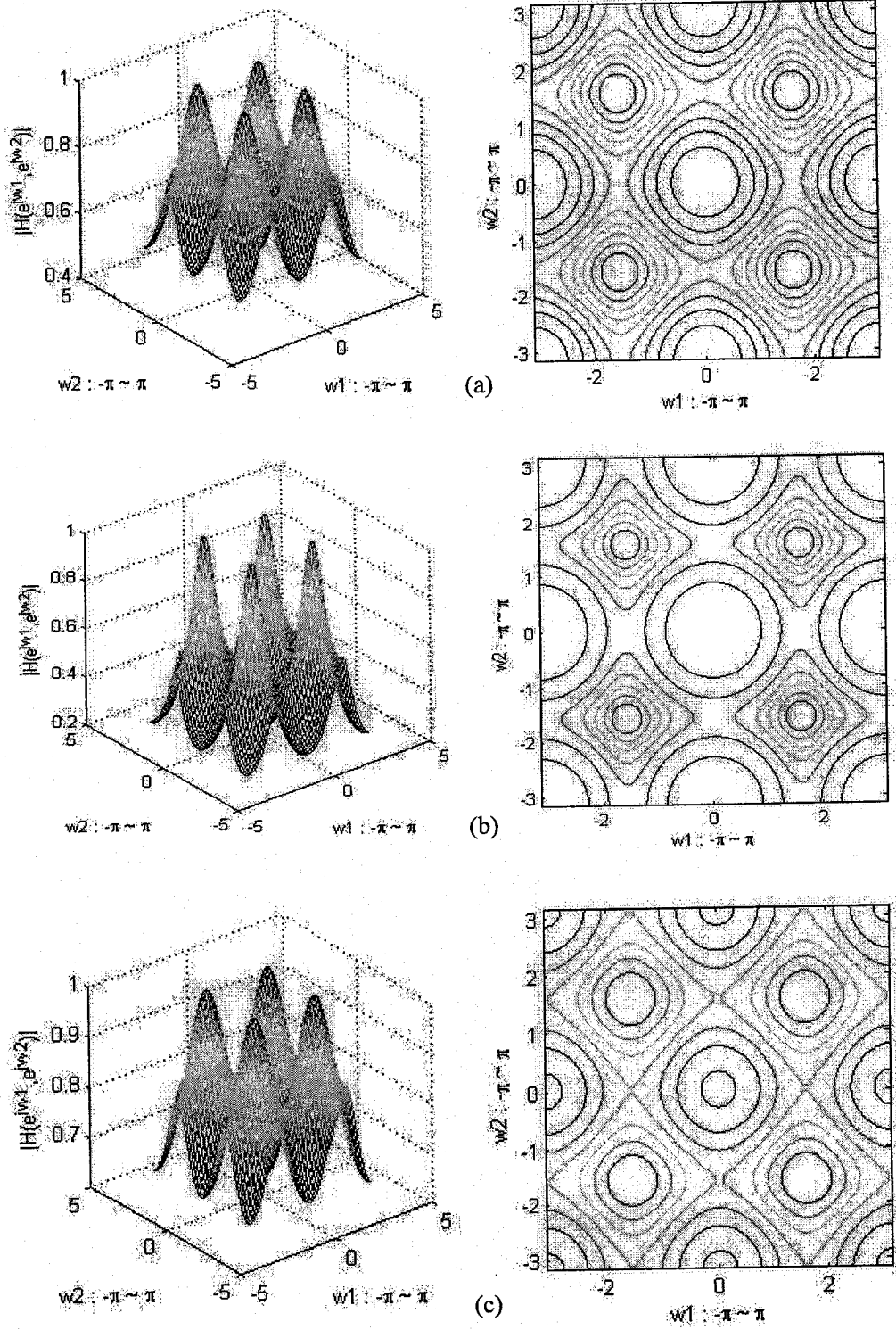


Fig.3.7 2-D Butterworth of LP00 (a) $k_1=k_2=0$; (b) $k_1=k_2=1.8$; (c) $k_1=k_2=-1.8$

3.4.2 LP01 with different values of k

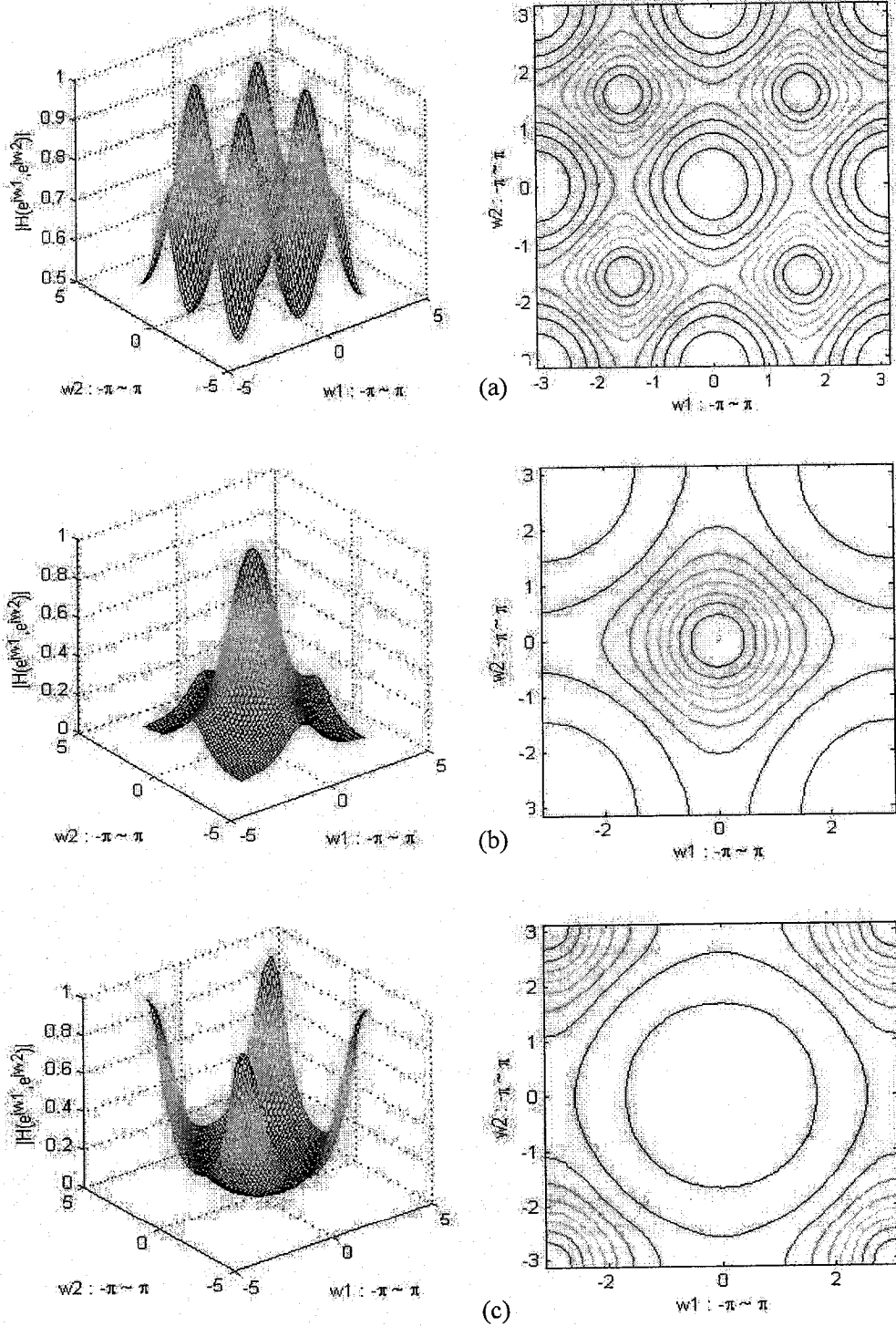


Fig.3.8 2-D Butterworth of LP01 (a) $k_1=k_2=0$; (b) $k_1=k_2=2.5$; (c) $k_1=k_2=-2.5$

3.4.3 LP02 with different values of k

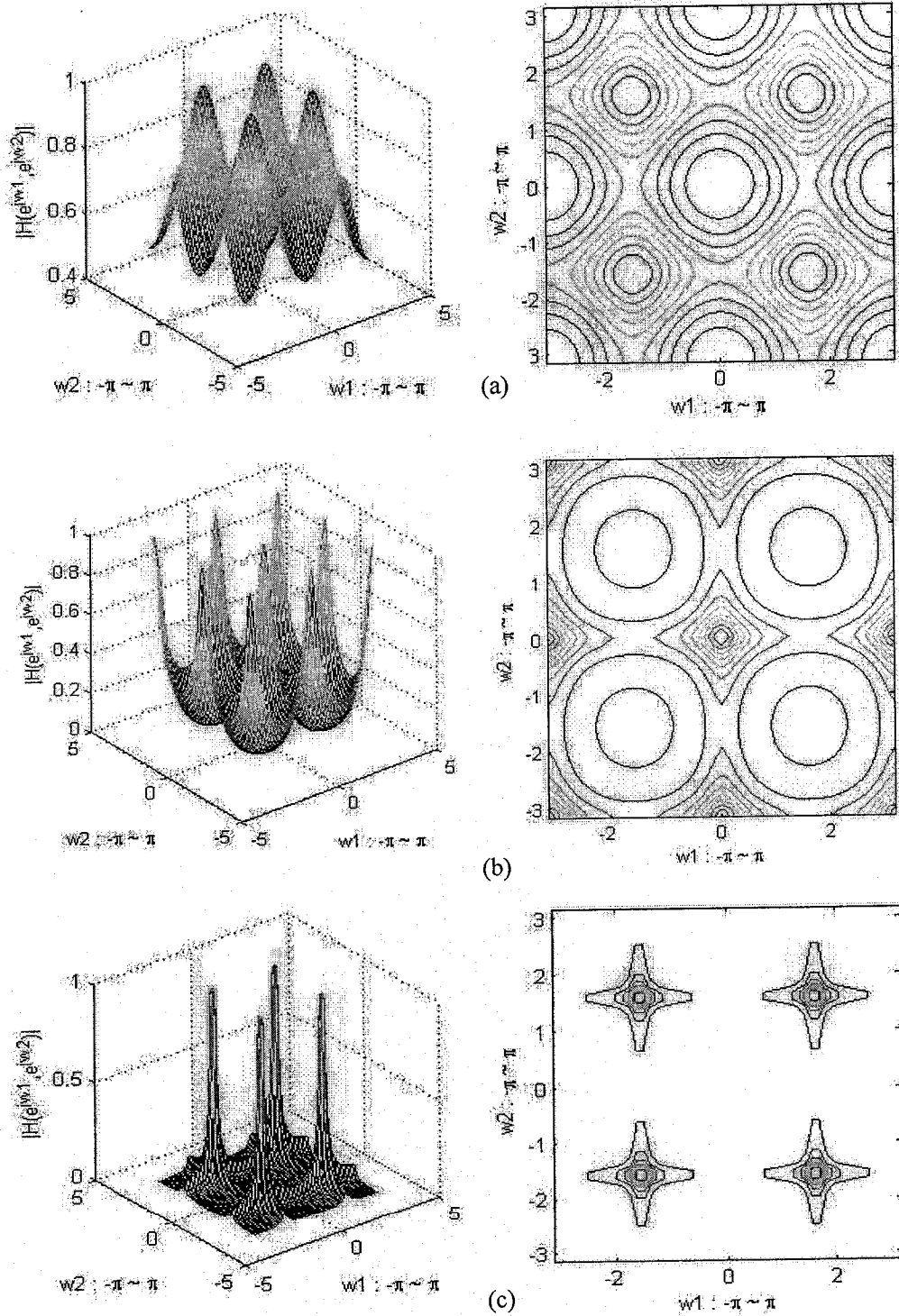


Fig.3.9 2-D Butterworth of LP02 (a) $k_1=k_2=0$; (b) $k_1=k_2=2.5$; (c) $k_1=k_2=-2.5$

3.4.4 LP11 with different values of k

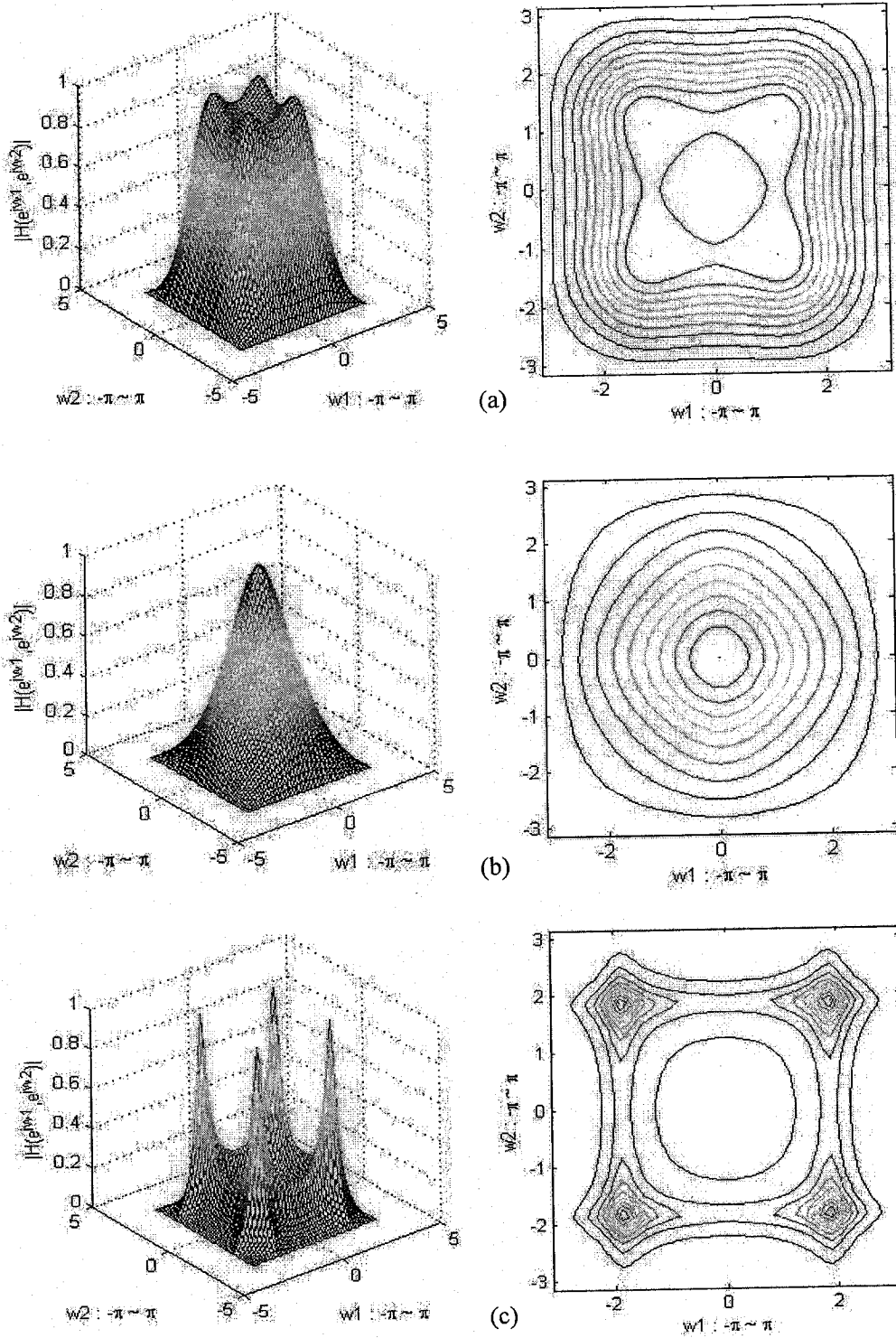
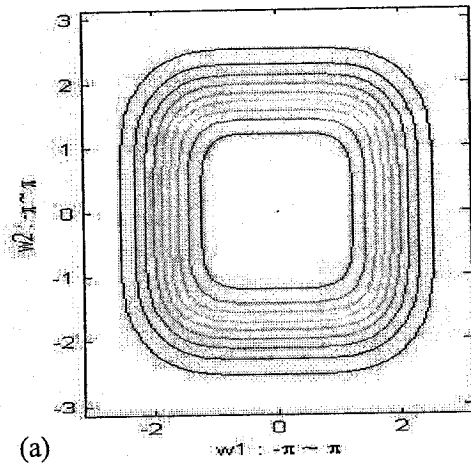
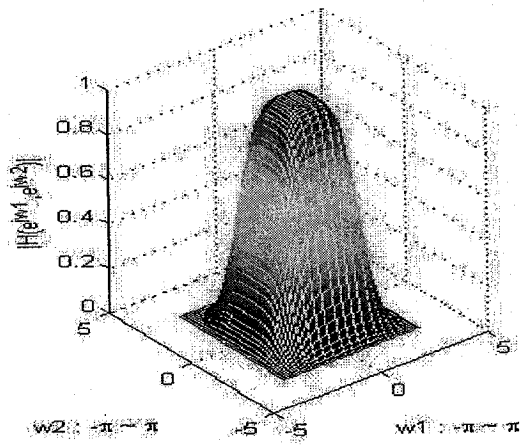
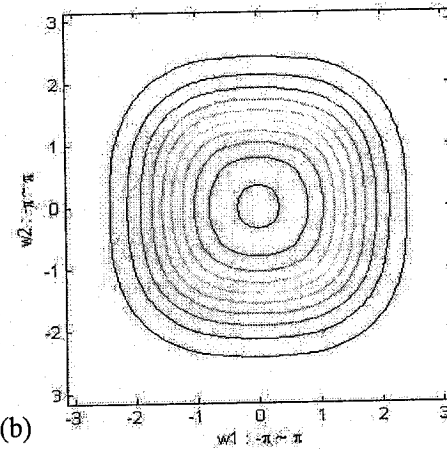
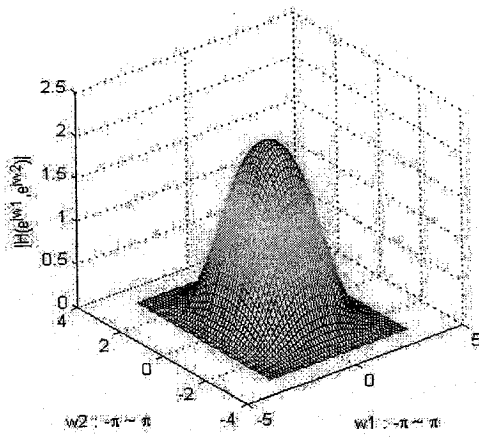


Fig.3.10 2-D Butterworth of LP11 (a) $k_1=k_2=0$; (b) $k_1=k_2=0.7$; (c) $k_1=k_2=-1.7$

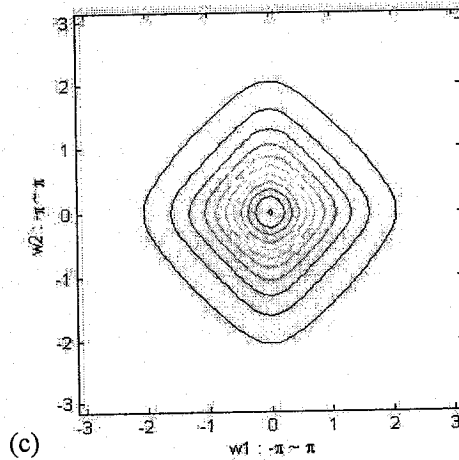
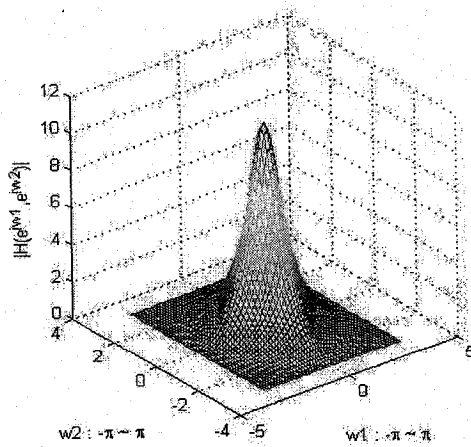
3.4.5 LP20 with different values of k



(a)



(b)



(c)

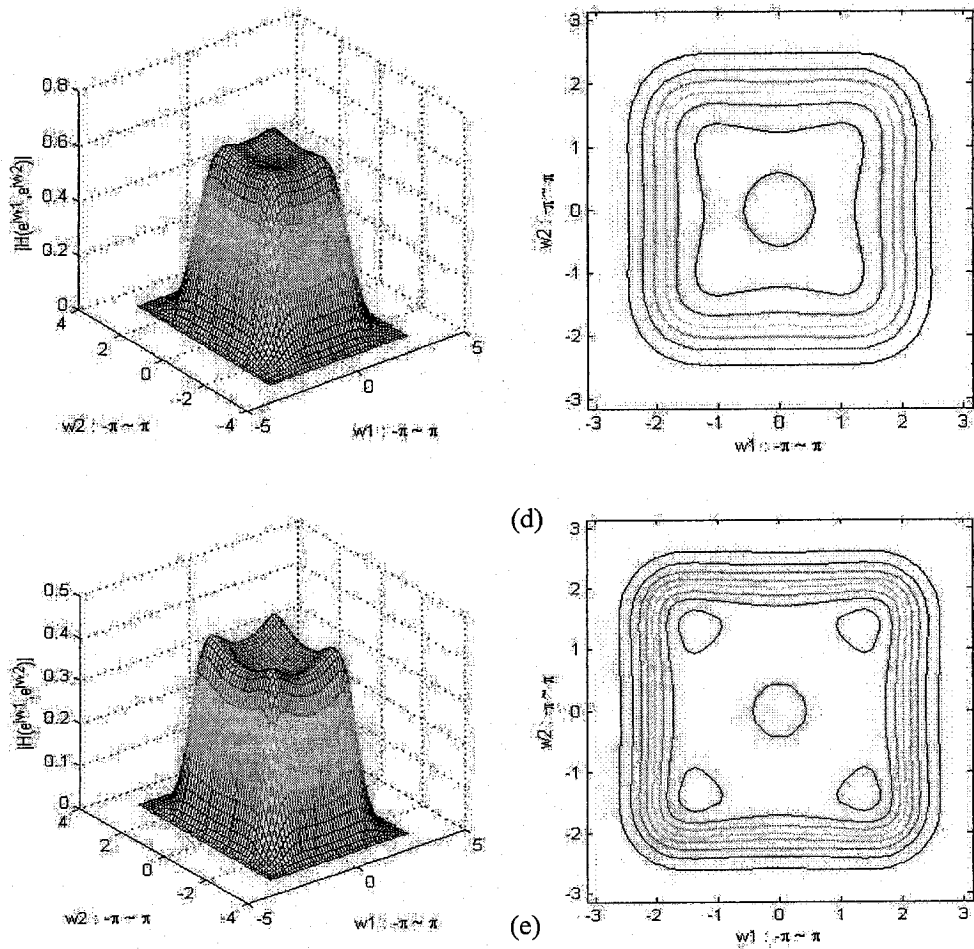


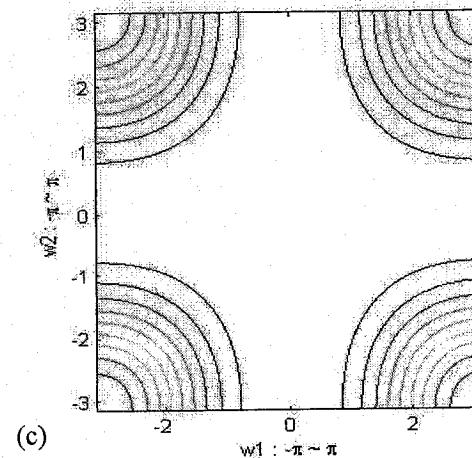
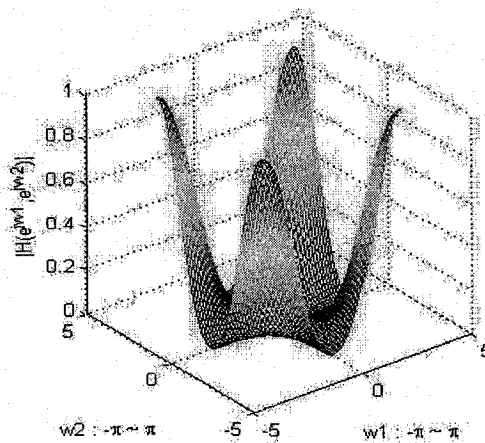
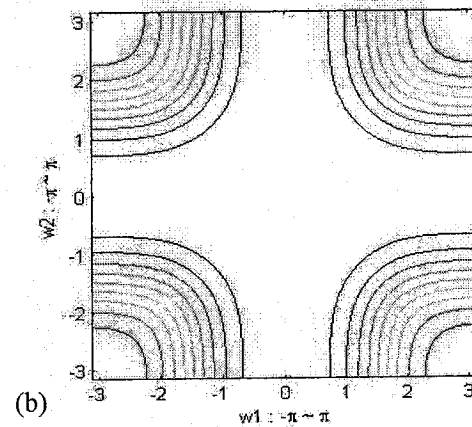
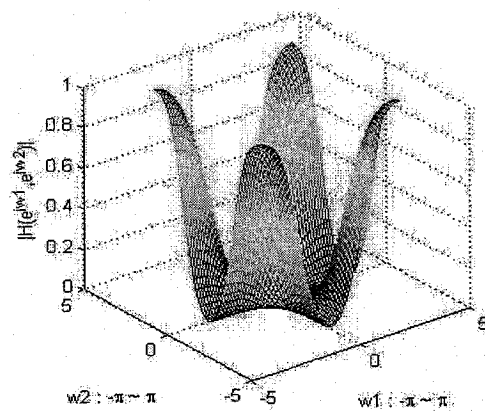
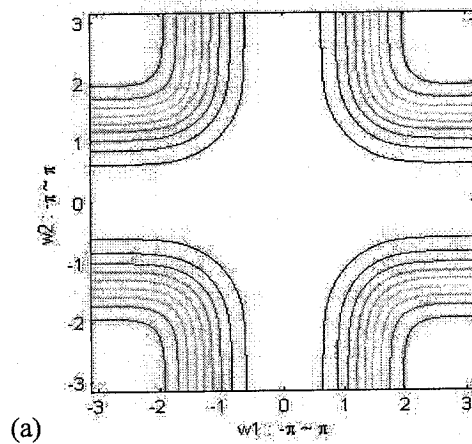
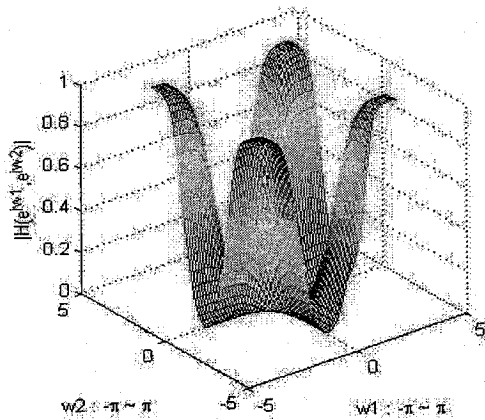
Fig.3.11 2-D Butterworth of LP20
 (a) $k_1=k_2=0$; (b) $k_1=k_2=0.3$; (c) $k_1=k_2=0.7$; (d) $k_1=k_2=-0.3$; (e) $k_1=k_2=-0.7$

With different stable k values, and because of the same low-pass filters with same coefficients and feedbacks, the response shows octagonal symmetry. The center part always shows near-circular symmetry and the contour is composed of circle-like patterns.

And also by changing k within the stable range given in Table 3.1, one can get near-circular symmetry when $k > 0$. By increasing positive k value, the pass-band frequency shrinks and the transient-band becomes wider. While $k < 0$, by increasing the absolute value of k , the pass-band inflates and transient-band becomes sharper. And

simultaneously the flatness within the pass-band is worse.

3.4.6 HP with different values of k



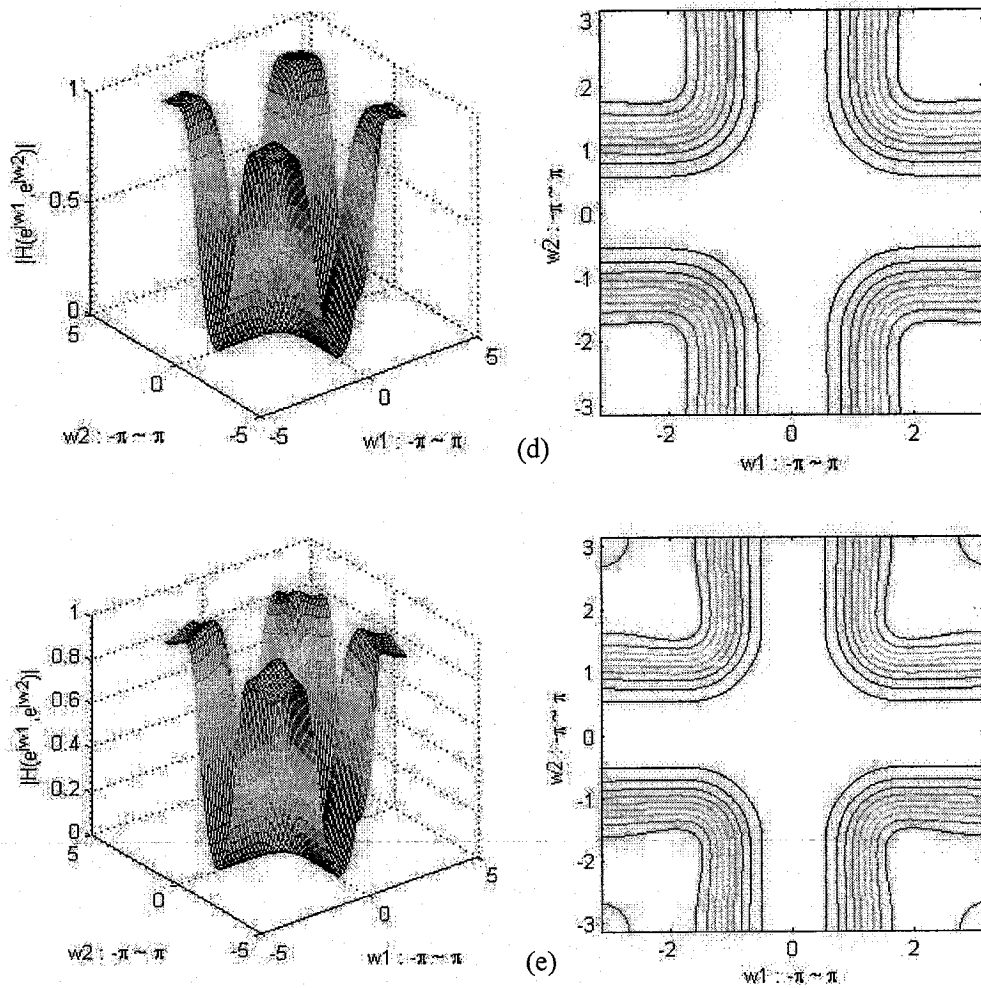


Fig.3.12 2-D Butterworth of HP

(a) $k_1=k_2=0$; (b) $k_1=k_2=0.2$; (c) $k_1=k_2=0.4$; (d) $k_1=k_2=-0.2$; (e) $k_1=k_2=-0.5$

For high-pass filters with different stable k values, the response remains octagonal symmetry. When $k > 0$, by increasing positive k value, the pass-band frequency shrinks and the transient-band becomes slightly wider. While $k < 0$, by increasing the absolute value of k , the pass-band inflates and the transient-band becomes slightly sharper. And simultaneously the flatness within the pass-band becomes worse.

3.4.7 BP01 with different values of k

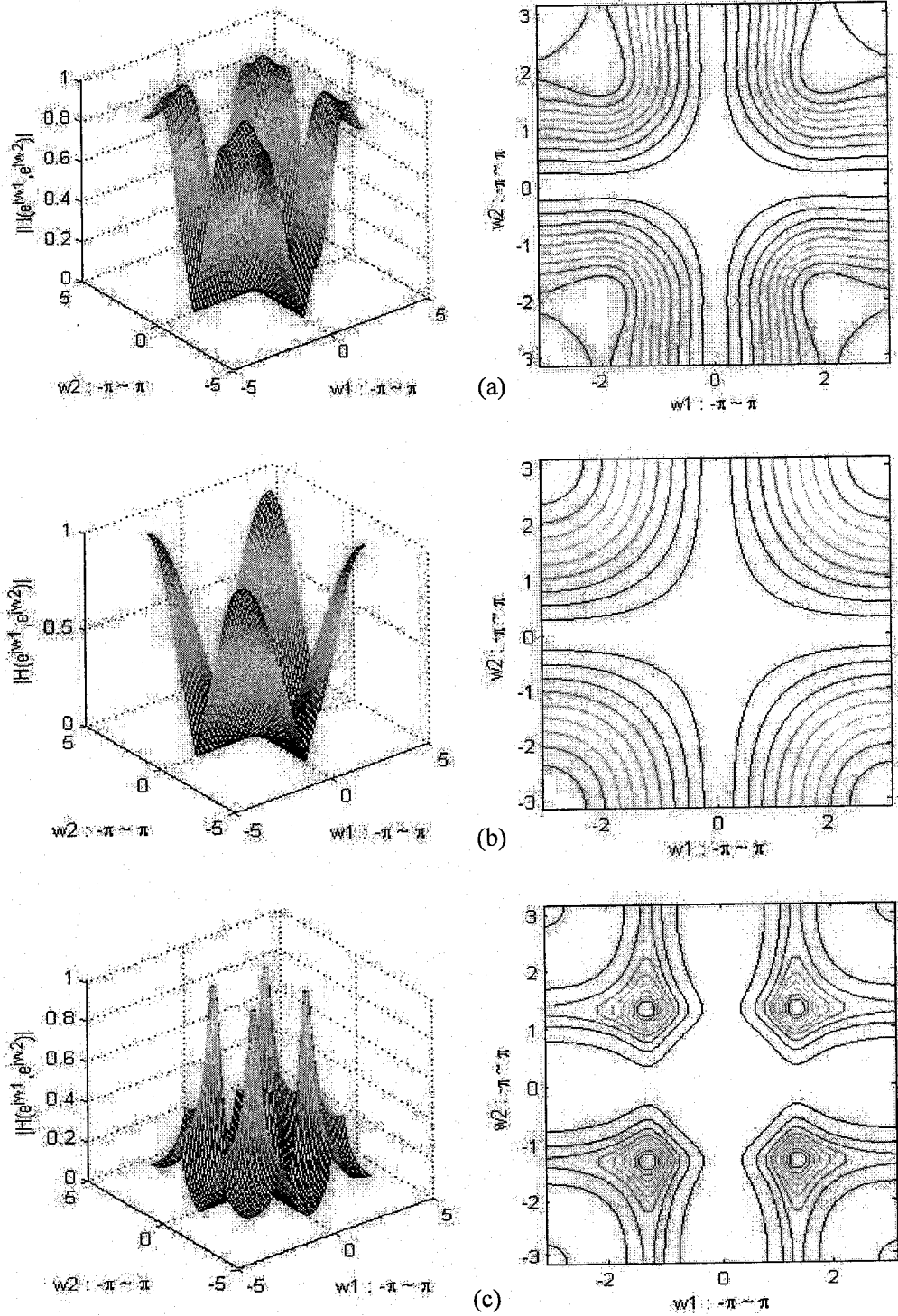
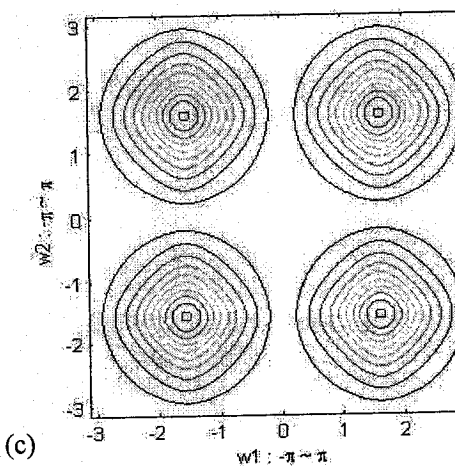
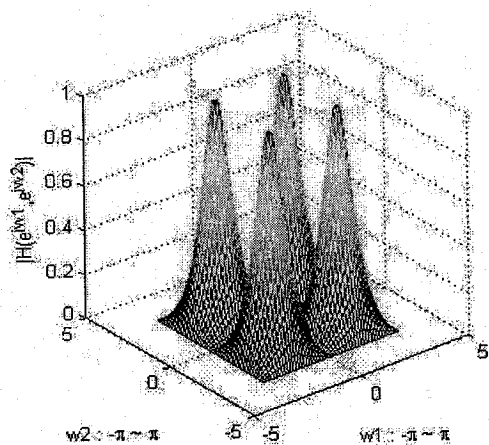
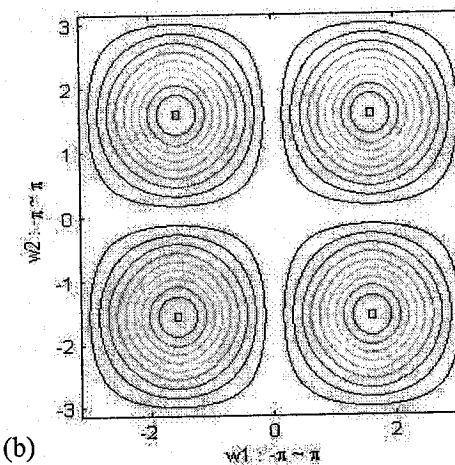
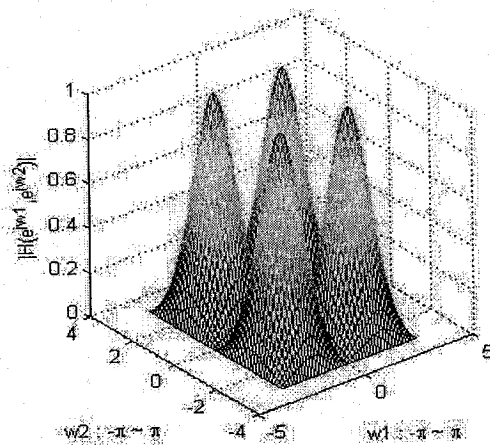
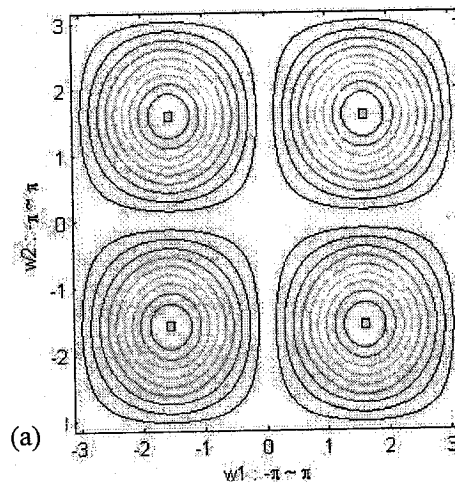
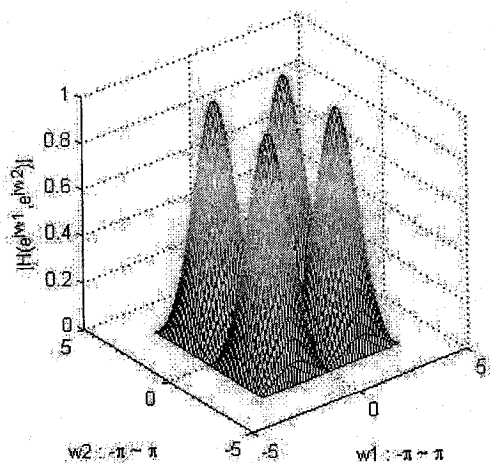


Fig.3.13 2-D Butterworth of BP01 (a) $k_1=k_2=0$; (b) $k_1=k_2=0.5$; (c) $k_1=k_2=-1.5$

3.4.8 BP10 with different values of k



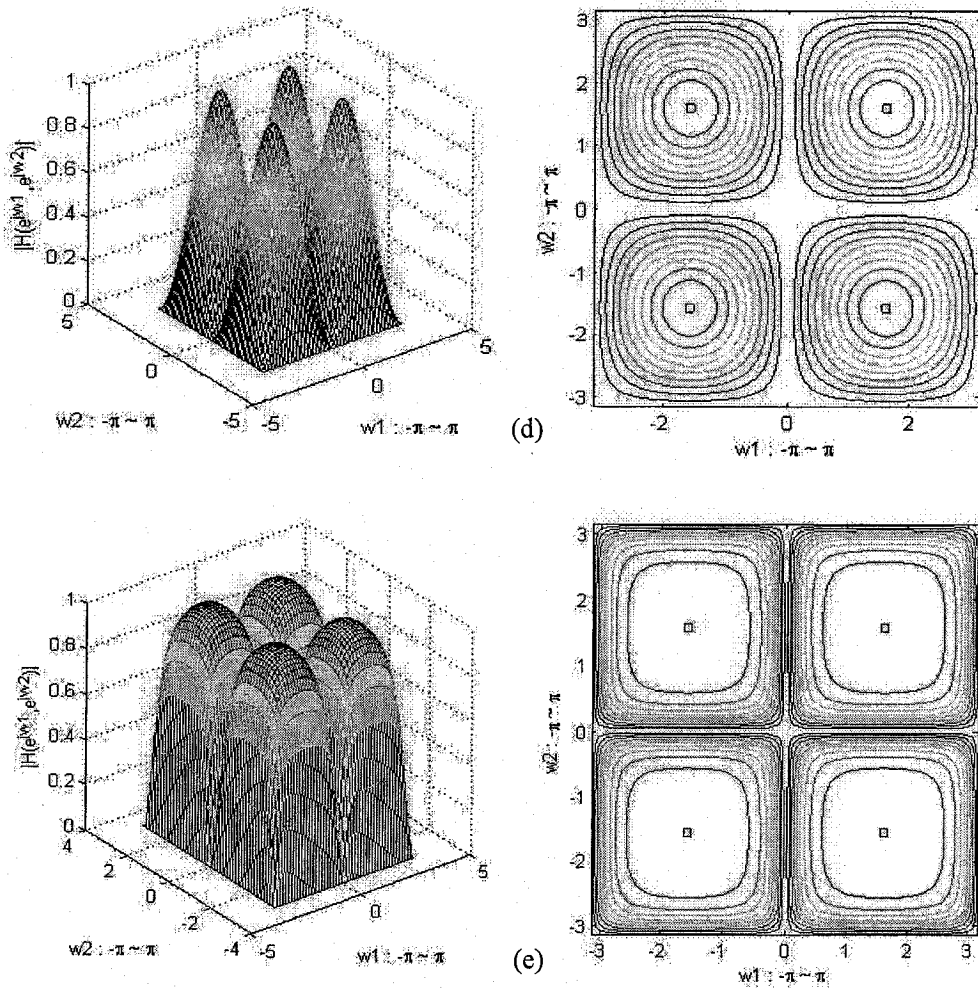


Fig.3.14 2-D Butterworth of BP10

(a) $k_1=k_2=0$; (b) $k_1=k_2=0.1$; (c) $k_1=k_2=0.5$; (d) $k_1=k_2=-0.5$; (e) $k_1=k_2=-1.5$

For band-pass filters with different stable k values, the response remains octagonal symmetry. When $k > 0$, by increasing positive k value, the pass-band frequency shrinks and the transient-band nearly remains the same. While $k < 0$, by increasing the absolute value of k , the pass-band inflates and the transient-band becomes much sharper. And the flatness within the pass-band is sustained.

3.5 Frequency responses of various filters with $k_1 \neq k_2$

Now the same type of filters in z_1 and z_2 domains is considered, but with different values of k 's. They are discussed below.

3.5.1 Dimension-unbalanced LP00

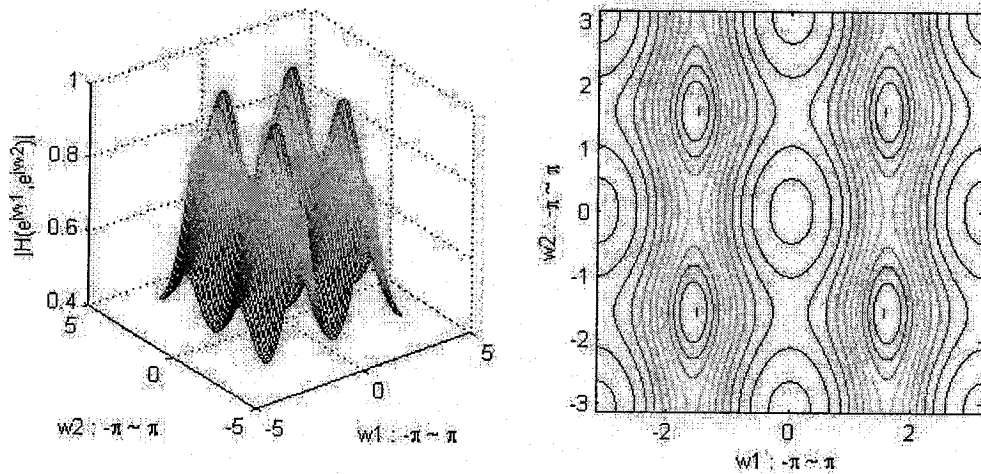


Fig.3.15 2-D Butterworth of LP00 $k_1 = 1.5, k_2 = -2$

3.5.2 Dimension-unbalanced LP01

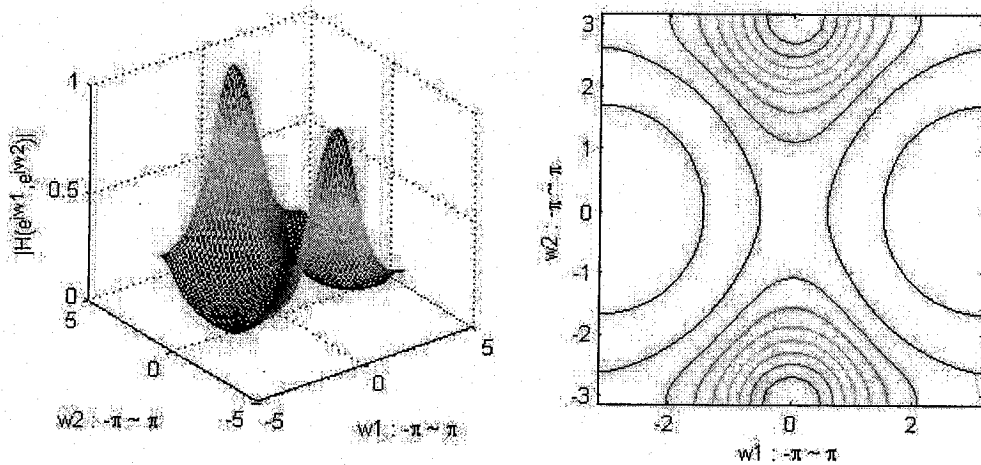


Fig.3.16 2-D Butterworth of LP01 $k_1 = 2.5, k_2 = -2.5$

3.5.3 Dimension-unbalanced LP02

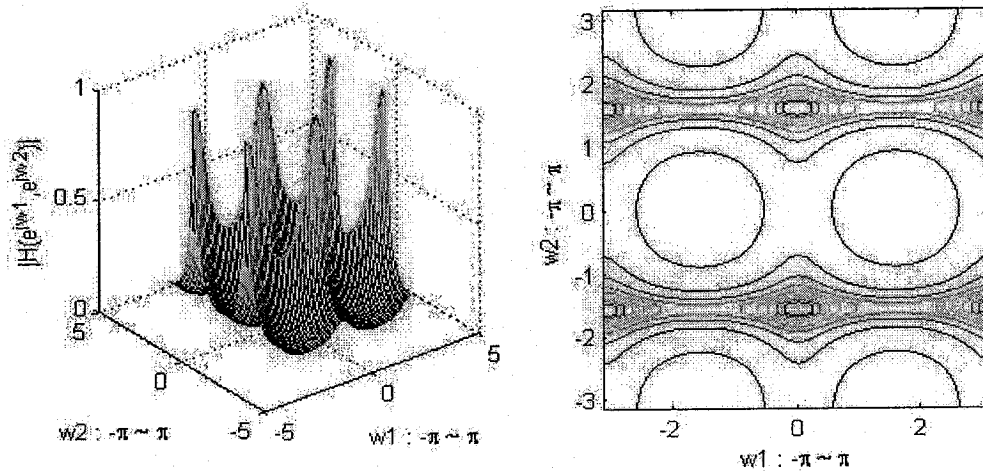


Fig.3.17 2-D Butterworth of LP02 $k_1=2, k_2=-2$

3.5.4 Dimension-unbalanced LP11

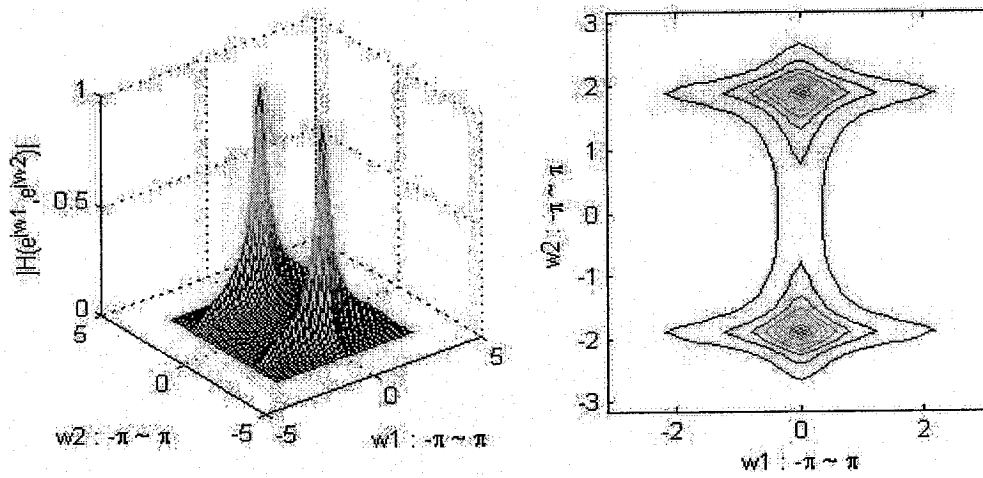


Fig.3.18 2-D Butterworth of LP11 $k_1=1.5, k_2=-2$

3.5.5 Dimension-unbalanced LP20

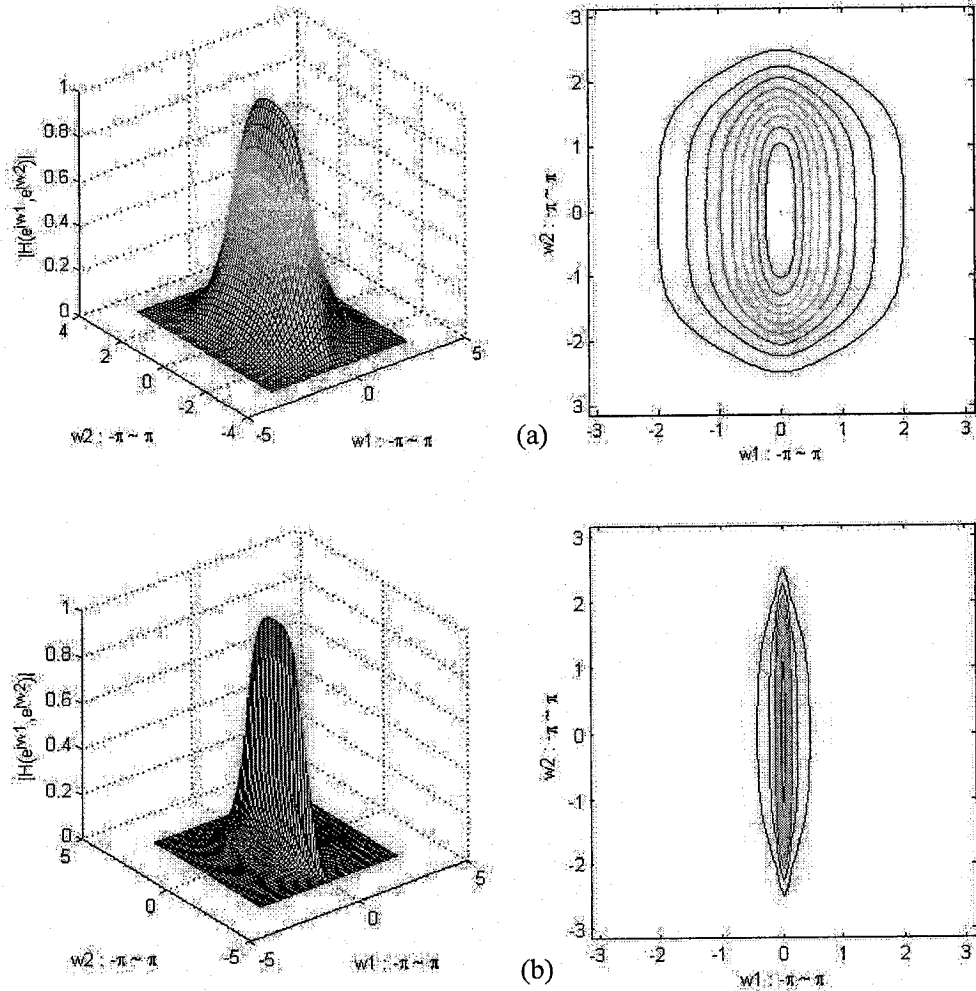


Fig.3.19 2-D Butterworth of LP20 (a) $k_1=0.7, k_2=0.1$; (b) $k_1=0.97, k_2=0.1$

For low-pass filters with different k 's, quadrantal symmetry holds. By changing one of the two dimensional feedbacks, the response of this dimension changes significantly. Increasing a positive k value can obtain a narrow pass-band in this dimension, which can satisfy some special requirement.

3.5.6 Dimension-unbalanced HP

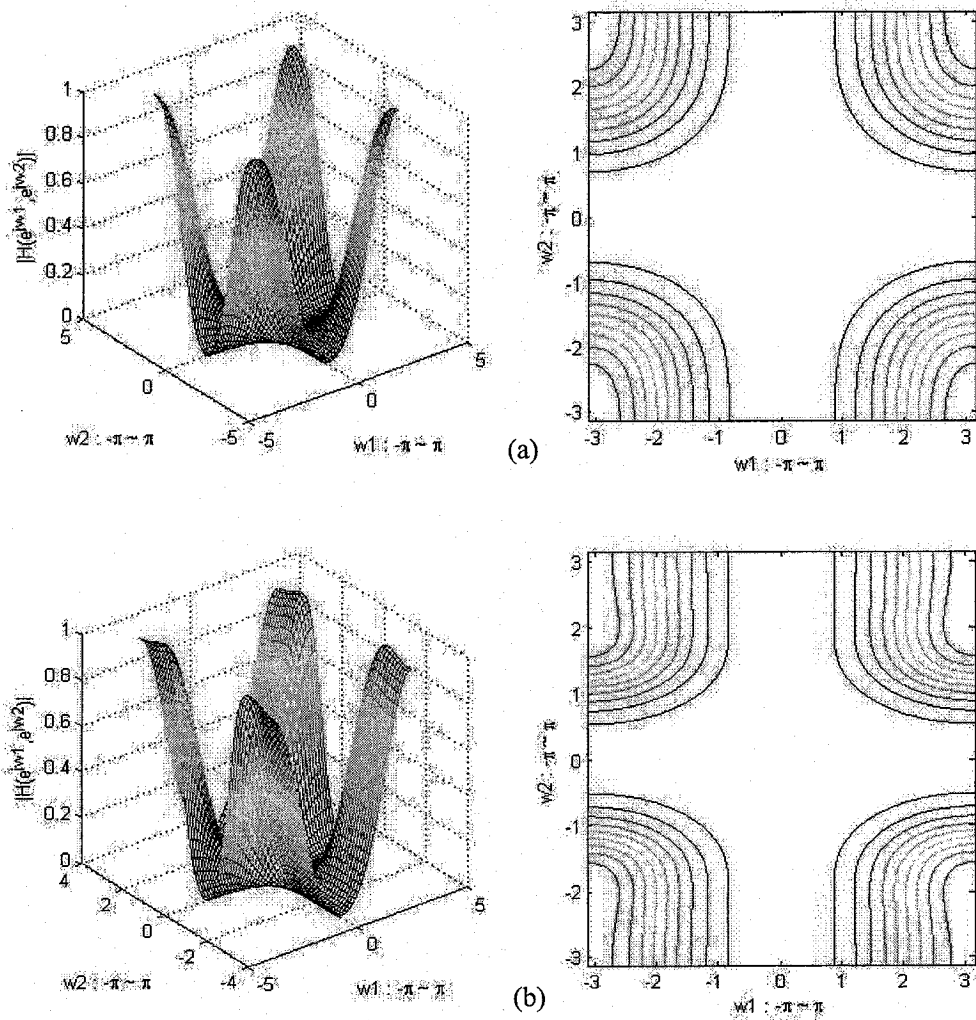


Fig.3.20 2-D Butterworth of HP (a) $k_1=0.45, k_2=0.2$; (b) $k_1=0.45, k_2=-0.4$

Likewise, for high-pass filters with different k 's, quadrantal symmetry holds. By changing one of the two dimensional feedbacks, the response of this dimension changes.

Decreasing a k value can obtain a wider pass-band in this dimension.

3.5.7 Dimension-unbalanced BP01

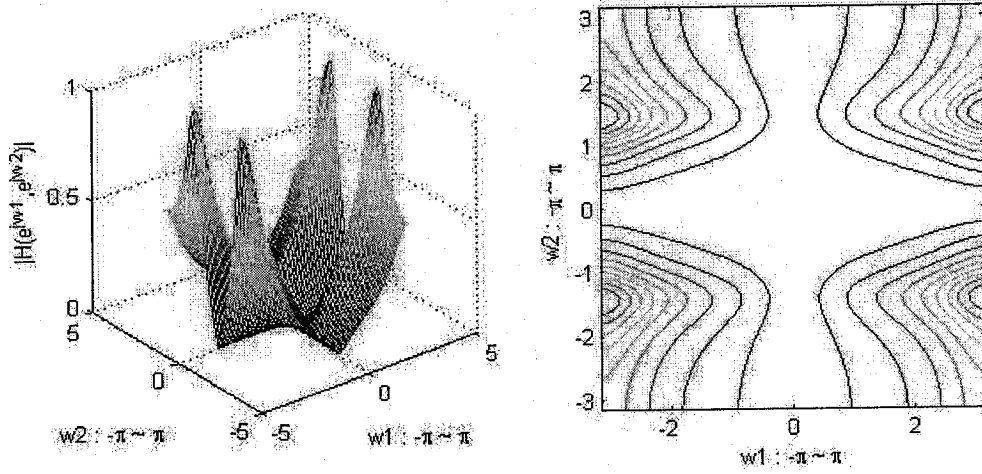
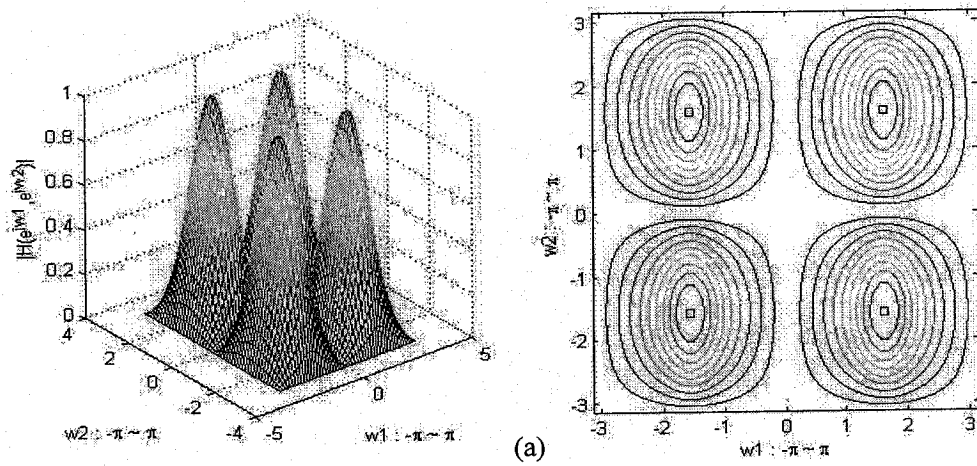


Fig.3.21 2-D Butterworth of BP01 $k_1=1, k_2=-1$

3.5.8 Dimension-unbalanced BP10



(a)

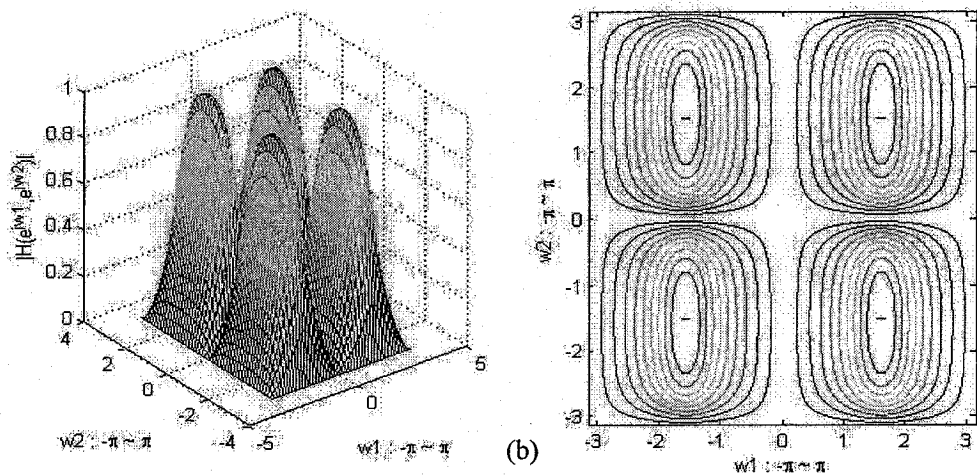


Fig.3.22 2-D Butterworth of BP10 (a) $k_1=0.5, k_2=-0.5$; (b) $k_1=0.5, k_2=-2.5$

For band-pass filters with different k 's, quadrantal symmetry holds. By changing one of the two dimensional feedbacks, the response of this dimension changes. Decreasing a k value can obtain a wider pass-band in this dimension.

In this section, since $k_1 \neq k_2$, not octagonal but quadrantal symmetry holds. Dimension-unbalanced variable characteristics can be observed.

3.6 Frequency responses of combinations of filters with $k_1=k_2$

Now, different filters with the same feedbacks are considered. In view of large number of possibilities, some representative filters are selected.

3.6.1 LP20/HP

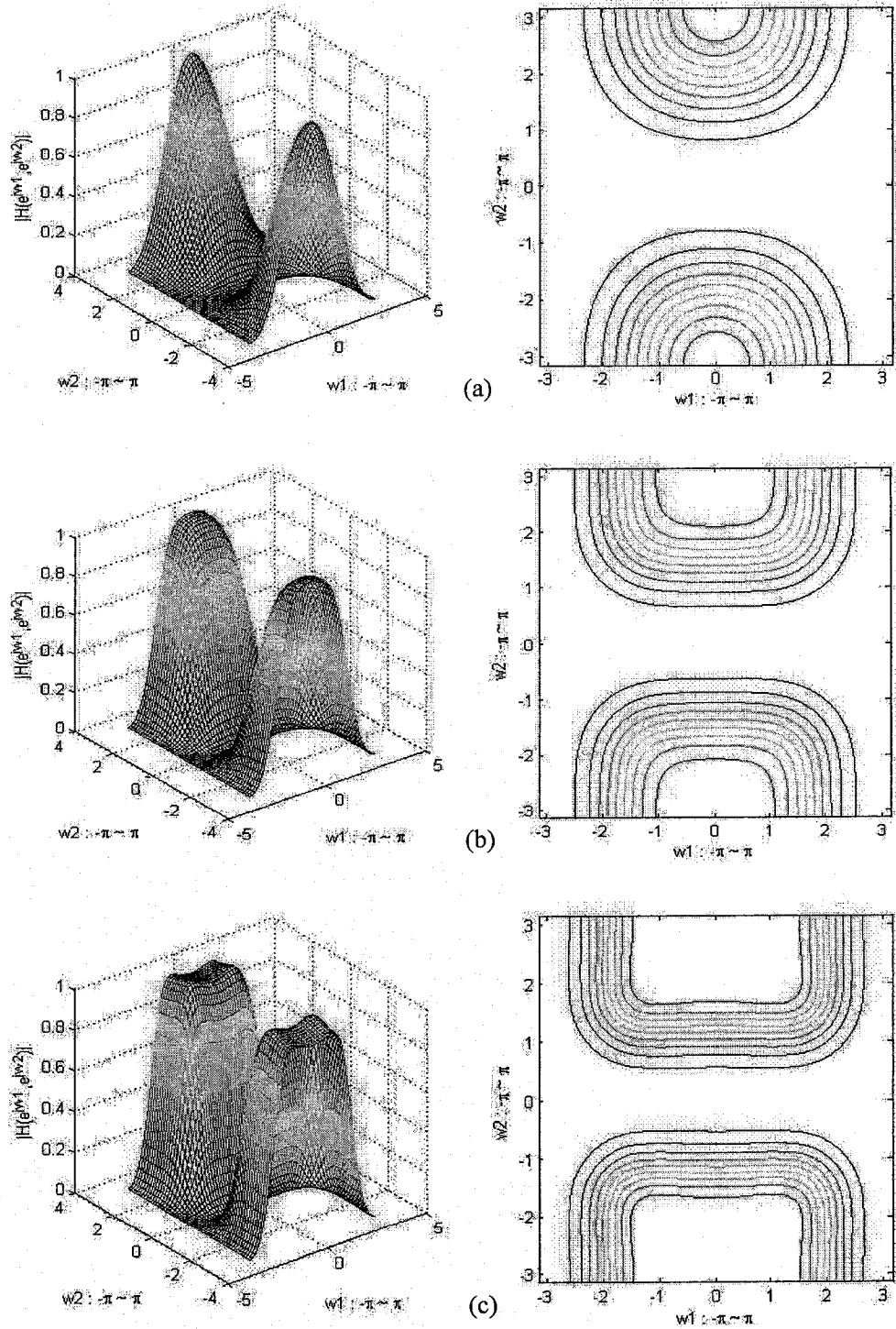
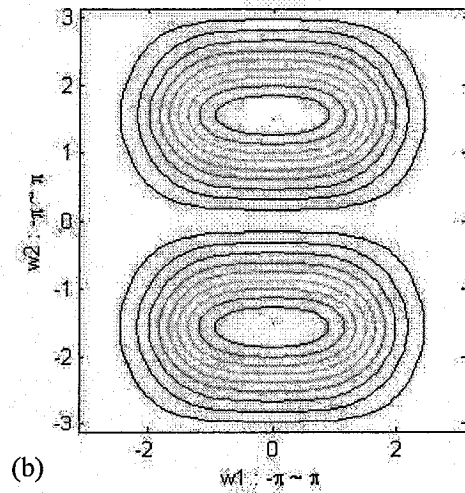
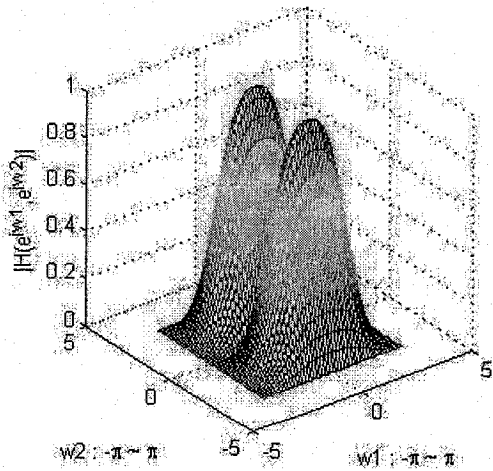
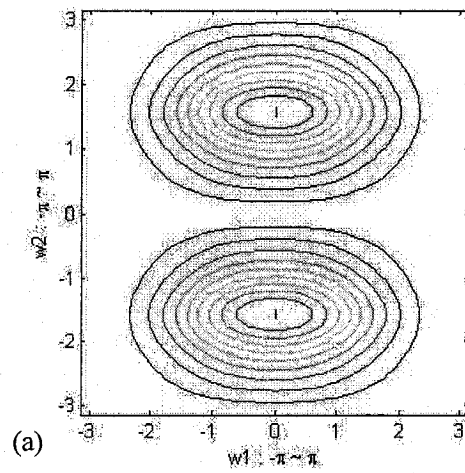
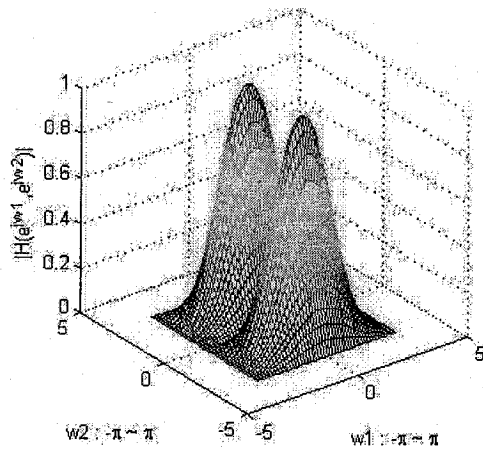


Fig.3.23 Butterworth of LP20/HP (a) $k_1=k_2=0.4$; (b) $k_1=k_2=0.1$; (c) $k_1=k_2=-0.3$

For low-pass and high-pass filters with same k values, quadrantal symmetry holds. By changing the two dimensional feedbacks simultaneously, the response changes according to the rule of each dimension. Decreasing the k values can widen the pass-bands in both dimensions.

3.6.2 LP20/BP10



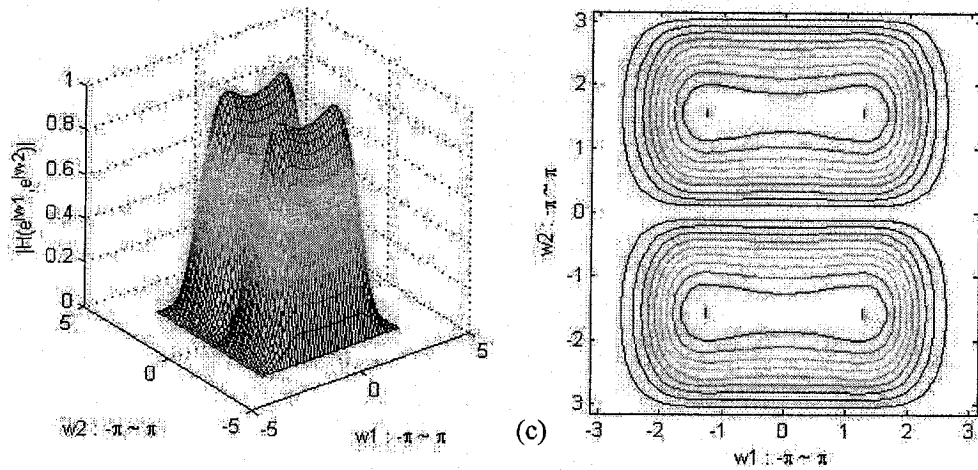
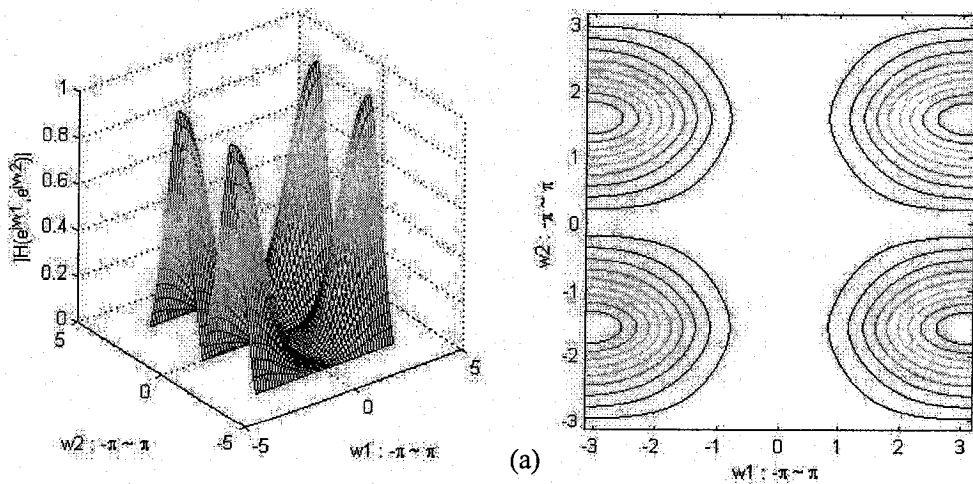


Fig.3.24 Butterworth of LP20/BP10 (a) $k_1=k_2=0.4$; (b) $k_1=k_2=0.2$; (c) $k_1=k_2=-0.5$

For low-pass and band-pass filters with same k values, quadrantal symmetry holds. The response changes according to the rule of each dimension. Decreasing the k values can widen the pass-bands in both dimensions.

3.6.3 HP/BP10



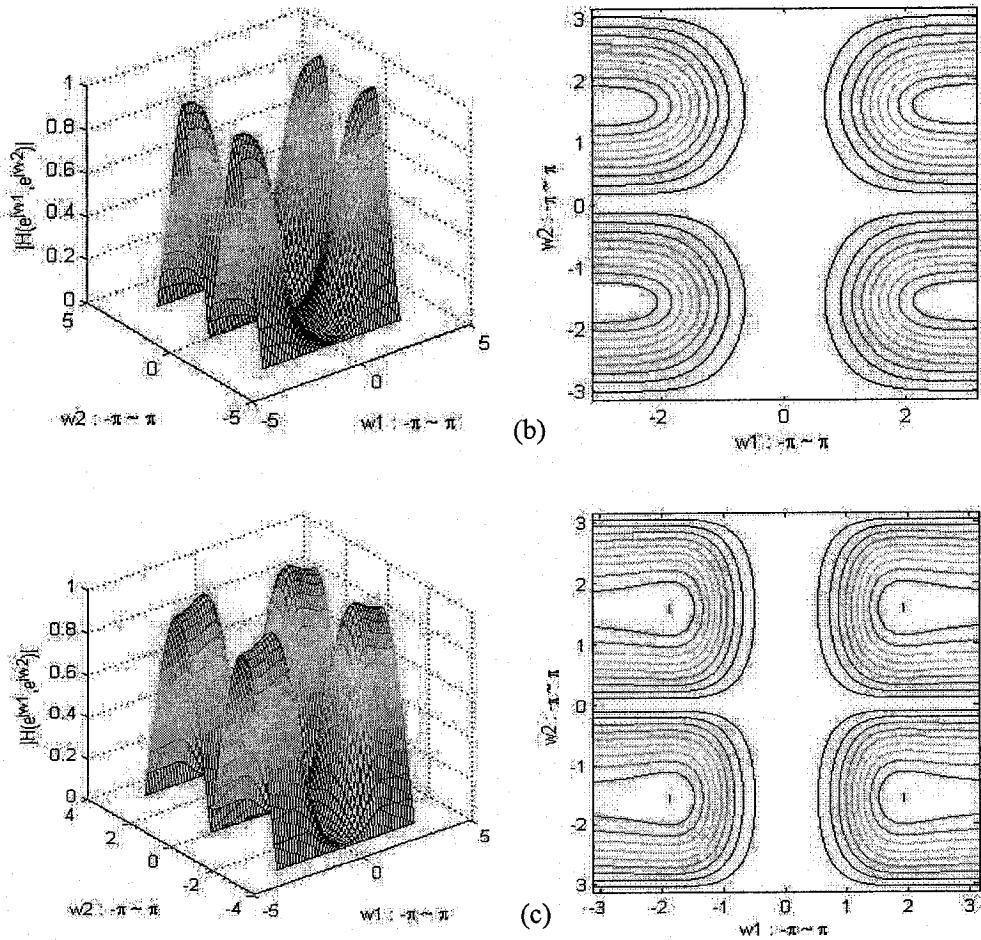


Fig.3.25 Butterworth of HP/BP10 (a) $k_1=k_2=0.4$; (b) $k_1=k_2=0.1$; (c) $k_1=k_2=-0.5$

For high-pass and band-pass filters with same k values, quadrantal symmetry holds.

Decreasing the k values can widen the pass-bands in both dimensions.

In this section, even with $k_1=k_2$, different filters still offer dimension-unbalanced variable characteristics. But quadrantal symmetry always holds.

3.7 Frequency responses of combinations of filters with $k_1 \neq k_2$

Now, different filters with different feedbacks are considered, with values that point to the opposite side of each other dimensions.

3.7.1 LP20/HP

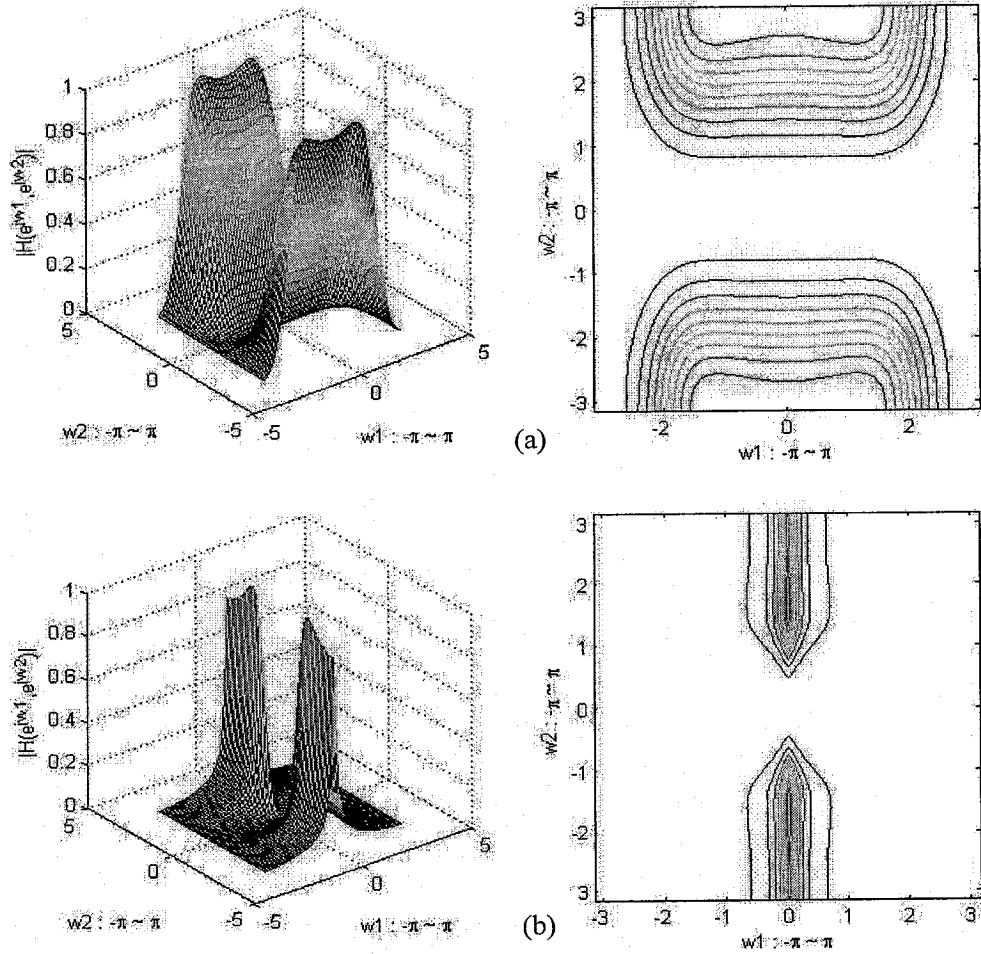


Fig.3.26 Butterworth of LP20/HP (a) $k_1=-0.4, k_2=0.4$; (b) $k_1=0.95, k_2=-0.9$

For low-pass and high-pass filters with different k values pointing to the opposite sides to each other, quadrantal symmetry holds. The response changes according to the rule in each dimension. While decreasing the pass-band of low-pass filter and increase it for high-pass filter, a near-fan-filter can be obtained(see Fig 3.26 b).

3.7.2 LP20/BP10

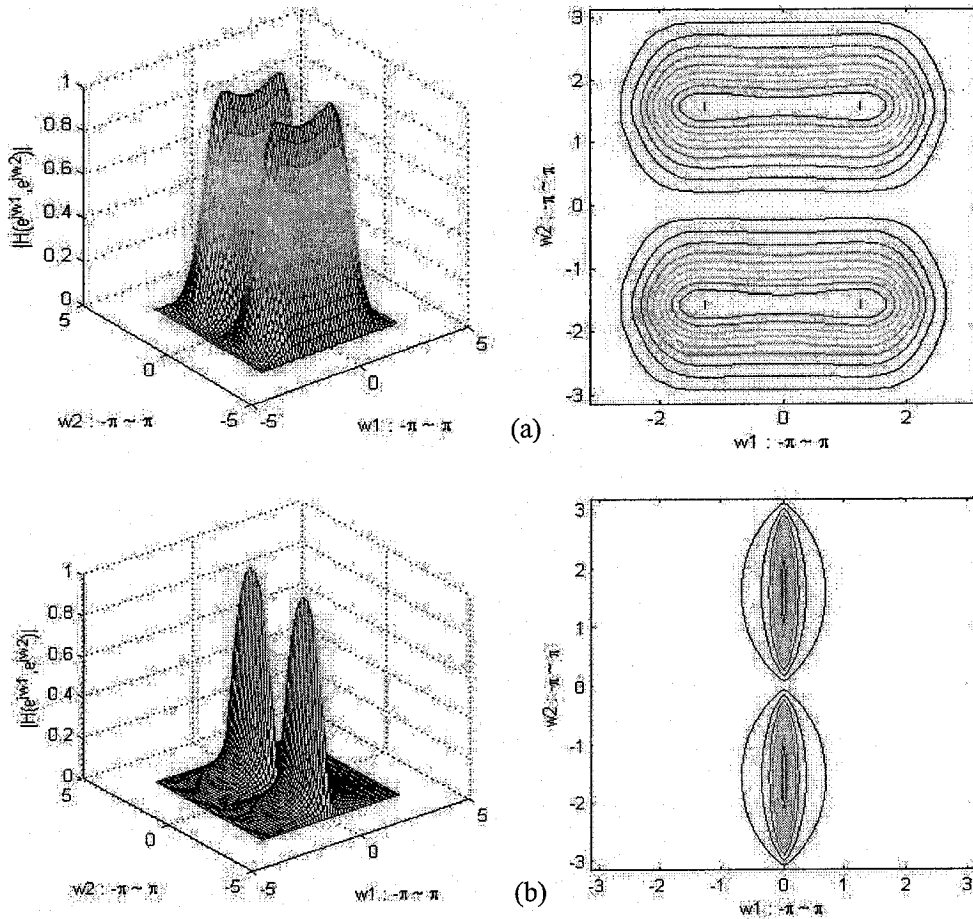


Fig.3.27 Butterworth of LP20/BP10 (a) $k_1=-0.5, k_2=0.5$; (b) $k_1=0.95, k_2=-0.95$

Likewise, for low-pass and band-pass filters with different k values pointing to the opposite sides to each other, quadrantal symmetry holds. While decreasing the pass-band of low-pass filter and increase it for high-pass filter, a near-fan-filter can be obtained.

3.7.3 HP/BP10

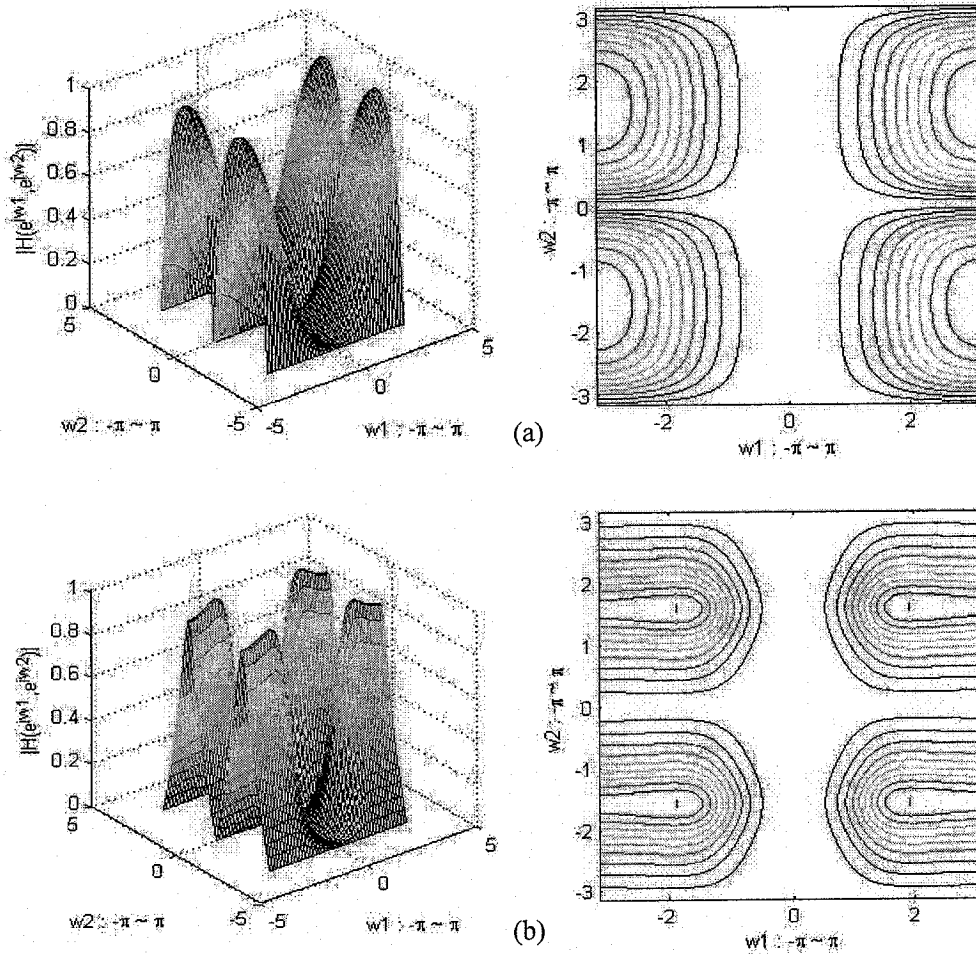


Fig.3.28 Butterworth of HP/BP10 (a) $k_1=-0.5, k_2=0.5$; (b) $k_1=0.95, k_2=-0.95$

For high-pass and band-pass filters with different k values pointing to the opposite sides to each other, quadrantal symmetry holds. The response changes according to the rule in each dimension.

In this section, different filters with $k_1 \neq k_2$ give us dimension-unbalanced variable patterns but quadrantal symmetry remains.

3.8 Summary and Discussions

In this chapter, Low-order filters such as Generic Biquadratic Butterworth are considered. With values inside the stability range of k , 1-D frequency magnitude responses have been shown without any singularity. Also the 1-D variable magnitude characteristics within the whole stability area of k are displayed.

Then two kinds of general 2-D frequency specification of filter design are introduced, namely quadrantal and circular frequency requirements.

In order to show the effects of 2-D variable magnitude response with stable value of k , different situations are considered: Same filters in z_1 and z_2 domains with the same values of k ; Same filter with different values of k ; Different filters with same k 's; Different filters with different k 's.

For the first situation, octagonal symmetry (both quadrantal and diagonal four-fold reflection symmetries) is obtained inherently. Near-circular symmetries can also be observed. The variable characteristics are dimension-symmetrical.

For other three situations, quadrantal symmetry always holds and many kinds of variable dimension-unbalanced characteristics are obtained.

In all these situations, the 2-D magnitude responses vary significantly within stability range of k . Hence different kinds of 2-D requirements can be achieved or approached. The rough characteristics of relations between the responses and the change of k values are observed and briefly discussed.

CHAPTER 4 Analysis and Response of Higher Order Filters

4.1 Algorithms for higher order filters

Having obtained 2-D variable characteristics with lower order filters, theoretically one can build higher order VCTF systems by cascading more than one of such lower-order systems with their feedback k 's. Adjusting these different k values can be done. However, for higher-order systems considered in $D_1(z_1)$ or $D_2(z_2)$ the evaluation of k will be quite difficult. So for higher order systems, high-order filters as a whole with unique feedbacks need to be considered.

For higher-order filters, the product decomposition of the polynomials is difficult and hence the complexity of the analysis increases significantly. In order to extend such an analysis to IIR filters or even FIR filters with non-zero feedbacks, which make them the same order of IIR systems, one needs to simplify the analysis of product-separable 2-D IIR filter design for higher orders. And this method also needs to be automatically adaptive from one set of coefficients to another.

A computer assisted analysis always serves this purpose. In this chapter, a computerized analysis methodology and algorithm are proposed and the 2-D response of medium order filters are studied.

4.1.1 Algorithm Selection

Based on the purpose of this computerized system, the requirement can be described as following:

- (i) System must be adaptive for any 2-D product-separable filters with any orders;
- (ii) Computation result must give correct stable range area for any input set of coefficients;
- (iii) The computation complexity shall be as small as possible;

According to the properties of Schussler polynomial and also that they are sufficient and necessary conditions, as long as one finds the zeros of the mirror-image and anti-mirror-image polynomial of the denominator on the unit circle, one can easily determine if it is stable or not. And to find out the zeros for the two polynomials with order as same as the denominator, there are two possible methods:

Method 1: Just like the analysis carried out, one can use a certain computerize algebra equation solving program to get the answers for the mirror-equation and anti-mirror-equation as following:

According to (1.19)~(1.27), with given conditions including parameter k and $D(z)$'s coefficient elements, the final coefficients of denominator $[D(z)-kN(z)]$ and its mirror-image and anti-mirror-image polynomials contain k and those elements. Then one can get a bunch of equations with unknown variables of α_i and β_i . For order less or equal to 3, single-variable/single-order equations can be obtained, which are easy to

solve.

Therefore one can get single-variable/single-order equations with variable of k according to (1.24) and (1.27) so that the stable ranges are obtained. However, with order of five or higher, multi-variable/multi-order equations with α_i and β_i are obtained, which are too complex to solve with either derivation or computerized algebra programs.

So this method can be accurate but only works with lower orders. The computation complexity depends on the specific one-variable/one-order algebra derivation program.

Method 2: To avoid solving those multi-variable/multi-order equations and make this method universal with any order, an approximation way can achieve this purpose.

For a certain value of k and a certain set of coefficient values, the program detects if those stable conditions of the system are satisfied or not. Or with a certain given range of k , the program can scan with certain step values through the range and output the approximately stable sub-ranges among it. These ranges can allow the designer to have a rough idea about the available ranges of k . Any chosen k value can be further verified with the same program to ensure it finally.

The algorithm is this: For a certain set of k and coefficients, mirror-image and anti-mirror-image polynomials are determined. Then one can scan the upper semi-circle of the unit circle from -1 all the way to 1 with an adequate small step values as shown in Fig.4.1. Every complex z value is taken into the two polynomials and we get an array for each polynomial. Consider functions:

$$G_1(z) = |F_1(z)| = \left| \sum_{v=0}^n d_v z^v \right| \quad (4.1)$$

And

$$G_2(z) = |F_2(z)| = \left| \sum_{v=0}^n g_v z^v \right| \quad (4.2)$$

For $|z|=1$ and $\text{Im}(z) \geq 0$, as shown in Fig.4.1, one can get a non-negative curve, which may touch the horizontal axis at certain points. And if those location points for $G_1(z)$ and $G_2(z)$ are all their zeros and they separate each other, this situation will satisfy the stability conditions.

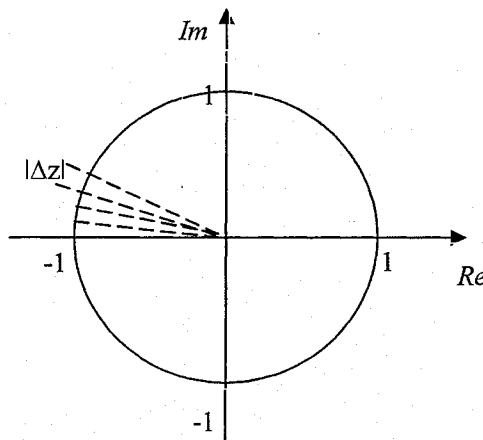


Fig.4.1 Variable z picked from -1 to 1 on the unit circle with small step value of Δz

In order to determine if a very low point of the curve is a zero point or not, it is assumed that in the very close neighbourhood of a real zero point or a regional lowest point of this function, the curve is monotonous with each side of the zero point. The small neighbourhood here means that it is far less than the minimum distance between any two zeros. $|\Delta z| \ll |z_i - z_j|, (i \neq j)$, z_i and z_j denote any zeros.

So in computerized approximation, the first scan step value must be far less than $\frac{1}{n}$ to ensure that at least three of the step points can be located inside a zero candidate

point's left and right neighbourhoods. The zero candidate neighbourhoods can be detected by getting the derivative from the samples of the curve. Then the regional lowest bottoms are picked as zero candidates. Because of the monotonous characteristics, one can use a much less step value to re-scan between the left and right point beside the zero candidate point. And then the newest zero candidates are picked with their own neighbour points at this stage, because it is known that the real zero point may be located between these neighbour points. Then one can continue this work by decreasing the step value for each stage until a preset threshold value is reached. The threshold value depends on the precision of the computer system or, for example 10^{-6} or even smaller. Once the threshold is reached and this point can be approximately regarded as a zero point, otherwise the candidates will be discarded.

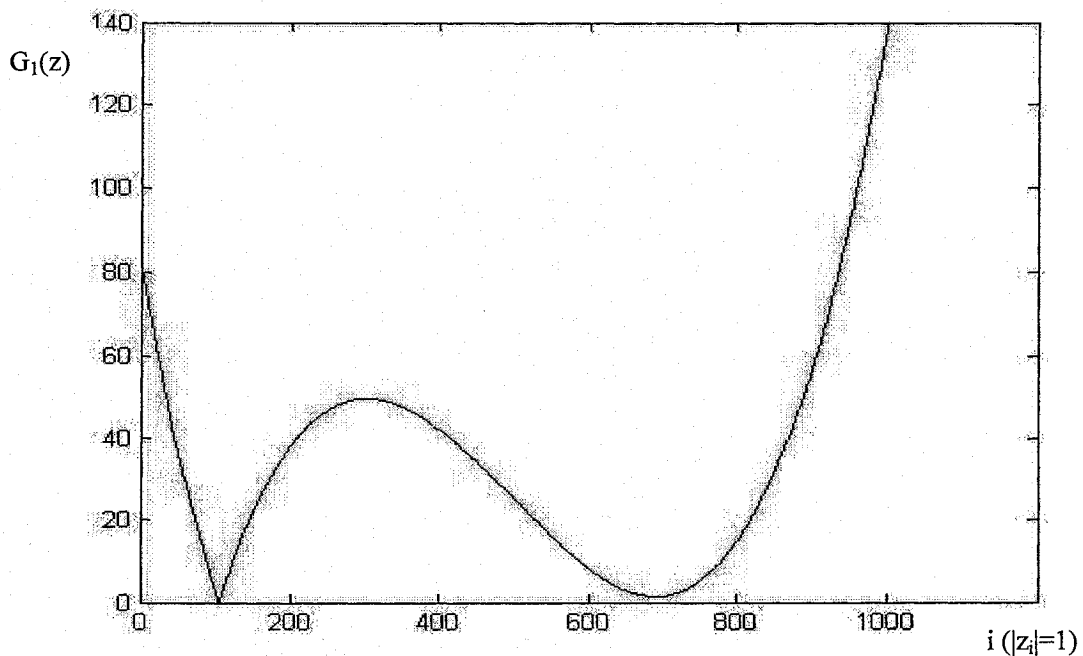


Fig.4.2 Example of $G_1(z)$ along semi unit circle, $n=6$, $|\Delta z| = 0.001\pi$, i : Sample number

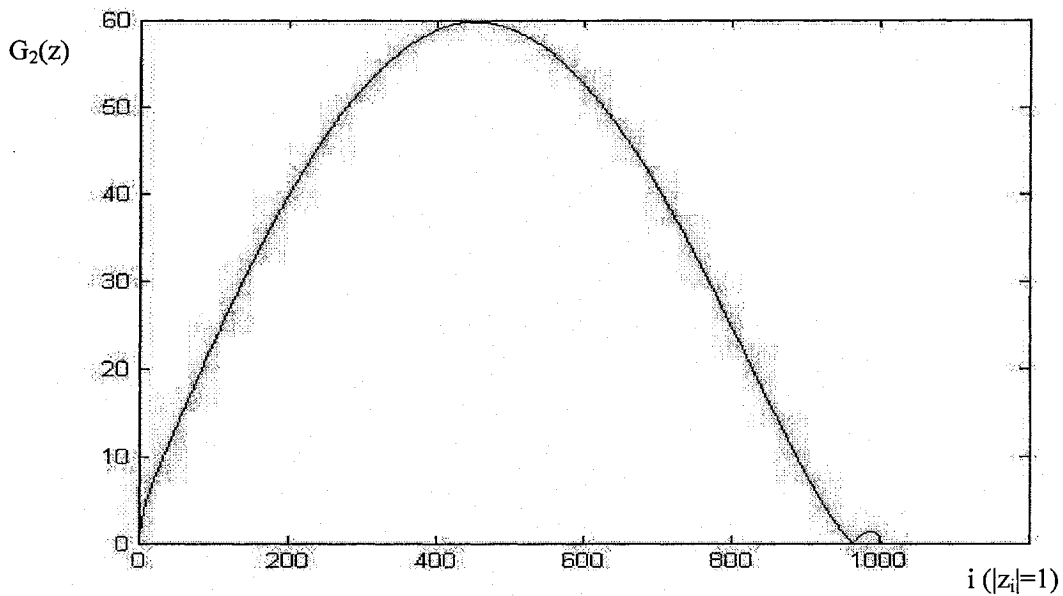


Fig.4.3 Example of $G_2(z)$ along semi unit circle, $n=6$, $|\Delta z| = 0.001\pi$, i : Sample number

Fig.4.2 and Fig.4.3 show examples of 6 order with $\Delta z = 0.001$, $G_1(z)$ can have two zero candidates and can eliminate the false one, while $G_2(z)$ has 3 zeros.

The remaining thing is to pick a certain step value of k and do the scanning within the interesting range. Each k is inputted to the program above and marked as stable or unstable based on the result of the judgment. A sub-range that starts from the first encountered stable k value and ends at the last consecutive stable one is the approximate stable area of k . Still the step value of k needs to be small enough, say, $|\Delta k| \ll \frac{C_a}{n}$, to avoid possibly having some unstable areas between two neighbour samples of k . (C_a denotes the average value of the coefficients)

This method is easier to implement. It also shows a great improvement of computation complexity because of Schussler's theorem. Comparing with the basic stability theorem, the scan is in 1-D domain (the semi unit circle) only, while for the other

the whole area inside the unit circle needs to be scanned, which is 2-D domain and the zeros need to be found out. So the computation complexity relation ratio of them is approximately $2r:r^2$ (r denotes the scan points on the semi unit circle).

The disadvantage of this method is that it is an approximation. One cannot get a determined cut-off point through it. The computer precision, choose of step values and threshold values of zero affect the computation time and the boarder's clearance.

4.1.2 Implementation and simulation

4.1.2.1 Algorithm flow chart

Fig.4.4 shows the flow chart of the algorithm(method 2):

The simulation programming is done with Matlab 7.0.

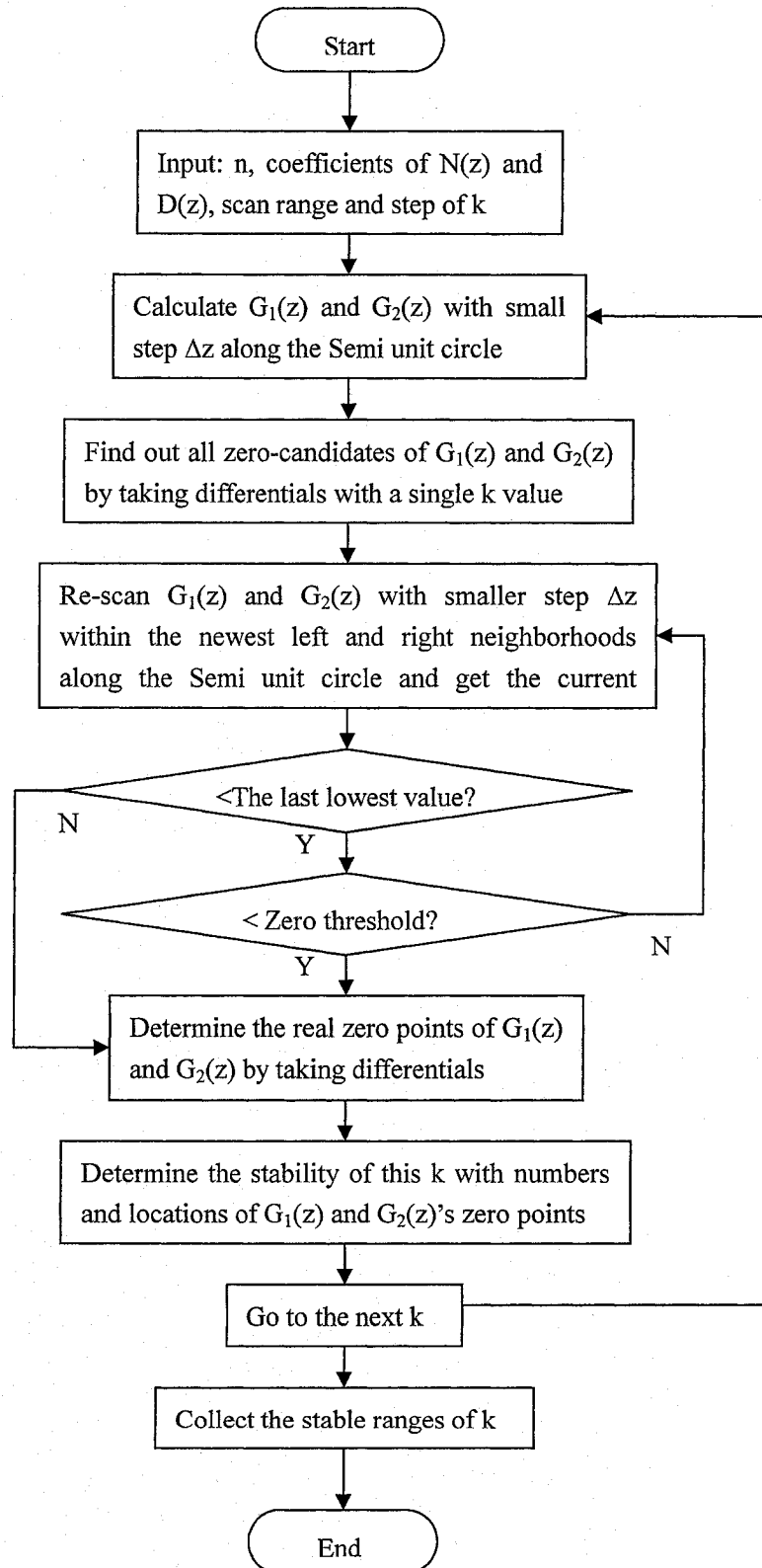


Fig.4.4 The flow chart of the algorithm

4.1.2.2 Implementation examples

A 6th order Butterworth low-pass filter with pass-band of 0.5π is chosen. The coefficients of $N(z)$ and $D(z)$ are obtained from Matlab function *butter()* and listed in Table.4.1. The calculated stable range of k is shown in Fig.4.5. The range of k is chosen from -4 to 4 because there is no more stable area far away from the average level of all the coefficients. The system frequency response for all the stable area of k is shown in Fig.4.6 (it is forced to zero within the unstable area).

Table 4.1 Example of high order coefficients

Order #.	0th	1st	2nd	3rd	4th	5th	6th
N(z) coefficients	0.0296	0.1775	0.4438	0.5918	0.4438	0.1775	0.0296
D(z) coefficients	1.0000	0	0.7777	0	0.1142	0	0.0018

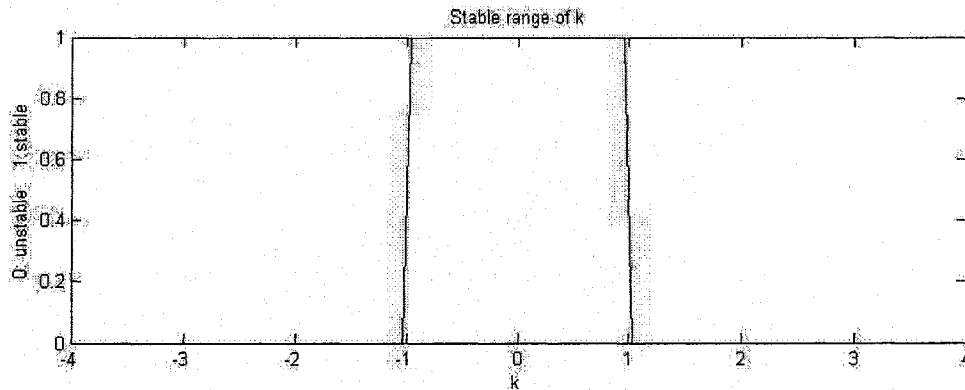


Fig.4.5 Calculated stable range of k ($\Delta k = 0.08$, $|\Delta z| = 0.001\pi$)

With smaller Δk one can get closer to the real boarder, so the stable range of k for this filter is approximately within $-1\sim 1$. The actual running time of this example by using PC (Intel Pentium CPU, 1.4GHz, 256MB SD RAM, Windows XP) is 8437 ms.

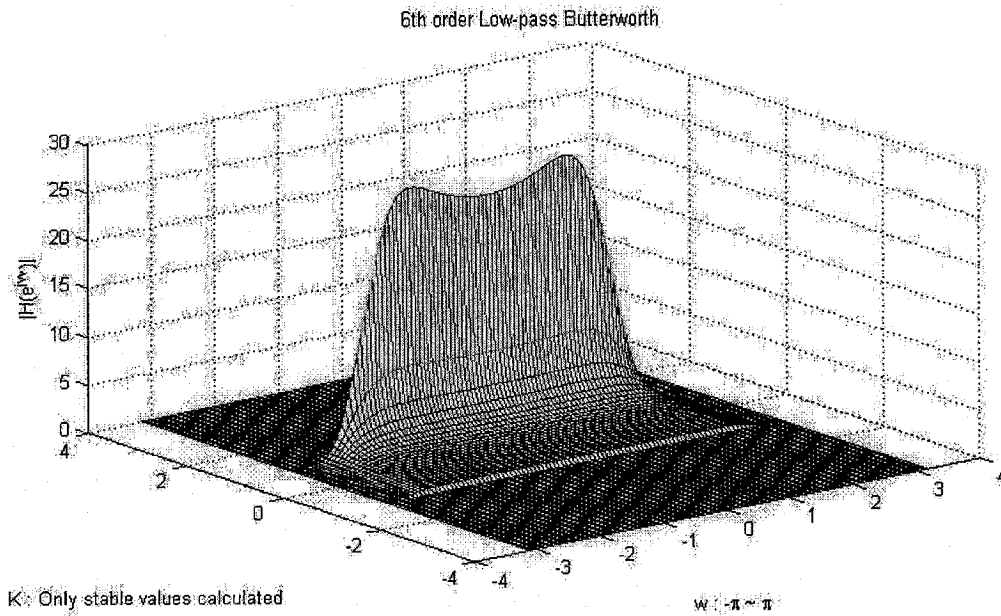


Fig.4.6 1-D response with stable range of k

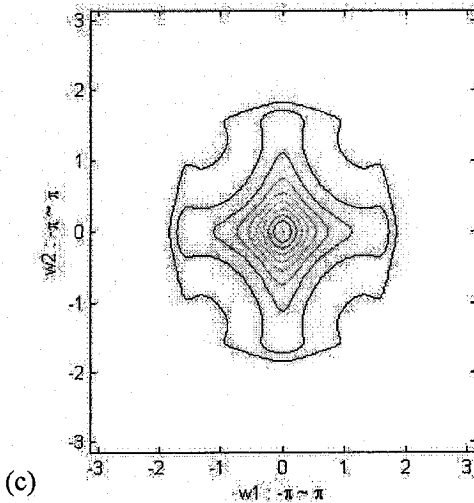
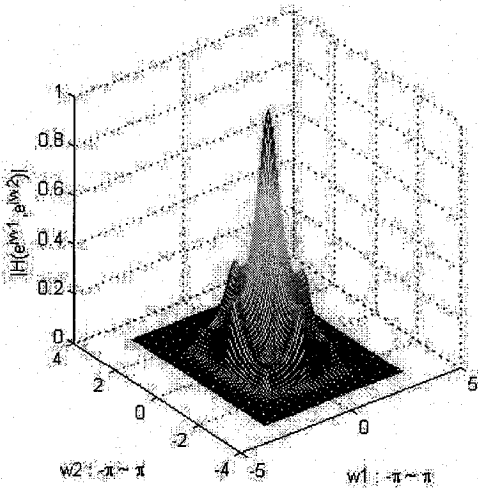
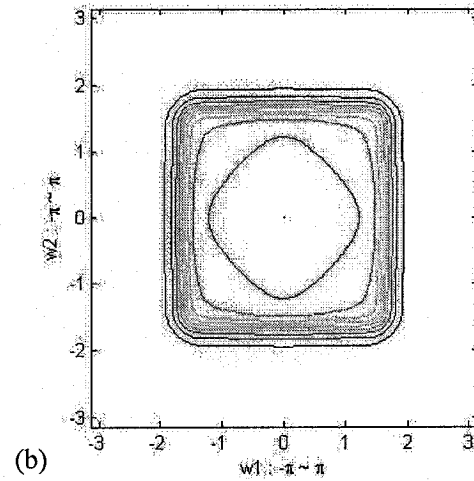
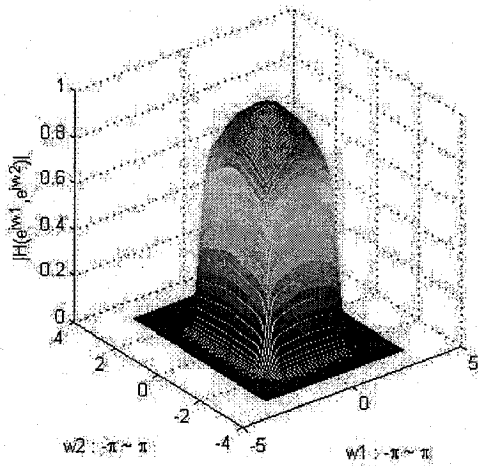
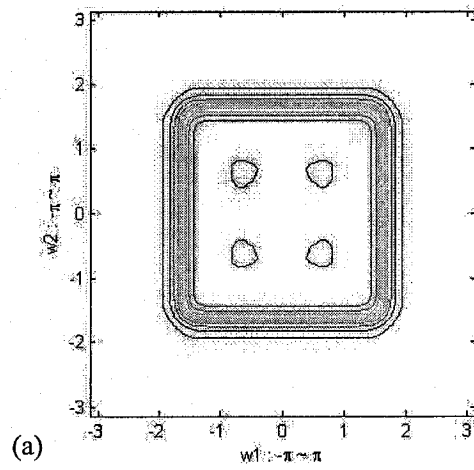
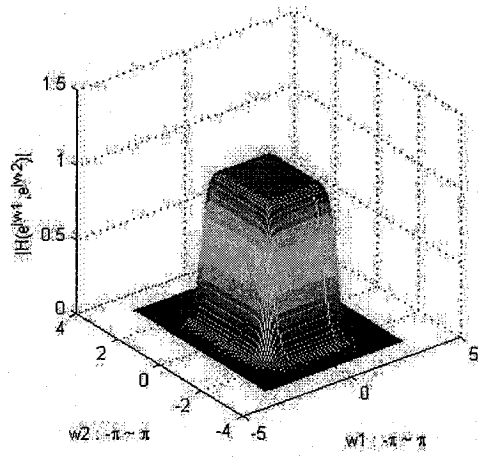
As one can see from Fig.4.6, with different stable k values, the shape of the 1-D response of the system changes accordingly and remains stable.

Simulation results have been verified by comparing the them with the derivation results obtained in Table.3.1.

4.2 2-D response of higher order filters

4.2.1 IIR filters

The 6th order Butterworth Low-pass and High-pass filters are chosen here. And for simplicity, only same filters with same k values for two dimensions are illustrated. The variable k value are picked within their calculated stable ranges.



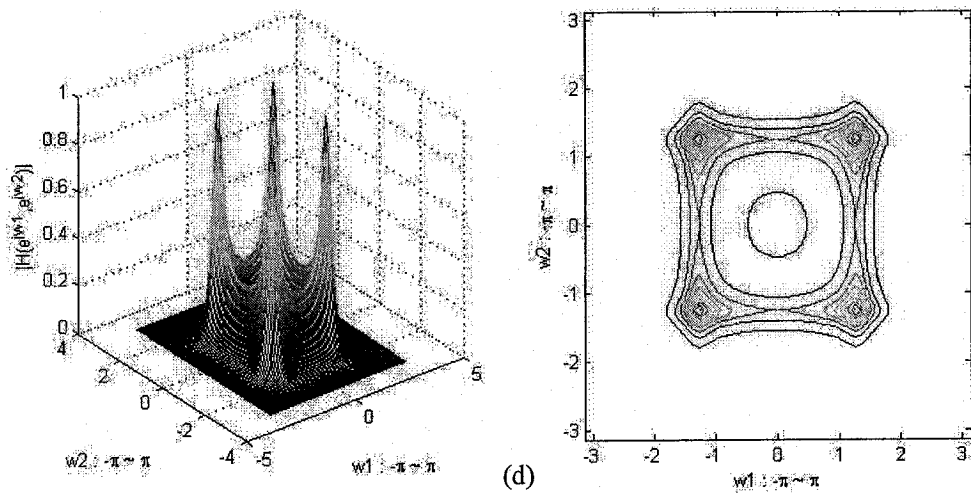


Fig.4.7 2-D response with 6th order Butterworth low-pass filters(0.5π)

(a) $k_1=k_2=0$; (b) $k_1=k_2=0.05$; (c) $k_1=k_2=0.55$; (d) $k_1=k_2=-0.55$

For the low-pass filters, the positive feedback values give us smaller pass-band with near-circular symmetry, the edge of the pass-band is rounded off. While the negative values sink the low-frequency in the pass-band and make the filter become near-band-pass filter. The flatness in the stop-band remains.

Like low-order responses, the octagonal symmetry holds and near-circular symmetry can be obtained with certain k values.

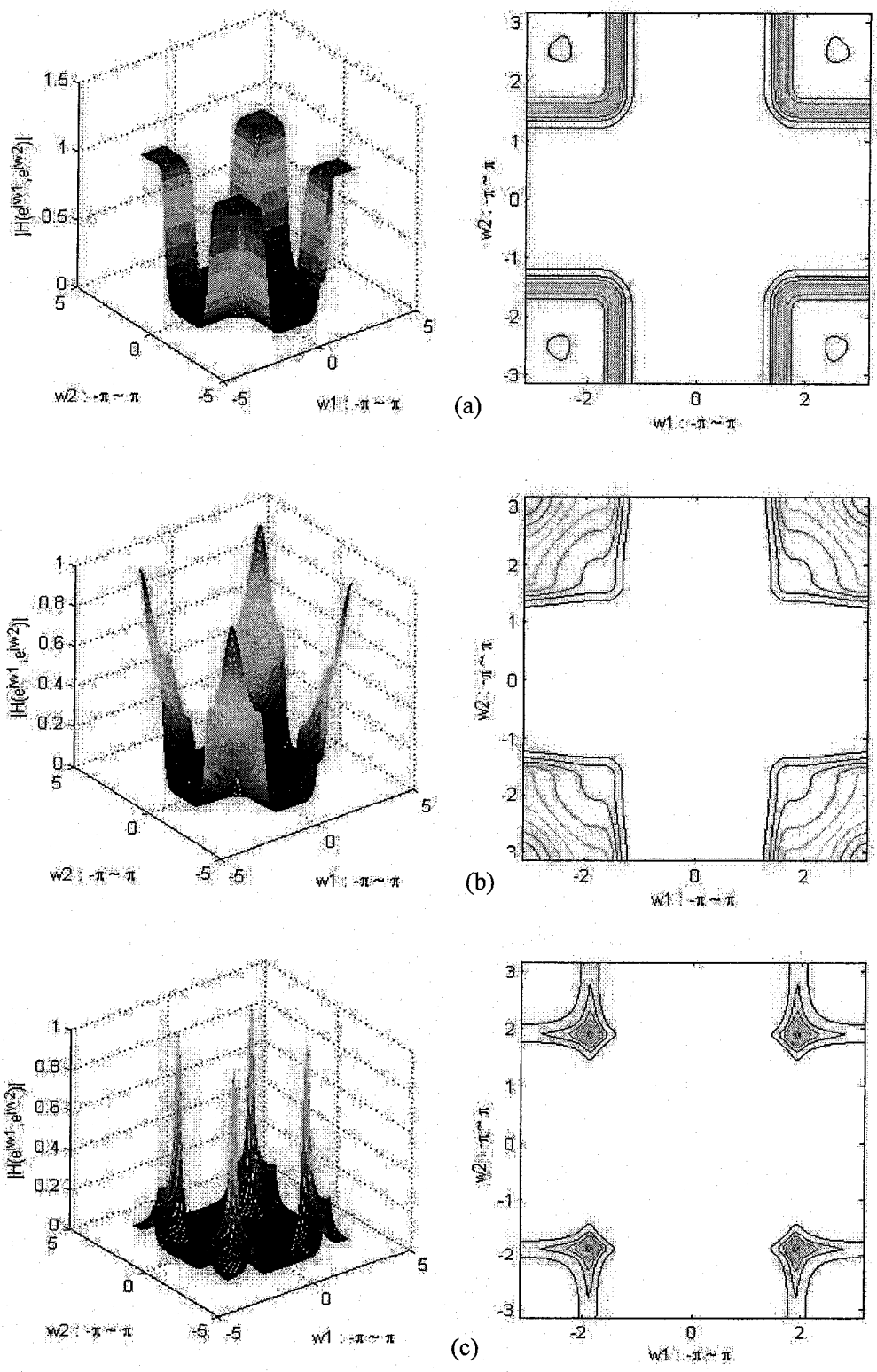


Fig.4.8 2-D response with 6th order Butterworth high-pass filters(0.5π)

(a) $k_1=k_2=0$; (b) $k_1=k_2=0.3$; (c) $k_1=k_2=-0.7$

For the high-pass filters, the positive feedback values give us smaller pass-band with the pass-band edge being rounded off, while the negative values sink the high frequency in the pass-band and make the filter become band-pass filter. The flatness in the stop-band remains. The octagonal symmetry holds and near-circular symmetry can be obtained with certain k values.

As one can see from above, since higher-order filters' pass-band characteristics are affected by multiple poles, once the locations of these poles change and the shape of the response becomes complex patterns.

Furthermore, instead of putting a feedback to get variable characteristics by changing all the poles, one can also work inside the IIR filter's coefficients. Any change of the numerator does not affect the stability hence it is not the concern. And it also may ruin the stop-band flatness because the zero locations are changed. So when working with the denominator, each time only one coefficient needs to be changed and this coefficient is regarded as a variable a_i . By using the similar algorithm the stable range of this coefficient can be obtained.

Fig.4.9 and Fig.4.10 show examples of 6th order Butterworth filters with modified but still stable coefficients:

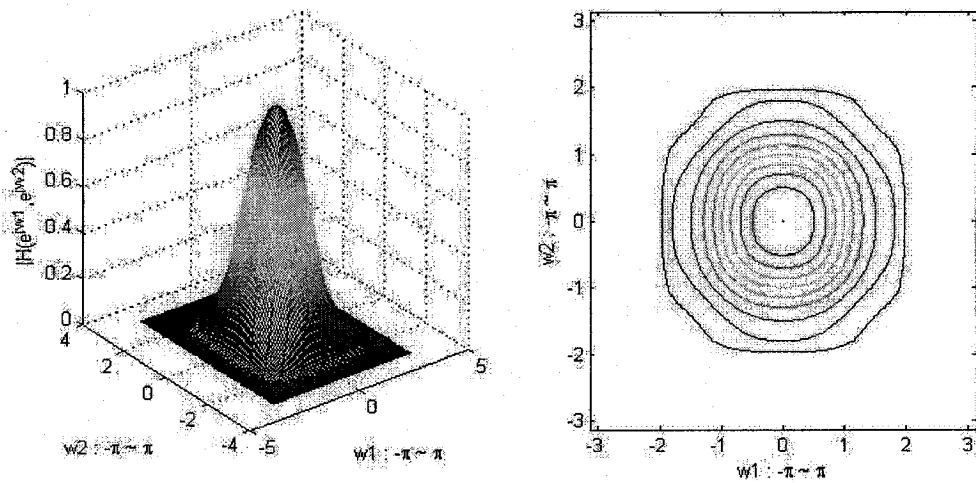


Fig.4.9 2-D response of modified 6th order Butterworth low-pass filter

Coefficients a_2 and a_3 are changed to 0.5558 and 0.2959

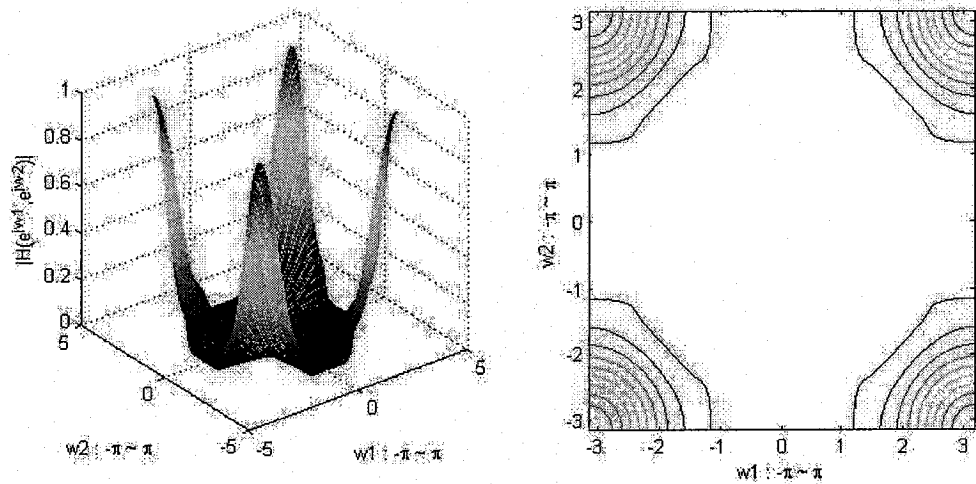


Fig.4.10 2-D response of modified 6th order Butterworth high-pass filter

Coefficients a_2 and a_3 are changed to 0.467 and 0.3965

By carefully changing one or more coefficients of the denominator under the stability conditions, one can get variable characteristics like very-near-circular symmetry with unchanged stop-band flatness.

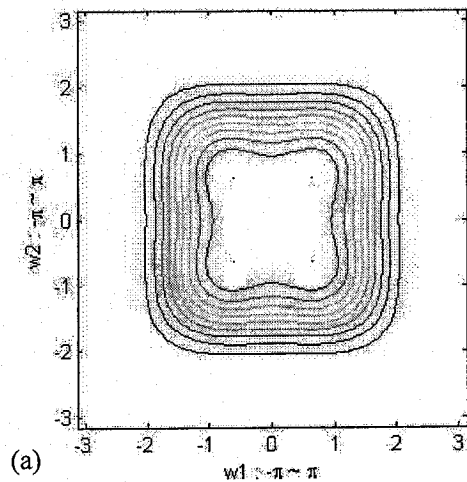
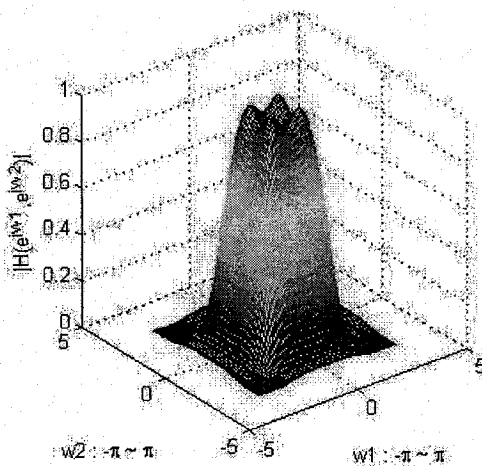
4.2.2 FIR filters

Since there exists a large variety of kinds of FIR filters, so once the stability detection is solved, one can even use an FIR filter with a feedback loop, which makes the whole system become an IIR system. The analysis method can be used the same way with $D_1(z_1^{-1})=1$ and $D_2(z_2^{-1})=1$.

The following example of 6th order FIR filters are generated by Matlab function *firhalfband()*. The coefficients are shown in Table.4.2.

Table 4.2 Example of high order FIR coefficients

Order of z^{-1} .	0th	1st	2nd	3rd	4th	5th	6th
$N(z^{-1})$ coefficients	-0.0635	0	0.3007	0.5000	0.3007	0	-0.0635
$D(z^{-1})$ coefficients	1.0000	0	0	0	0	0	0



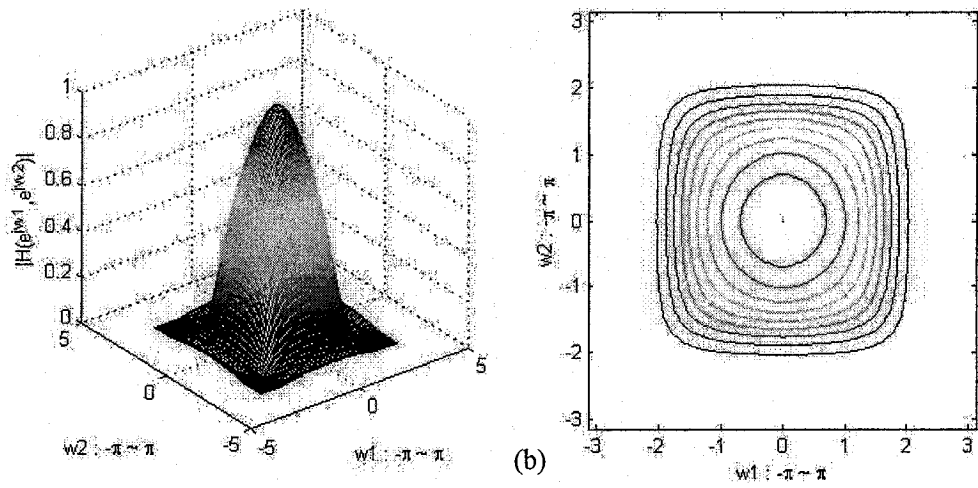


Fig.4.11 2-D magnitude response of 6th order FIR high-pass filters with feedbacks

(a) FIR with feedback $k_1=k_2=0$; (b) $k_1=k_2=0.1$

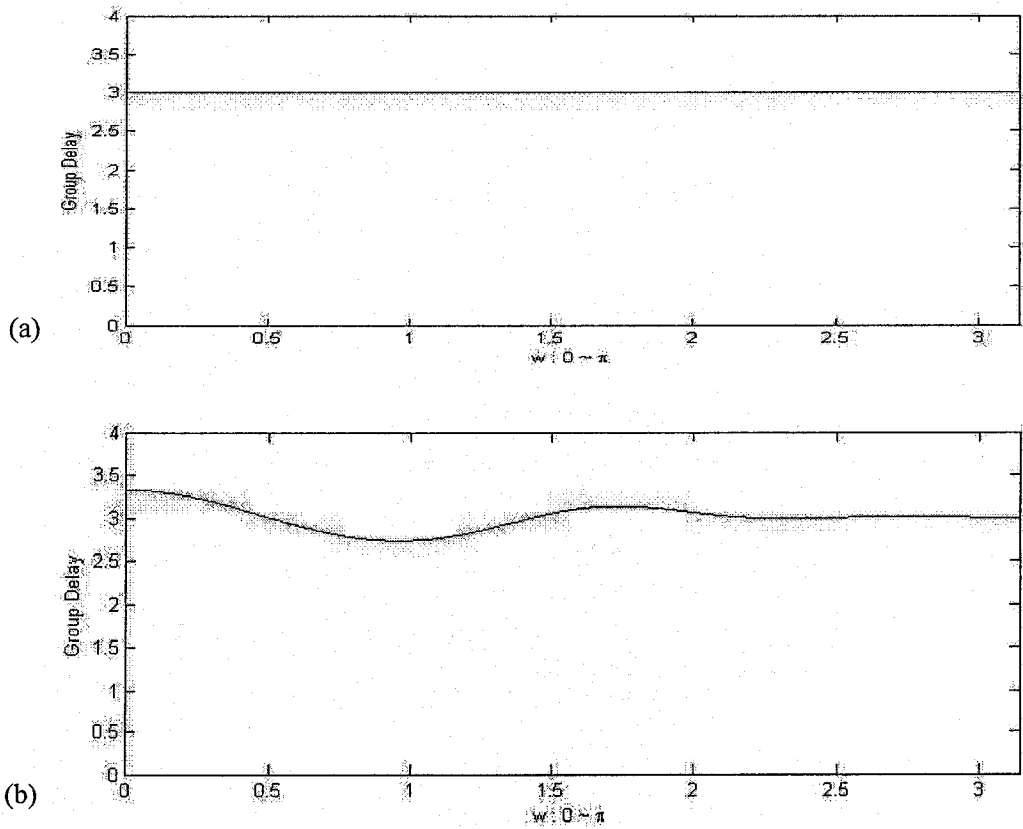


Fig.4.12 1-D group delay of 6th order FIR high-pass filters with feedbacks

(a) FIR with feedback $k=0$; (b) $k=0.1$

As one can see from Fig.4.11 and Fig.4.12, by using FIR as the original filters, variable magnitude of near-circular symmetry can be obtained. And also since a small value of feedback is used, the 1-D group delay of the new constructed IIR filters is near constant. Since the 2-D system studied is product-separable, the 2-D group delay is simply the two 1-D group delays in each dimension.

Since FIR filters have the advantages including linear phase and constant group delay, which is suitable for application of image processing without worrying about the stability, one can take this advantage and get variable magnitude characteristics simultaneously with stable response.

4.3 Summary

In this chapter, first a computer assisted analysis algorithm has been discussed and proposed to conduct the analysis and get the approximate stable ranges of feedback gain. Two methods have been discussed and the approximation method is chosen, which can work for filters with any orders with relatively low computation complexity. This algorithm is based on the same stability theorem used for analysis with 2-D lower order IIR systems. Implementation and simulation are conducted with high order frequency response samples and low-order analysis results in Chapter 3.

By using this algorithm, the analysis is then extend to higher order systems composed of high order IIR or even FIR filters with unique feedbacks, which are able to be adjusted to offer us variable characteristics uniquely.

The high order 2-D frequency responses are illustrated first with 6th order Butterworth filters with same variable feedbacks in both dimensions. Different k values change the pass-band characteristics significantly. Multiple patterns with octagonal or even near-circular symmetries can be obtained. Thereafter by changing one or more coefficients of the denominator, one can get very-near-circular symmetrical response.

Having solved the stability detection for any order of IIR filters, FIR filters with feedbacks are also studied. With $D_1(z_1^{-1})=1$ and $D_2(z_2^{-1})=1$, variable characteristics of 2-D response of FIR filters are observed. But most importantly, by using small values of k , a near-constant group delay in each dimension can be obtained while pass-band characteristics are changed significantly. It is enlightening to make balance between 2-D response of magnitude and dimensional group delay in 2-D filter design.

CHAPTER 5 2-D Applications and Simulations

5.1 2-D filters derived from low-pass and high-pass filters

Having obtained 2-D low-pass and high-pass IIR VCTF filters, one can then derive other 2-D filters such as band-pass and band-elimination filters by connecting them in parallel and cascade respectively. For simplification, same k values are used for both low-pass and high-pass filters.

6th order Butterworth low-pass and high-pass filters are still considered with certain cut-off frequencies. For band-pass filters, the two pass-band frequencies overlap to get a common pass-band as shown in Fig.5.1, while band-elimination filters are built with non-overlapping pass-band frequencies to get a common stop-band as shown in Fig.5.2:

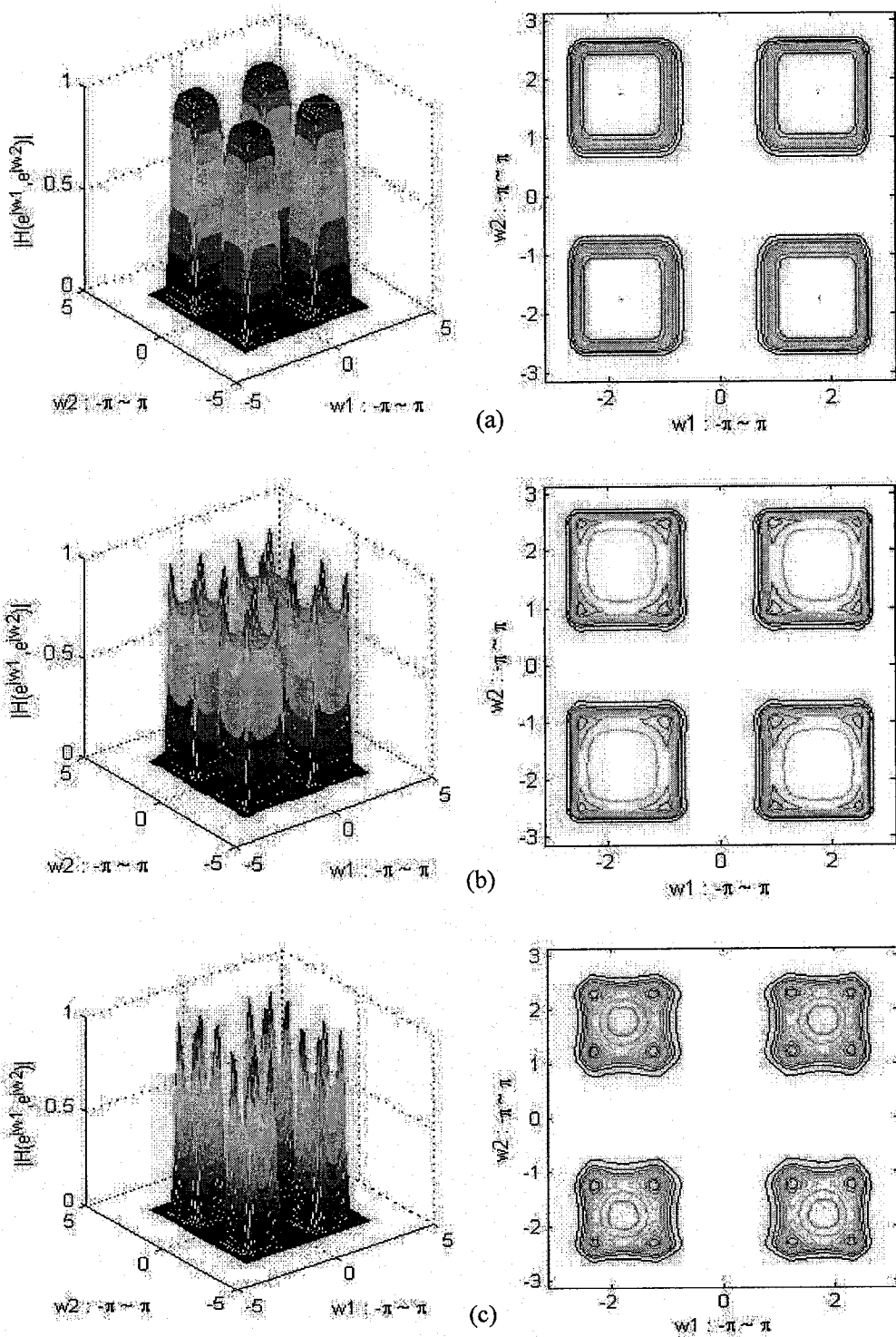
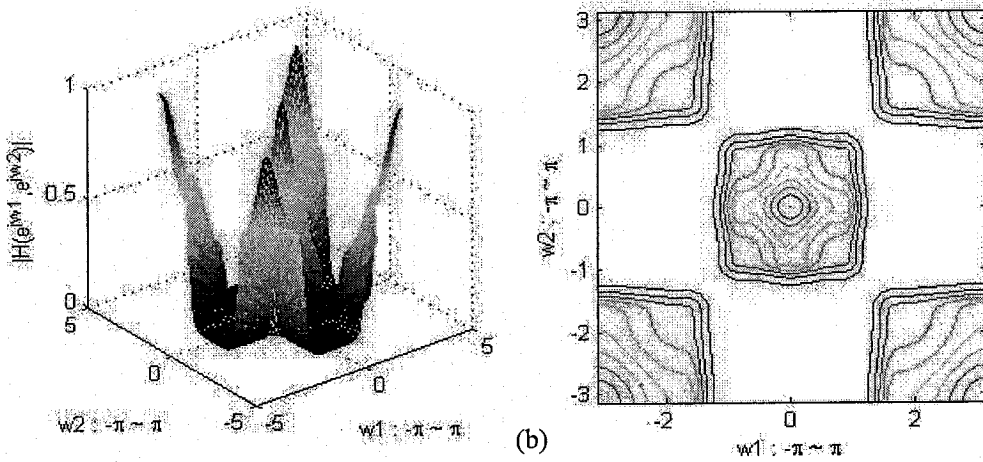
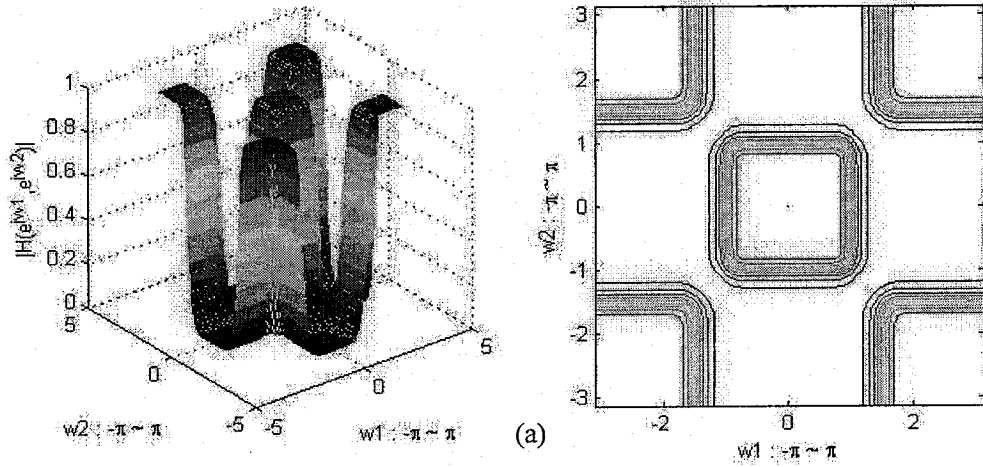


Fig.5.1 2-D band-pass filters built with 6th order Butterworth filters

Pass-band: $0.3\pi \sim 0.8\pi$; (a) $k=0$; (b) $k=0.5$; (c) $k=-0.5$

As one can see from above, for composed 2-D band-pass filters, positive k values strengthen the corners of the four pass-band areas while negative values sink the centers of the areas. Octagonal symmetry holds still.



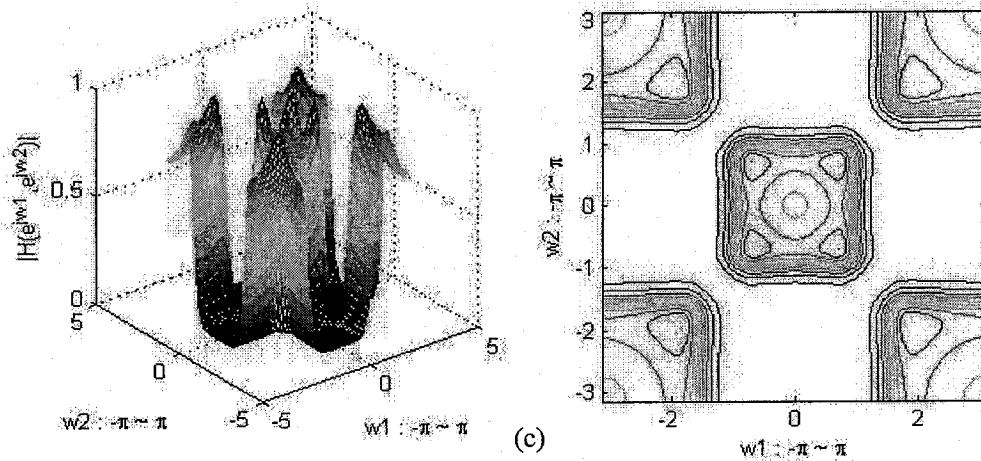


Fig.5.2 2-D band-elimination filters built with 6th order Butterworth filters
 Pass-band: $0 \sim 0.3\pi$, $0.5\pi \sim \pi$; (a) $k=0$; (b) $k=0.5$; (c) $k=-0.5$

For composed 2-D band-elimination filters above, positive k values round off the borders of the pass-band while negative values sink the center of the areas. Octagonal symmetry holds.

So for composed 2-D filters, by adjusting the two feedbacks, significantly variable characteristics of the component filters are obtained. Some other specific 2-D filters can also be expected by using different filters and different connections.

5.2 Space-domain response

According to digital image processing [11], images are applied to the stable systems to verify the effect of the 2-D processing. Some systems analyzed to be stable are simulated. For simplification, only square black/white digital images are used and their FFT [10] are taken. Then they are multiplied by the systems' frequency responses. For

filters other than high-pass, the 2-D frequency response at origin is scaled to 1 in order to keep the DC level of the image. For high-pass filters, the images are highlighted to be displayed properly. After taking I-FFT [10] of the product matrices, the time/space [11] domain matrices are displayed, which are the processed images.

Fig.5.1 shows two 256×256 pixel original images and their noised images with additive normally distributed noise (zero-mean, $\sigma = 15$)

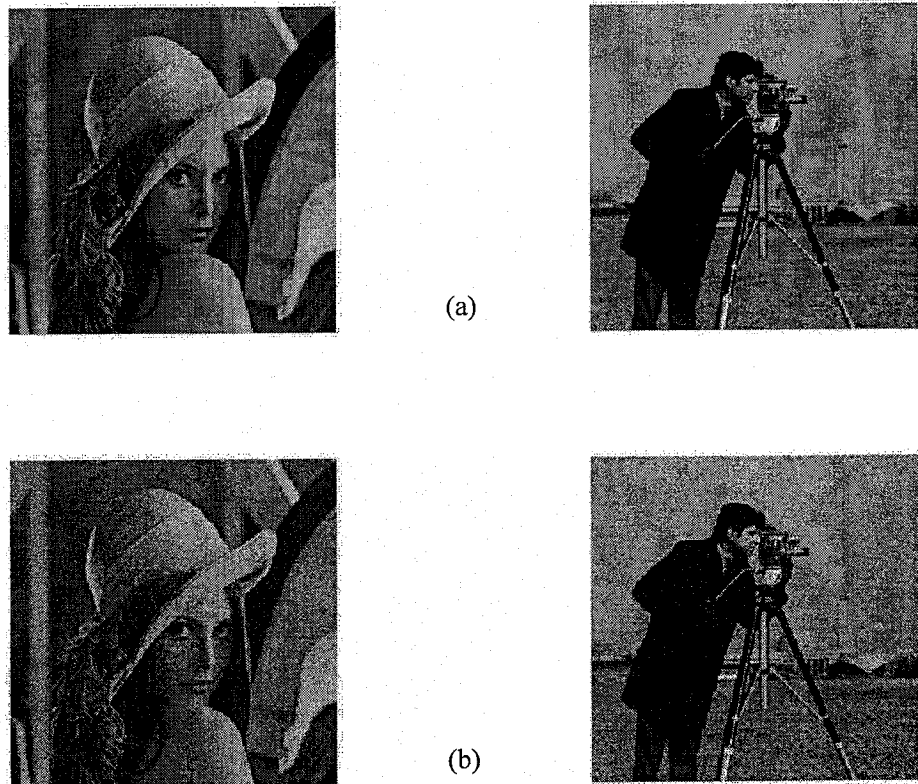
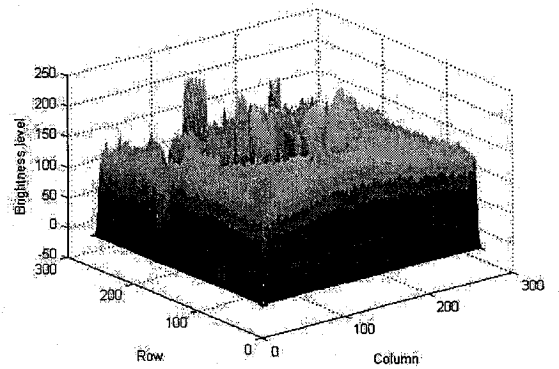
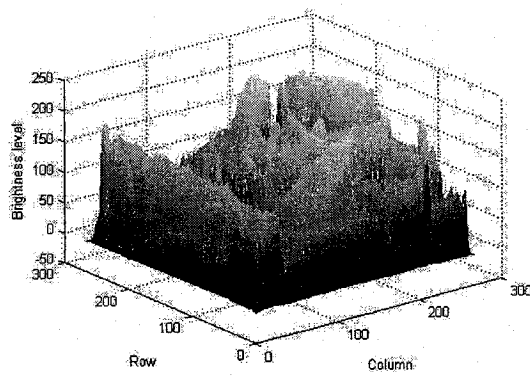


Fig.5.3 (a) Image Lena and Photographer; (b) Noised added images

In order to avoid signal aliasing [10], the images are first zero-padded before being processed. The results will have black backgrounds around the images, which can be ignored in image processing.



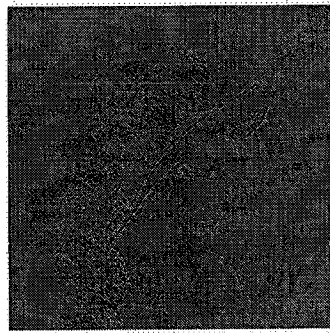
(a)



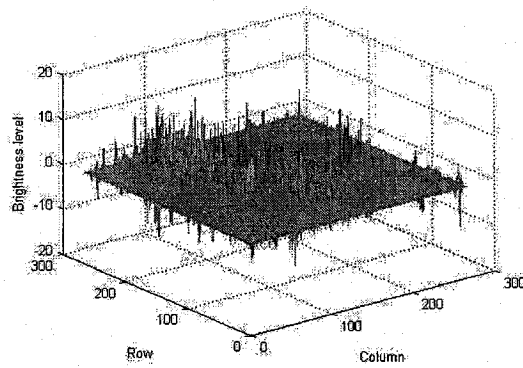
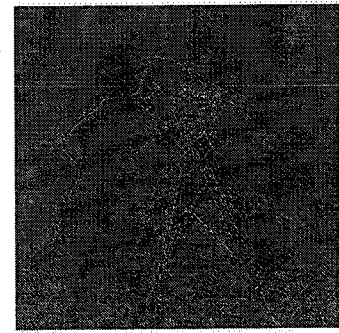
(b)

Fig.5.4 (a) Image denoised with 2-D LP11 Biquadratic filters ($k_1 = k_2 = 0.2$)
(b) Output matrix values

With low-pass filters like LP11 with a feedback loop, as shown above, the noised images are denoised by removing some high-frequency signals. The matrices show the stable responses in space domain.



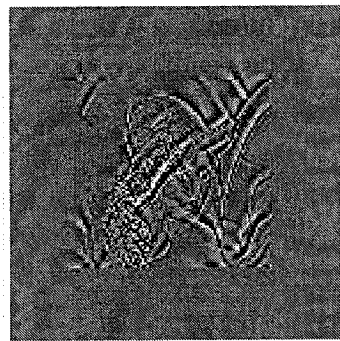
(a)



(b)

Fig.5.5 (a) Original images processed with 2-D BP01 Biquadratic filters ($k_1=k_2=0.2$);
(b) Output matrix values

With BP01 with feedback loop, which is a band-pass filter, the lowest and highest frequency signals of the images are removed. The remaining contours of the images show the medium frequency signals and the matrix show the stable response.



(a)

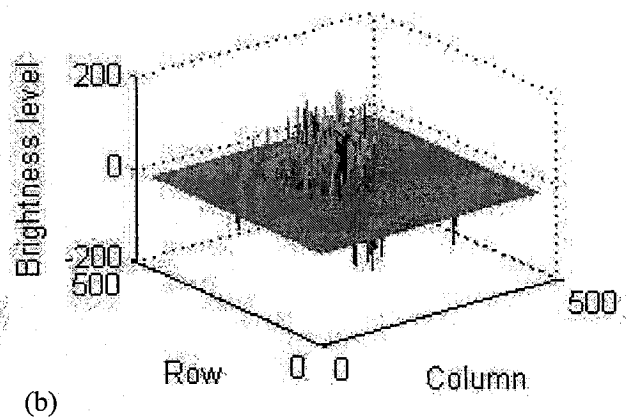
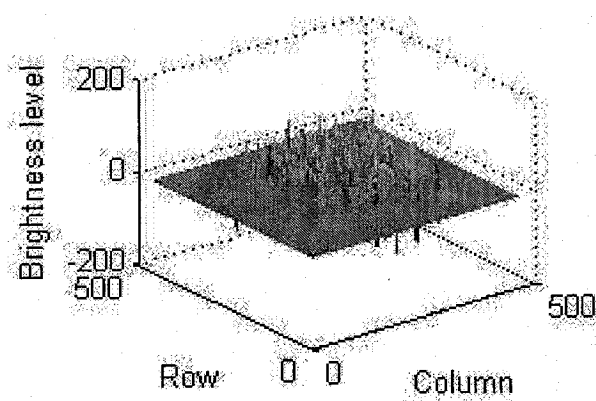
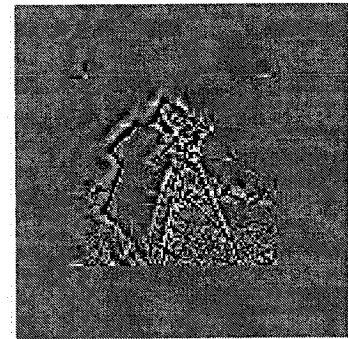
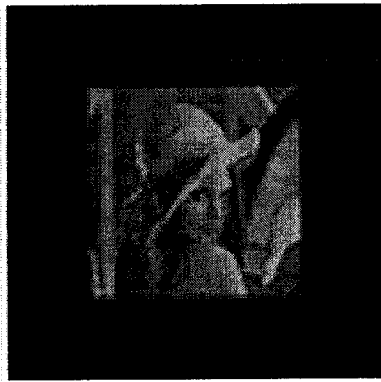


Fig.5.6 (a) Processed with 2-D Butterworth high-pass filters (2^{nd} order, 0.05π , $k_1 = k_2 = 0.1$); (b) Output matrix

With wide pass-band high-pass filters like 2^{nd} order Butterworth (0.05π) with feedback loop, the processed images contain more medium frequency signals as shown above. The matrices show the stable space-domain response.



(a)

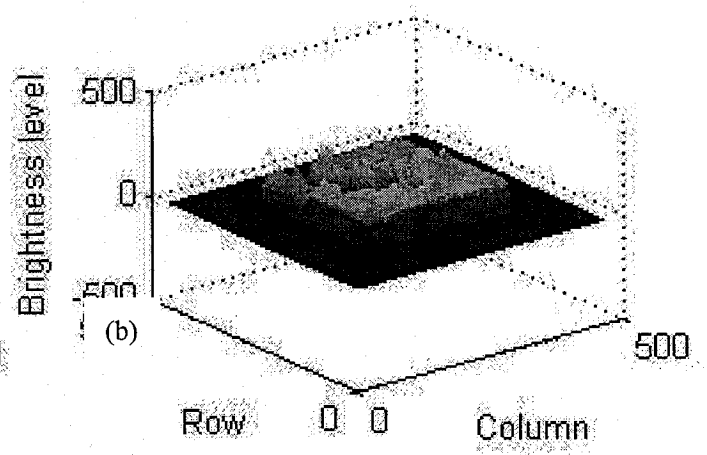
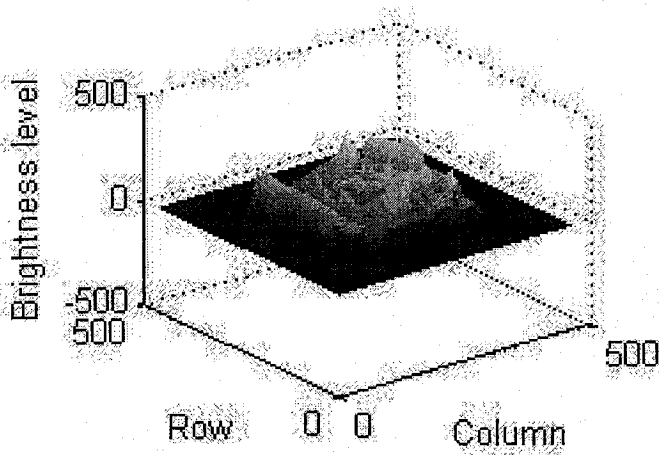


Fig.5.7 (a) Processed with 2-D Butterworth band-elimination filters ($0.15\pi \sim 0.5\pi$);

(b) Output matrix

With band-elimination filters with feedback loops, the processed images lose some of medium frequency signals as shown above. The matrices show the stable response.

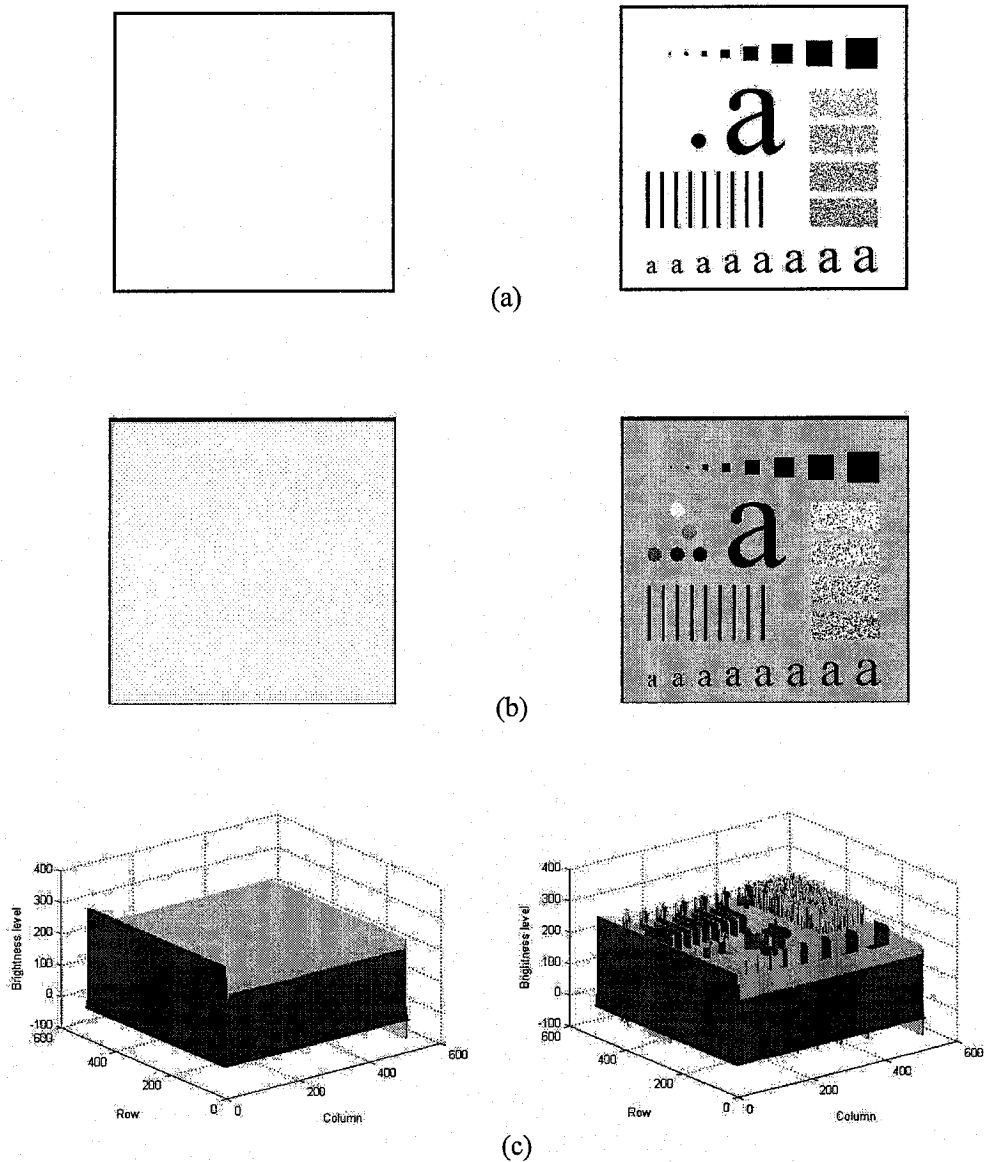


Fig.5.8 (a) Plain white and template images; (b) Processed with LP00-LP02 Biquadratic filters ($k_1 = k_2 = 0.1$); (c) Output matrix values

With plain white image and template images, dimension-unbalanced 2-D filters with same feedback values are applied. The processed images show the corresponding characteristics. For the white plain image that represents constant strong low frequency

impulses, and for the template image that stands for strong signals for all frequency components, there is no singularity in the space-domain response.

5.3 Summaries

In this chapter, 2-D band-pass and band-elimination filters are first built with low-pass and high-pass filters containing feedbacks. The same feedback values for the two component filters are considered and the 2-D responses are illustrated. These changes of feedback hence cause variable characteristics of the built filters as shown in frequency domain. Different changes of the pass-band characteristics with positive and negative feedback values are observed and discussed.

Then in order to briefly illustrate the applications in image processing field, which represents space-domain response, some of the 2-D filters with stable k values in previous chapters are used to process digital images.

For 2-D low-pass filters, the most frequent application is image denoising. Images with additive random noise have been denoised by the low-pass filters with feedbacks. Also for other filters like high-pass, band-pass and band elimination filters with feedbacks, the corresponding effects are shown after the processing with original images.

To further emphasize the stability warranty in the system design in time/space domain, a white plain and a template images, which represent strong signal impulses, are processed and no singularity occurs.

CHAPTER 6 Conclusions

6.1 The investigations carried out

For 2-D system designing with IIR VCTF filters, it has always been a main concern that the system stability needs to be known. The complexity of stability analysis limits the use of IIR filter bank. A simple and solid way of stability analysis is needed.

The product-separable 2-D discrete VCTF system is composed with two cascaded 1-D IIR systems with a feedback for each system has been analyzed. This stability analysis is strictly based on Schussler's theorem and one of the methods of generation of VSHP. The results focus on the feedback value range with respect of coefficients of the 1-D sub-systems.

After the introduction of the theorem, an equivalent and more explicit expression is given, which plays an important role in the following analysis. For simplification, typical types of 1-D filters with order up to 2 such as Generic Biquadratic filters are considered. Conditions of feedback value k are obtained with respect of typical coefficients of the system's numerator and general form coefficients of the denominator.

The 2-D system stable conditions rely on their two 1-D sub-systems. Conditions of k_1 and k_2 can vary with different forms of filters chosen. Butterworth filters are considered for purpose of simulations. Once the denominator is determined to be Butterworth's form, the equations of k can be solved and the range for stability is obtained for each type of

Biquadratic Butterwoth filter. Then different combinations of non-singularity 2-D frequency response are simulated with certain stable feedback values.

Before observing 2-D frequency responses in Chapter 3, some important specifications for 2-D filter design like quadrantal and circular frequency requirements are introduced. The observation starts from lower order 2-D filters response with real numbers. Four different situations are considered, namely: same filters in z_1 and z_2 domains with the same values of k ; same filters with different values of k ; different filters with same k 's; different filters with different k 's. Octagonal, quadrantal and near-circular symmetries can be observed and many kinds of variable dimension-unbalanced characteristics are obtained.

In all these situations, the 2-D magnitude responses vary significantly within stability range of k . Hence different kinds of 2-D requirements can be achieved or approached. The corresponding trends of changes with positive and negative k values within pass-band are observed and briefly discussed.

In order to simplify the analysis with this theorem and also make it adaptive for any order including high orders, a computerized analysis method has been proposed and simulated. The algorithm of this method is one of approximation and is analyzed. It has less computation complexity than other methods and most of its computations focus on the semi-unit circle with the two mirror-polynomials. The principle is strictly based on the stability theorem in Chapter 1 and 2. With any input of coefficients the approximate stable range of k can be obtained. The algorithm is verified with the analysis results in

Chapter 2 and also with high order examples.

Since the stability analysis for this kind of 2-D IIR system is completed, and also a computerized approximation is proposed and proven to be robust, the design work can be extended to wider scopes and higher efficiency. The simplicity of the stability analysis can also allow medium or higher order IIR and FIR system consideration for special applications. The higher order 2-D frequency responses are illustrated in Chapter 4 with IIR and FIR filters with feedbacks. Similar observations and discussions are conducted and the characteristics of near-constant group delay are emphasised.

So for both lower and high order systems, 2-D separable digital filters with variable feedbacks, one can obtain variable characteristics with stable systems. The magnitude characteristics can cover most of the symmetry specifications.

Then in Chapter 5, further stability verification is done by composing 2-D filters with the fundamental filters and using different 2-D systems to process digital images. The 2-D frequency responses of designed filters are shown with same variable k values in the component filters. The symmetries and changes of the characteristics are corresponding to the two filters.

For applications in image processing, different 2-D filters with feedbacks are applied to images. Corresponding results like denoising or contour extraction are observed and the stability in space domain is confirmed with template image processing.

So, the strict and efficient stability analysis for product-separable discrete 2-D filter design with variable characteristics has been achieved.

6.2 Related and future works

There exist many researches about 2-D VCTF filter design from analog domain, and by using generalized bilinear transformations, the 2-D VCTF digital filters are obtained. The design of 2-D discrete VCTF IIR filters with dimension-independent feedbacks directly in digital domain is firstly studied in this thesis.

Having done all these analysis, proposal of algorithm, simulations and observations, future works related to this thesis could be focused on with the following aspects:

(i) Research of relationship in detail between the feedback, coefficients and the characteristics of response, which can allow us to reach the specification easily;

For different kinds of given filters, a mapping can be established between the feedback gain and the pass-band frequencies, flatness within pass-band and variance of group delay, etc; And also in some cases the relationship between the feedback and the symmetries of frequency response can be studied in details, say, the extent of approaching to circular symmetry. Such a relationship can also lead to algorithms for us to design dynamic adaptive 2-D filters with this structure.

(ii) Research of similar structures with additional variable numerators in each dimension;

Since the studied system structure has variable denominators, which mainly changes the pass-band characteristics because of variable locations of poles, one can also consider simultaneous changes in the numerators. Therefore variable stop-band characteristics can also be obtained because of the changes of the zero locations.

(iii) Research of non-product-separable digital IIR systems with additional universal feedbacks for variable characteristics;

So far only product-separable systems have been considered, if an additional feedback gain is applied for the whole system, it will become a non-product-separable system. Predictable variable characteristics will be obtained and the stability needs to be studied.

References

- [1] M. E. Van Valkenburg, "Analog Filter Design", Holt, Rinehart and Winston, 1982
- [2] A. Antonious "Design Filters: Analysis, Design and Applications", McGraw-Hill Inc., 1993
- [3] C. S. Gargour, V. Ramachandran, Ravi P. Ramachandran and F. S. Awad, "Variable Magnitude Characteristics of 1-D IIR Discrete Filters by a Generalized Bilinear Transformation", pp. 1270-1273, *Processing of 43rd IEEE Midwest Symposium on Circuits and Systems*, Lansing MI, August 8-11, 2000
- [4] V.Ramachandran and C.S.Garour, "Generation of Very Strict Hurwitz Polynomials and Applications to 2-D Filter Design", *Multidimensional Systems: Signal Processing and Modeling Techniques*, Academic Press Inc., Vol. 69, 1995, pp 211-254
- [5] C.S.Garour and V.Ramachandran, "Generation of Stable 2-D Transfer Functions Having Variable Magnitude Characteristics", *Multidimensional Systems: Signal Processing and Modeling Techniques*, Academic Press Inc., Vol. 69, 1995, pp 255-297
- [6] Hans W. Schussler, "A Stability Theorem for Discrete Systems", *IEEE transactions on acoustics, speech, and signal processing*, vol. ASSP-24, No.1, February 1976
- [7] Spryos G. Tzafestas, "Mulutidimensional Systems: Techniques and Applications", Amrcei Dekker. Inc., 1986

- [8] V.Ramachandran and C.S.Garour, "Implementation of a stability test of 1-D discrete system based on Schussler's theorem and some consequent coefficient conditions", Journal of Franklin Institute, Vol.317, No.5, pp.341-358, May 1984
- [9] P.E.Fleischer and K.R.Laker, "A Family of Active Switched Capacitor Biquad Buiding Blocks", The Bell System Technical Journal, vol.58, No.10, December 1979.
- [10] Alen V.Oppenheim, Ronald W.Schafer and John R.Buck, "Discrete-Time Signal Processing", Prentice Hall
- [11] Rafael C. Gonzalez, Richard E. Woods, "Digital Image Processing", Prentice Hall, ISBN number 0201180758
- [12] J. S. Lim, "Two-dimensional Signal and Image Processing", Prentice Hall Inc., 1990
- [13] D.E. Dudgeon and R. M. Mersereau, "Multidimensional Digital Signal Processing", Englewood Cliffs, NJ: Prentice Hall Inc., 1984
- [14] T. W. Parks and C. S. Burrus, "Digital Filter Design", John Wiley & Sons Inc., 1987
- [15] M. N. S. Swamy, P. Karivaratha Rajan, "Symmetry in Two-Dimensional Filters and Its Application", in Multidimensional Systems: Techniques and Applications (Edited by S. G. Tafestas). New York: Marcel Dekkar, 1986, Chapter 9
- [16] Haric Reddy, I-Hung Khoo, P. K. Rajan and Allenr Stubberud, "Symmetry in the Frequency Response of Two-dimensional { } Complex Plane Discrete-time

- Systems”, *Processing of IEEE*, (Part V), pp. 66-69, 1998
- [17] V. Rajaravivarma, P. K. Rajan and H. C. Reddy, “Symmetry Study on 2-D Complex analog and Digital Filter Functions”, *Multidimensional Systems and Signal Processing*, Vol. 2, p. 161-187, 1991
- [18] Brian T. O’Connor and Thomas S. Huang, “Stability of General Two-dimensional Recursive Digital Filters”, *IEEE Transactions on Acoustics, Speech and Signal Processing*, ASSP-26, No.6, pp. 550-560, Dec, 1978
- [19] John L. Shanks, Sven Treitel, and James H. Justice, “Stability and Synthesis of Two-dimensional Recursive Filters”, *IEEE Transactions on Audio and Electroacoustics*, ASSP-24, No.5, pp.426-427, Oct, 1976
- [20] C. S. Gargour and V. Ramachandran, “Design of 2-D Low Pass Digital Filter Having Variable Magitude Characteristics”, *IEEE International Symposium on Circuit and Systems*, Vol. 3 of 6, pp. 1424-1427, San Diego, CA, May 10-15, 1992
- [21] James H. McClellan, “The Design of Two-Dimensional Digital Filters by Transformations”, *Proceeding of 7th Annual Coefferenc on Information Sciences and Systems*, pp. 247-251, 1973
- [22] S. K. Mitra, Y. Neuvo, and H. Roivaninen, “Design of Recursive Filters with Variable characteristics,” *Journal of Circuit Theory Applications*, vol. 18, pp. 107-119, 1990
- [23] P. K. Rajan, H. C. Reddy, M. N. S. Swarmy and V. Ramachandran, “Generation of Two-Dimensional Digital Functions without Nonessential singularities of the Second Kind”, *IEEE Transactions on Acoustics, Speech, and Signal Processing*, vol. ASSP-28, No. 5, pp. 373-380, November 1983